Journal Pre-proof

Bilaterally nonlocal dynamics of layer-by-layer assembly of double-walled carbon nanotubes accounting for intertube rigorous van der Waals forces

Keivan Kiani, Hossein Pakdaman

PII: S0997-7538(18)30662-4

DOI: https://doi.org/10.1016/j.euromechsol.2019.103876

Reference: EJMSOL 103876

To appear in: *European Journal of Mechanics / A Solids*

Received Date: 31 August 2018

Revised Date: 10 October 2019

Accepted Date: 13 October 2019

Please cite this article as: Kiani, K., Pakdaman, H., Bilaterally nonlocal dynamics of layer-by-layer assembly of double-walled carbon nanotubes accounting for intertube rigorous van der Waals forces, *European Journal of Mechanics / A Solids* (2019), doi: https://doi.org/10.1016/j.euromechsol.2019.103876.

Bilaterally nonlocal dynamics of layer-by-layer assembly of double-walled carbon nanotubes accounting for intertube rigorous van der Waals forces

Keivan Kiani[†,*], Hossein Pakdaman[†]

[†]Department of Civil Engineering, K.N. Toosi University of Technology,

P.O. Box 15875-4416, Valiasr Ave., Tehran, Iran.

[*]Corresponding author. Email(s): k_kiani@kntu.ac.ir; keivankiani@yahoo.com

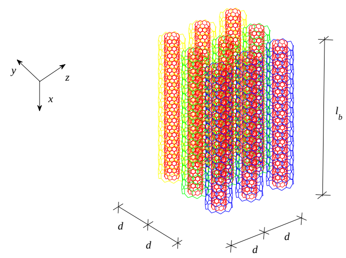

(a)

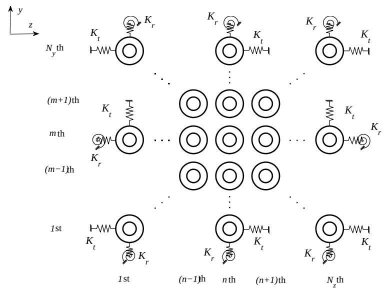

(b)

Elastically confined layer-by-layer assembly of DWCNTs: (a) atomic structure representation; (b) top view of the nonlocal continuum-based structure.

Summary

Bilaterally free vibrations of vertically aligned jungles of DWCNTs, confined in an elastic matrix, are going to be explored using nonlocal elasticity theory of Eringen. Through developing appropriate discrete and continuous models, the influential factors on vibrations of the nanosystem are examined in details.

Bilaterally nonlocal dynamics of layer-by-layer assembly of double-walled carbon nanotubes accounting for intertube rigorous van der Waals forces

Keivan Kiani[a,*], Hossein Pakdaman[a]

[a]*Department of Civil Engineering, K.N. Toosi University of Technology, Valiasr Ave., P.O. Box 15875-4416, Tehran, Iran*

Abstract

Based on appropriate nonlocal continuum models, free vibrations of a group of double-walled carbon nanotubes (DWCNTs) with forest configuration are going to be studied carefully. The nanosystem has been embedded in an elastic material such that the exterior nanotubes interact with the adjacent environment. The constitutive tubes of the nanosystem are modeled via nonlocal Rayleigh and high-order beams and all existing van der Waals forces between the walls of different DWCNTs are appropriately included in the developed models. Using the Hamilton's principle, the complex equations of motion of the nanosystem are obtained by exploiting two continuous and discrete models with some effort. For two conditions of the exterior tubes, the frequency analyses are carried out using assumed mode method and Galerkin approach based on discrete and continuous models. A close comparison of the results of the discrete models and those of the continuous ones demonstrates the success of the newly developed continuous models. These models would be very useful in the analysis of populous nanosystems. Finally, the crucial roles of the geometry of the nanotubes, intertube distance, lateral stiffness of the nearby matrix, and the nonlocality on the frequencies are investigated.

Keywords: Vertically aligned double-walled carbon nanotubes; Jungle configuration; Nonlocal continuum-based modeling; Discrete and continuous-based models; Elastic matrix; Dynamic analysis.

1. Introduction

Among the numerous configurations of carbon nanotubes (CNTs), single- and multi-walled, random and aligned, semiconducting and metallic, aligned CNTs are of particular importance because fundamental physics investigations as well as several crucial applications will not be conceivable in the lack of alignment. So far, enormous scientific works have been reported on synthesizing, exploring, physics of their alignment, and exploitation of aligned CNTs in numerous features; nevertheless, their various mechanical aspects have not been scrutinized completely yet. A forest of vertically aligned double-walled carbon nanotube (DWCNTs) is an inimitable micro-scaled structure consisting of DWCNTs oriented along their major axes, which are perpendicular to the surface of the substrate. These special microstructures own a specific morphology that could be regulated accurately. This fact plus to the extraordinary physical and mechanical properties of CNTs accelerate studies on their potential applications as field-emission devices (Chen et al. 2008; Liu et al. 2009a; Sohn et al. 2011), carbon fiber ropes (Jiang et al. 2002, 2011; Liu et al. 2009b), adhesive films (Qu and Dai 2007; Qu et al. 2008), blackbody absorber (Yang et al. 2008), gas sensors (Dragoman et al. 2007; Wei et al. 2006), dampers (Koratkar et al. 2002, 2003; Suhr et al. 2005), transistors (Choi et al. 2004, 2001; hu et al. 2004), thermal interface materials (Lin et al. 2009; Ngo et al. 2004; Tong et al. 2007), nanocomposites (Cebeci et al. 2009; Ogasawara et al. 2011; Yamamoto et al. 2009). Other crucial applications of vertically aligned CNTs have been scrutinized and explained with more details by Lan et al. (2011) and Chen et al. (2016). For most of these applications, mechanical behavior of jungles of vertically aligned CNTs and their elasto-dynamic interactions with the surrounding medium should be appropriately realized and explained.

For a densely synthesized DWCNTs array, the van der Waals (vdW) forces are among

*Corresponding author. Tel: +98 21 88779473; Fax: +98 21 88779476.
Email address: k\relax $\@@underline {\hbox {~}}\mathsurround \z@ $\relax kiani@kntu.ac.ir;~keivankiani@yahoo.com (Keivan Kiani)

the major intertube forces that should be taken into account in the mechanical analysis of such a nanosystem. For each DWCNTs, there exist rigorous vdW forces between the atoms of the innermost tube and those of the outermost one. Such crucial forces are responsible for the rigorous variation of the vdW forces due to the relative transverse motion of these tubes. By assuming a linear relationship between these factors, the parameter of this proportionality (which is commonly called the coefficient of vdW force) could be determined. For transverse vibrations of DWCNTs in a most general form, the existing vdW forces in both lateral directions are commonly modeled by two springs with the same constants due to the symmetry and coaxial of the cross-section of the innermost and outermost tubes. For doubly parallel-nearby DWCNTs with different geometry, it could be easily researched that all vdW interactional forces could be modeled by linear springs with at least eight constants (as shown in Fig. A1, each curvy spring has two transverse constants along the y and z directions). In the case of doubly identical DWCNTs, the number of constants is reduced from eight to seven. By following this procedure, we should appropriately consider all existing transverse vdW forces between constitutive tubes appropriately when transverse vibrations of forests of vertically aligned DWCNTs are of concern. The main made assumptions for modeling of vdW forces and their variations in the presented continuum-based models are the linear-like action of these forces (i.e., excluding the higher-order or nonlinear terms) and their uniform action along the tubes (due to averaging the non-uniform vdW forces and their variations due to the transverse vibrations). For more accurate modeling of the vdW forces, these two effects should be suitably taken into account. Thereby, the resulting equations of motion of the nanosystem would become nonlinear and integro-type and surely some difficulties arrive into the dynamic analysis of the nanosystem. Herein, without making the problem so difficult, we are interested in developing linear models for variation of vdW forces to arrive at a simple model for the vibrations of vertically aligned DWCNTs arrays as well as their influential factors. Surely, more complementary studies on this subject by making the above-mentioned more accurate assumptions lead to new insights on the problem at hand.

When a carbon atom vibrates, this vibration is induced to its neighboring atoms. The classical theory of elasticity could not take into account such a bizarre effect in its constitutive equations. To conquer this drawback of this concept, several size-dependent theories have been developed in the past century. One of the most well-known of these theories is the nonlocal continuum field theory established by Eringen (1966, 1972, 2002). This sophisticated model is not only applicable to elasticity problems but also to any field at the nanoscale to take into account the nonlocality. From nonlocal elasticity point of view, this theory basically explains that the state of stresses at a point of a continuum does not only depend on the stresses at that point but also to those act at its neighbor points. Mathematically, it could be written: $\sigma_{ij}^{nl}(\mathbf{x},t) = \int_{\Omega} K(||\mathbf{x}' - \mathbf{x}||; e_0 a)\, \sigma_{ij}^{l}(\mathbf{x}',t)\, \mathrm{d}\Omega'$, where Ω is the spatial domain of the continuum, K is the kernel function, $||\mathbf{x}' - \mathbf{x}||$ denotes the Euclidean distance between two points of coordinates $\mathbf{x}$ and $\mathbf{x}'$, $\mathrm{d}\Omega'$ is the infinitesimal portion of the continuum, $\sigma_{ij}^{l} = \sigma_{ij}^{l}(\mathbf{x},t)$ and $\sigma_{ij}^{nl} = \sigma_{ij}^{nl}(\mathbf{x},t)$ in order are the local and the nonlocal stress fields, and $e_0 a$ is the small-scale or the nonlocal parameter. The kernel function has a compact support domain such that $\int_{\Omega} K\left(||\mathbf{x}' - \mathbf{x}||; e_0 a\right)\, \mathrm{d}\Omega' = 1$, and various kernel functions for mechanical analysis of one-, two-, and three-dimensional domains have been introduced by Eringen in his book (Eringen 2002). Since lateral vibrations of CNTs of the nanosystem are of our concern in the present paper, we employ Rayleigh and higher-order beams for modeling of their vibrations on the basis of the concept of equivalent continuum structure (ECS) (Batra and Sears 2007; Gupta and Batra 2008; Gupta et al. 2010). For such one-dimensional elements, the above-mentioned nonlocal constitutive equation could also be presented in a simpler form: $\sigma_{ij}^{nl}(x,t) - (e_0 a)^2 \dfrac{\partial^2 \sigma_{ij}^{nl}}{\partial x^2}(x,t) = \sigma_{ij}^{l}(x,t)$. Until now, the nonlocality has been incorporated into the governing equations describe vibrations of nano-scaled rod, beam, plate, and shell structures (Akgoz and Civalek 2017; Barretta et al. 2016; Civalek et al. 2010; Demir and Civalek 2017a,b; Ghavanloo and Fazelzadeh 2013; 2015; Meng et al. 2018; Mercan and Civalek 2017; Murmu et al. 2012; Numanoglu et al. 2018; Rahmani et al. 2017). Additionally, various mechanical responses of DWCNTs have been widely investigated by various researchers. For instance, elastic waves and transverse vibrations (Heireche et al. 2008; Hoseinzadeh and Khadem 2014; Hu et al. 2008; Wang and Varadan 2006), nonlinear vibrations (Fang et al. 2013; Ke et al. 2009), vibration signature analysis for detecting nano-objects (Patel and Joshi 2014), free vibrations in the presence of magnetic fields (Murmu et al. 2012) and thermal fields (Besseghier et al. 2011; Tounsi et al. 2013, 2008), forced vibrations (Chang 2013), buckling and postbuckling (Shen and Zhang 2010; Sudak 2003) of DWCNTs have been explained by the nonlocal elasticity theory. However, free transverse vibrations of elastically embedded-vertical DWCNTs arrays in the context of the nonlocal continuum field theory of Eringen have not been examined up until now.

Concerning mechanical behavior of vertically aligned single-walled carbon nanotubes (SWCNTs) with membrane morphology, their transverse vibrations (Kiani 2014a) and free vibration under magnetic field (Kiani 2016) have been addressed. Regarding mechanical analysis of these nanostructures with jungle configuration, their free vibrations (Kiani 2014b), elastic wave analysis (Kiani 2015), elastic waves in the presence of longitudinal magnetic field (Kiani 2018a), and magneto-thermo-elastic vibrations (Kiani 2018b; Kiani and Wang 2018) have been investigated using nonlocal beam models. Recently, transverse vibrations of membranes made from DWCNTs subjected to longitudinal gradient temperatures were examined by Kiani and Pakdaman (2018) using nonlocal beam models. In contrast to the undertaken works on buckling, waves, and vibrations of membranes and jungles of vertically aligned SWCNTs, mechanical behaviors of jungles of vertically aligned DWCNTs embedded in an elastic matrix have not been comprehensively studied to date.

In the present work, we are eagerly interested in examining free lateral vibrations of jungles of vertically aligned DWCNTs embedded in an elastic matrix. To this end, variation of the vdW forces between constitutive tubes of the assembly of DWCNTs and its neighboring one due to the lateral motion of the tubes are visualized by transversely linear springs. In a deep sight, we confront a nonlocally modeled nanosystem composed of vertically aligned tubes that linked each other through a complex net of springs. The constitutive tubes are modeled by non-localized Rayleigh and higher-order beam models. By employing the Hamilton's principle, the linear equations of motion for such a nanosystem are methodically derived. Actually, these are discrete models since such models and their governing equations are constructed on the basis of the mechanical behavior of individual tubes. The idea of developing of continuous models for groups of SWCNTs (Kiani 2014b, 2015, 2018a) is now generalized for the problem at hand. Then the efficiency of the suggested continuous models is displayed, and it is declared that the free vibration of highly populated nanosystems could be efficiently explained by such models.

2. Description of the nanomechanical problem

Consider a forest structure composed of vertically aligned DWCNTs with a uniform distribution as shown in Fig. 1. The number of layers of DWCNTs along the y and z axes are represented by N_y and N_z, respectively, while the intertube distance (i.e., the distance between the major axes of doubly nearby DWCNTs) in both directions is denoted by d. By considering ECS associated with each tube, transverse vibrations of vertically aligned DWCNTs could be mechanically modeled by a double-circular-cylindrical beam-like structures whose length, wall's thickness, cross-sectional area, mean radius, Young's modulus, shear elastic modulus, and density of the innermost/outermost tubes in order are l_b, t_b, A_{b_1}/A_{b_2}, r_{m_1}/r_{m_2}, E_{b_1}/E_{b_2}, G_{b_1}/G_{b_2}, and ρ_{b_1}/ρ_{b_2}. Due to the existence of the vdW forces between the carbon atoms of the innermost and outermost walls as well as carbon atoms of doubly adjacent DWCNTs, the constitutive DWCNTs of the vertically aligned nanosystem are tightly interacted dynamically. It means that we should be aware regarding the resulted variation of the vdW forces because of the relative transverse displacements of nearby DWCNTs. By assuming a linear relationship between these factors, the coefficient of vdW forces for the above-mentioned interactional vdW forces should be evaluated by some effort. The details of calculations of these coefficients ($C_{v[.](i,j)}$ and $C_{d[.](i,j)}$ where $[.]=\|$ or $\perp$)

have been given in Appendix A. All exterior nanotubes of the nanosystem are under static and dynamic interactions with the elastic surrounding medium. Such interactions have been modeled by continuous transverse and rotational springs with constants K_t and K_r, respectively (see Fig. 2). The transverse dynamic displacements of the constitutive tubes of DWCNTs along the y and z directions in order are denoted by V_{mni} and W_{mni} where those with i=1 and i=2 correspond to the innermost and outermost tubes, respectively.

In the following parts, the nonlocal discrete-based and continuous-based models according to the nonlocal Rayleigh and higher-order beam theories (NRBT and NHOBT) are developed for examining free transverse vibrations of elastically embedded layer-by-layer assembly of vertically aligned DWCNTs.

3. Discrete modeling of jungle-like configuration of vertically aligned DWCNTs

3.1. Application of the NRBT for frequency analysis

This section displays an energy-based methodology for extracting the explicit-complex equations of motion of the nanosystem whose constitutive tubes have been modeled on the basis of the Rayleigh beam theory by consideration of the nonlocality. The main assumption of this theory is that each plane perpendicular to the neutral axis remains normal after deformation. This hypothesis is the same as that of the Euler-Bernoulli beam model; however, the rotary inertia of the beam is also incorporated into the kinetic energy while such an important factor is excluded in the Euler-Bernoulli-based beams. In this view, the whole kinetic energy of the nanosystem is provided by:

$$T^R\left(t\right) = \frac{1}{2}\sum_{i=1}^{2}\sum_{m=1}^{N_y}\sum_{n=1}^{N_z}\int_0^{l_b} \rho_{b_i} \left(\begin{array}{c} A_{b_i}\left(\left(\frac{\partial V^R_{mni}}{\partial t}\right)^2 + \left(\frac{\partial W^R_{mni}}{\partial t}\right)^2 \right) \\ +I_{b_i}\left(\left(\frac{\partial^2 V^R_{mni}}{\partial t \partial x}\right)^2 + \left(\frac{\partial^2 W^R_{mni}}{\partial t \partial x}\right)^2 \right) \end{array} \right) \mathrm{d}x. \tag{1}$$

In discrete modeling of the nanosystem, each nanotube is modeled separately from its surrounding tubes such that the dynamic-lateral interactions between them due to the vdW forces could be visualized by elastic layers. The constants of such layers are the slope of variation of the transverse vdW forces as a function of relative transverse displacements of adjacent tubes (for details of calculations of coefficients of vdW forces, please see Appendix A). As a result, the total strain energy of the elastically embedded jungle-like nanosystem accounting for the nonlocality, $U^R(t)$, on the basis of the NRBT is expressed by:

$$
\begin{aligned}
&U^R(t) = \frac{1}{2}\sum_{i=1}^{2}\sum_{m=1}^{N_y}\sum_{n=1}^{N_z}\int_0^{l_b}\left\{-\frac{\partial^2 V_{mni}^R}{\partial x^2}\left(M_{bz_{mni}}^{nl}\right)^R - \frac{\partial^2 W_{mni}^R}{\partial x^2}\left(M_{by_{mni}}^{nl}\right)^R + \right.\\
&C_{v\|_{(i+2,i)}}\left[\left(V_{mni}^R - V_{(m+1)ni}^R\right)^2\left(1-\delta_{mN_y}\right) + \left(V_{mni}^R - V_{(m-1)ni}^R\right)^2\left(1-\delta_{1m}\right)\right] +\\
&C_{v\perp_{(i,3-i)}}\left(V_{mni}^R - V_{mn(3-i)}^R\right)^2 + C_{v\|_{(i+1,4-i)}}\left[\left(V_{mni}^R - V_{(m+1)n(3-i)}^R\right)^2\left(1-\delta_{mN_y}\right)\right.\\
&\left. + \left(V_{mni}^R - V_{(m-1)n(3-i)}^R\right)^2\left(1-\delta_{1m}\right)\right] + C_{v\perp_{(i+2,i)}}\left[\left(V_{mni}^R - V_{m(n-1)i}^R\right)^2\left(1-\delta_{1n}\right)\right.\\
&\left. + \left(V_{mni}^R - V_{m(n+1)i}^R\right)^2\left(1-\delta_{nN_z}\right)\right] + C_{v\perp_{i(3-i)}}\left(V_{mni}^R - V_{mn(3-i)}^R\right)^2\\
&+C_{v\perp_{(i+1,4-i)}}\left[\left(V_{mni}^R - V_{m(n-1)(3-i)}^R\right)^2\left(1-\delta_{1n}\right) + \left(V_{mni}^R - V_{m(n+1)(3-i)}^R\right)^2\left(1-\delta_{nN_z}\right)\right]\\
&+C_{d\|_{(i+2,i)}}\left(X_{mni}^R - X_{(m-1)(n-1)i}^R\right)^2\left(1-\delta_{1n}\right)\left(1-\delta_{1m}\right) + C_{d\|_{(i,3-i)}}\left(X_{mni}^R - X_{mn(3-i)}^R\right)^2\\
&+C_{d\|_{(i+1,4-i)}}\left(X_{mni}^R - X_{(m-1)(n-1)(3-i)}^R\right)^2\left(1-\delta_{1m}\right)\left(1-\delta_{1n}\right) + C_{d\|_{(i+2,i)}}\left(X_{mni}^R - X_{(m+1)(n+1)i}^R\right)^2\\
&\times\left(1-\delta_{nN_z}\right)\left(1-\delta_{mN_y}\right) + C_{d\|_{(i+1,4-i)}}\left(X_{mni}^R - X_{(m+1)(n+1)(3-i)}^R\right)^2\left(1-\delta_{nN_z}\right)\left(1-\delta_{mN_y}\right)\\
&+C_{d\|_{(i+2,i)}}\left(Y_{mni}^R - Y_{(m+1)(n-1)i}^R\right)^2\left(1-\delta_{1n}\right)\left(1-\delta_{mN_y}\right) + C_{d\|_{(i,3-i)}}\left(Y_{mni}^R - Y_{mn(3-i)}^R\right)^2\\
&+C_{d\|_{(i+1,4-i)}}\left(Y_{mni}^R - Y_{(m+1)(n-1)(3-i)}^R\right)^2\left(1-\delta_{1n}\right)\left(1-\delta_{mN_y}\right) + C_{d\|_{(i+2,i)}}\left(Y_{mni}^R - Y_{(m-1)(n+1)i}^R\right)^2\\
&\times\left(1-\delta_{nN_z}\right)\left(1-\delta_{1m}\right) + C_{d\perp_{(i+1,4-i)}}\left(Y_{mni}^R - Y_{(m-1)(n+1)(3-i)}^R\right)^2\left(1-\delta_{nN_z}\right)\left(1-\delta_{1m}\right)\\
&+C_{d\perp_{(i+2,i)}}\left(Y_{mni}^R - Y_{(m-1)(n-1)i}^R\right)^2\left(1-\delta_{1n}\right)\left(1-\delta_{1m}\right) + C_{d\perp_{(i,3-i)}}\left(Y_{mni}^R - Y_{mn(3-i)}^R\right)^2\\
&+C_{d\perp_{(i+1)(4-i)}}\left(Y_{mni}^R - Y_{(m-1)(n-1)(3-i)}^R\right)^2\left(1-\delta_{1n}\right)\left(1-\delta_{1m}\right) + C_{d\perp_{(i+2,i)}}\left(Y_{mni}^R - Y_{(m+1)(n+1)i}^R\right)^2\\
&\times\left(1-\delta_{nN_z}\right)\left(1-\delta_{mN_y}\right) + C_{d\perp_{(i+1,4-i)}}\left(Y_{mni}^R - Y_{(m+1)(n+1)(3-i)}^R\right)^2\left(1-\delta_{nN_z}\right)\left(1-\delta_{mN_y}\right)\\
&+C_{d\perp_{(i+2,i)}}\left(X_{mni}^R - X_{(m-1)(n+1)i}^R\right)^2\left(1-\delta_{nN_z}\right)\left(1-\delta_{1m}\right) + C_{d\perp_{(i,3-i)}}\left(X_{mni}^R - X_{mn(3-i)}^R\right)^2\\
&+C_{d\perp_{(i+1,4-i)}}\left(X_{mni}^R - X_{(m-1)(n+1)(3-i)}^R\right)^2\left(1-\delta_{nN_z}\right)\left(1-\delta_{1m}\right) + C_{d\perp_{(i+2,i)}}\left(X_{mni}^R - X_{(m+1)(n-1)i}^R\right)^2\\
&\times\left(1-\delta_{1n}\right)\left(1-\delta_{mN_y}\right) + C_{d\perp_{(i+1,4-i)}}\left(X_{mni}^R - X_{(m+1)(n-1)(3-i)}^R\right)^2\left(1-\delta_{1m}\right)\left(1-\delta_{mN_y}\right)\\
&\left. + \begin{pmatrix} K_t\left(V_{mni}^R\right)^2 + K_r\left(\dfrac{\partial V_{mni}^R}{\partial x}\right)^2 \\ K_t\left(W_{mni}^R\right)^2 + K_r\left(\dfrac{\partial W_{mni}^R}{\partial x}\right)^2 \end{pmatrix}\begin{pmatrix} \delta_{1n} + \delta_{1m} + \delta_{nN_z} + \delta_{mN_y} - \delta_{1m}\delta_{1n} - \\ \delta_{1m}\delta_{nN_z} - \delta_{1n}\delta_{mN_y} - \delta_{nN_z}\delta_{mN_y} \end{pmatrix}\left(1-\delta_{1i}\right)\right\}dx.
\end{aligned}
\tag{2}
$$

where $X_{mni}^R = \frac{\sqrt{2}}{2}\left(W_{mni}^R + V_{mni}^R\right)$, $Y_{mni}^R = \frac{\sqrt{2}}{2}\left(-W_{mni}^R + V_{mni}^R\right)$, and δ_{ij} is the Kronecker delta tensor. Using the nonlocal elasticity theory of Eringen (Eringen 1966, 1972), the nonlocal bending moments about the y and z axes (i.e., $(M_{by}^{nl})_{mni}^R$ and $(M_{bz}^{nl})_{mni}^R$) are linked to their corresponding local bending moments by:

$$
\begin{aligned}
&(M_{by}^{nl})_{mni}^{R} - (e_0 a)^2 \frac{\partial^2}{\partial x^2}(M_{by}^{nl})_{mni}^{R} = -E_{b_i} I_{b_i} \frac{\partial^2 W_{mni}^{R}}{\partial x^2},\\
&(M_{bz}^{nl})_{mni}^{R} - (e_0 a)^2 \frac{\partial^2}{\partial x^2}(M_{bz}^{nl})_{mni}^{R} = -E_{b_i} I_{b_i} \frac{\partial^2 V_{mni}^{R}}{\partial x^2},
\end{aligned}
\tag{3}
$$

where $E_{b_i} I_{b_i}$ represents the bending rigidity of the ith nanotube. Let us consider the following dimensionless quantities:

$$
\begin{aligned}
&\xi = \frac{x}{l_b},\ \overline{V}_{mni}^{R} = \frac{V_{mni}^{R}}{l_b},\ \overline{W}_{mni}^{R} = \frac{W_{mni}^{R}}{l_b},\ \tau = \frac{t}{l_b^2}\sqrt{\frac{E_{b_1} I_{b_1}}{\rho_{b_1} A_{b_1}}},\ \mu = \frac{e_0 a}{l_b},\ \lambda_1 = \frac{l_b}{\sqrt{\frac{I_{b_1}}{A_{b_1}}}},\\
&\varrho_1^2 = \frac{\rho_{b_2} A_{b_2}}{\rho_{b_1} A_{b_1}},\ \varrho_2^2 = \frac{\rho_{b_2} I_{b_2}}{\rho_{b_1} I_{b_1}},\ \varrho_3^2 = \frac{E_{b_2} I_{b_2}}{E_{b_1} I_{b_1}},\ \overline{C}_{v[\bullet]_{(i,j)}}^{R} = \frac{C_{v[\bullet]_{ij}} l_b^4}{E_{b_1} I_{b_1}},\ \overline{C}_{d[\bullet]_{(i,j)}}^{R} = \frac{C_{d[\bullet]_{ij}} l_b^4}{E_{b_1} I_{b_1}},\\
&\overline{K}_t^{R} = \frac{K_t l_b^4}{E_{b_1} I_{b_1}},\ \overline{K}_r^{R} = \frac{K_r l_b^2}{E_{b_1} I_{b_1}},\ \overline{d} = \frac{d}{l_z},\ l_z = (N_z - 1)\, d,\ [\bullet] = \parallel \ \text{ or } \perp.
\end{aligned}
\tag{4}
$$

In order to derive equations of motion of the jungle-like nanosystem, we employ the Hamilton's principle. For a nanosystem with $N_y N_z$ numbers of DWCNTs, we will arrive at $4N_y N_z$ dimensionless-partial differential equations of motion to study their lateral vibrations via the NRBT-based discrete model (see Appendix B).

For frequency analysis of the problem, we use assumed mode approach (AMA). Regarding lateral conditions of the group, we consider two cases: (i) all the outermost nanotubes on the edges of the nanosystem are laterally fixed; (ii) only those outermost tubes on the corners have been fixed. Concerning the ends' conditions of the constitutive DWCNTs, we restrict our analysis to the simply supported ends; however, free vibration behavior of the nanosystem for other boundary conditions could be readily investigated by AMA. Therefore, the deflection fields of the innermost and the outermost tubes with simple ends are expressed in terms of admissible mode shapes as follows:

$$
\overline{V}_{mni}^{R}(\xi,\tau) = \sum_{j=1}^{NM} \overline{V}_{mnij}^{R}(\tau)\sin(j\pi\xi),\quad \overline{W}_{mni}^{R}(\xi,\tau) = \sum_{j=1}^{NM} \overline{W}_{mnij}^{R}(\tau)\sin(j\pi\xi),
\tag{5}
$$

where NM denotes the number of vibration modes, $\overline{V}_{mnij}^{R}(\tau)$ and $\overline{W}_{mnij}^{R}(\tau)$ are the time-dependent parameters pertinent to the jth mode. By application of the Galerkin method to the governing equations of the elastically embedded group of DWCNTs (i.e., Eqs. (B.1) and (B.2)) and using orthogonal property of mode shapes, one can arrive at the following set of second-order ordinary differential equations: $\overline{\mathbf{M}}^R \frac{\mathrm{d}^2\overline{\boldsymbol{x}}^R}{\mathrm{d}\tau^2} + \overline{\mathbf{K}}^R\overline{\boldsymbol{x}}^R = \mathbf{0}$. Let us choose $\overline{\mathbf{x}}^R = \overline{\mathbf{x}}_0^R \exp(\mathrm{i}\varpi\tau)$, where $\mathbf{x}_0^R$ is the dimensionless amplitude vector, $\mathrm{i} = \sqrt{-1}$, and ϖ is the dimensionless natural frequency. The substitution of this form into the recently derived-discretized equations of motion leads to the following non-trivial solution: $\det\left(-\varpi^2\overline{\mathbf{M}}^R + \overline{\mathbf{K}}^R\right) = 0$. By solving this characteristic equation for ϖ, the natural frequencies of the nanosystem could be evaluated.

3.2. Application of the NHOBT for frequency analysis

In this part, we investigate transverse vibrations of elastically embedded jungles of DWCNTs using NHOBT. The most privilege of the NHOBT with respect to the NRBT is the consideration of shear deformation in its formulation. To this end, the longitudinal displacement is considered as a function of the slope of deflection (i.e., v^H and w^H) and the rotation angle (i.e., ψ_y^H and ψ_z^H) such that the shear strains at the farthest fibers of the cross-section of the ECS are vanished. This leads to a third-order function for the longitudinal displacement in terms of the distance from the neutral axis. Therefore, it is anticipated that the shear effect could be effectively captured and interpreted by the NHOBT.

Using the NHOBT, the kinetic energy of the vertically aligned jungles of DWCNTs embedded in an elastic matrix is calculated by:

$$T^H(t) = \frac{1}{2}\sum_{i=1}^{2}\sum_{m=1}^{N_y}\sum_{n=1}^{N_z}\int_0^{l_b} \left(\begin{array}{l} I_{0_i}\left(\left(\frac{\partial^2 V_{mni}^H}{\partial t\partial x}\right)^2 + \left(\frac{\partial^2 W_{mni}^H}{\partial t\partial x}\right)^2\right) + I_{2_i}\left(\frac{\partial \Psi_{y_{mni}}^H}{\partial t}\right)^2 + \\ \alpha_i^2 I_{6_i}\left(\frac{\partial \Psi_{y_{mni}}^H}{\partial t} + \frac{\partial^2 W_{mni}^H}{\partial t\partial x}\right)^2 - 2\alpha_i I_{4_i}\frac{\partial \Psi_{y_{mni}}^H}{\partial t}\left(\frac{\partial \Psi_{y_{mni}}^H}{\partial t} + \right. \\ \left. \frac{\partial^2 W_{mni}^H}{\partial t\partial x}\right) + I_{2_i}\left(\frac{\partial \Psi_{z_{mni}}^H}{\partial t}\right)^2 + \alpha_i^2 I_{6_i}\left(\frac{\partial \Psi_{z_{mni}}^H}{\partial t} + \right. \\ \left. \frac{\partial^2 V_{mni}^H}{\partial t\partial x}\right) - 2\alpha_i I_{4_i}\frac{\partial \Psi_{z_{mni}}^H}{\partial t}\left(\frac{\partial \Psi_{z_{mni}}^H}{\partial t} + \frac{\partial^2 V_{mni}^H}{\partial t\partial x}\right) \end{array} \right) \mathrm{d}x, \tag{6}$$

where $\alpha_i = \frac{1}{3r_{o_i}^2}$ and $I_{n_i} = \int_{A_{b_i}} \rho_{b_i} z^n \mathrm{d}A$ in which r_{o_i} is the outermost radius of the ith tube from the DWCNTs, V_{mni}^H and W_{mni}^H in order denote the transverse displacements of the ECS associated with the (m,n,i)th tube along the y and z axes, $\Psi^H_{y_{mni}}$ and $\Psi^H_{z_{mni}}$ represent the rotation angles of the aforementioned ECS about the y-axis and z-axis, respectively.

In the framework of the linear nonlocal theory of elasticity, the strain energy of the vertically aligned jungle-like DWCNTs which is embedded in an elastic matrix accounting for the intertube vdW interactional forces could be written as follows:

$$
\begin{aligned}
&U^H(t) = \frac{1}{2}\sum_{i=1}^{2}\sum_{m=1}^{N_y}\sum_{n=1}^{N_z}\int_0^{l_b}\left\{\frac{\partial \Psi^H_{y_{mni}}}{\partial x}\left(M^{nl}_{by_{mni}}\right)^H + \left(\Psi^H_{y_{mni}} + \frac{\partial W^H_{mni}}{\partial x}\right)\left(\alpha_i \frac{\partial\left(P^{nl}_{bz_{mni}}\right)^H}{\partial x} + \left(Q^{nl}_{bz_{mni}}\right)^H\right) + \right.\\
&\frac{\partial \Psi^H_{z_{mni}}}{\partial x}\left(M^{nl}_{bz_{mni}}\right)^H + \left(\Psi^H_{z_{mni}} + \frac{\partial V^H_{mni}}{\partial x}\right)\left(\alpha_i \frac{\partial\left(P^{nl}_{by_{mni}}\right)^H}{\partial x} + \left(Q^{nl}_{by_{mni}}\right)^H\right) + C_{v\|_{(i+2,i)}}\left[\left(V^H_{mni} - V^H_{(m+1)ni}\right)^2\right.\\
&\left.\times\left(1-\delta_{mN_y}\right) + \left(V^H_{mni} - V^H_{(m-1)ni}\right)^2\left(1-\delta_{1m}\right)\right] + C_{v\|_{(i,3-i)}}\left(V^H_{mni} - V^H_{mn(3-i)}\right)^2 + C_{v\|_{(i+1,4-i)}}\\
&\times\left[\left(V^H_{mni} - V^H_{(m+1)n(3-i)}\right)^2\left(1-\delta_{mN_y}\right) + \left(V^H_{mni} - V^H_{(m-1)n(3-i)}\right)^2\left(1-\delta_{1m}\right)\right] + C_{v\perp_{(i+2,i)}}\\
&\times\left[\left(V^H_{mni} - V^H_{m(n-1)i}\right)^2\left(1-\delta_{1n}\right) + \left(V^H_{mni} - V^H_{m(n+1)i}\right)^2\left(1-\delta_{nN_z}\right)\right] + C_{v\perp_{(i,3-i)}}\left(V^H_{mni} - V^H_{mn(3-i)}\right)^2\\
&+C_{v\perp_{(i+1,4-i)}}\left[\left(V^H_{mni} - V^H_{m(n-1)(3-i)}\right)^2\left(1-\delta_{1n}\right) + \left(V^H_{mni} - V^H_{m(n+1)(3-i)}\right)^2\left(1-\delta_{nN_z}\right)\right]\\
&+C_{d\|_{(i+2,i)}}\left(X^H_{mni} - X^H_{(m-1)(n-1)i}\right)^2\left(1-\delta_{1n}\right)\left(1-\delta_{1m}\right) + C_{d\|_{(i,3-i)}}\left(X^H_{mni} - X^H_{mn(3-i)}\right)^2\\
&+C_{d\|_{(i+1,4-i)}}\left(X^H_{mni} - X^H_{(m-1)(n-1)(3-i)}\right)^2\left(1-\delta_{1m}\right)\left(1-\delta_{1n}\right) + C_{d\|_{(i+2,i)}}\left(X^H_{mni} - X^H_{(m+1)(n+1)i}\right)^2\\
&\times\left(1-\delta_{nN_z}\right)\left(1-\delta_{mN_y}\right) + C_{d\|_{(i+1,4-i)}}\left(X^H_{mni} - X^H_{(m+1)(n+1)(3-i)}\right)^2\left(1-\delta_{nN_z}\right)\left(1-\delta_{mN_y}\right)\\
&+C_{d\|_{(i+2,i)}}\left(Y^H_{mni} - Y^H_{(m+1)(n-1)i}\right)^2\left(1-\delta_{1n}\right)\left(1-\delta_{mN_y}\right) + C_{d\|_{(i,3-i)}}\left(Y^H_{mni} - Y^H_{mn(3-i)}\right)^2\\
&+C_{d\|_{(i+1,4-i)}}\left(Y^H_{mni} - Y^H_{(m+1)(n-1)(3-i)}\right)^2\left(1-\delta_{1n}\right)\left(1-\delta_{mN_y}\right) + C_{d\|_{(i+2,i)}}\left(Y^H_{mni} - Y^H_{(m-1)(n+1)i}\right)^2\\
&\times\left(1-\delta_{nN_z}\right)\left(1-\delta_{1m}\right) + C_{d\|_{(i+1,4-i)}}\left(Y^H_{mni} - Y^H_{(m-1)(n+1)(3-i)}\right)^2\left(1-\delta_{nN_z}\right)\left(1-\delta_{1m}\right)\\
&+C_{d\perp_{(i+2,i)}}\left(Y^H_{mni} - Y^H_{(m-1)(n-1)i}\right)^2\left(1-\delta_{1n}\right)\left(1-\delta_{1m}\right) + C_{d\perp_{(i,3-i)}}\left(Y^H_{mni} - Y^H_{mn(3-i)}\right)^2\\
&+C_{d\perp_{(i+1,4-i)}}\left(Y^H_{mni} - Y^H_{(m-1)(n-1)(3-i)}\right)^2\left(1-\delta_{1n}\right)\left(1-\delta_{1m}\right) + C_{d\perp_{(i+2,i)}}\left(Y^H_{mni} - Y^H_{(m+1)(n+1)i}\right)^2\\
&\times\left(1-\delta_{nN_z}\right)\left(1-\delta_{mN_y}\right) + C_{d\perp_{(i+1,4-i)}}\left(Y^H_{mni} - Y^H_{(m+1)(n+1)(3-i)}\right)^2\left(1-\delta_{nN_z}\right)\left(1-\delta_{mN_y}\right)\\
&+C_{d\perp_{(i+2,i)}}\left(X^H_{mni} - X^H_{(m-1)(n+1)i}\right)^2\left(1-\delta_{nN_z}\right)\left(1-\delta_{1m}\right) + C_{d\perp_{(i,3-i)}}\left(X^H_{mni} - X^H_{mn(3-i)}\right)^2\\
&+C_{d\perp_{(i+1,4-i)}}\left(X^H_{mni} - X^H_{(m-1)(n+1)(3-i)}\right)^2\left(1-\delta_{nN_z}\right)\left(1-\delta_{1m}\right) + C_{d\perp_{(i+2,i)}}\left(X^H_{mni} - X^H_{(m+1)(n-1)i}\right)^2\\
&\times\left(1-\delta_{1n}\right)\left(1-\delta_{mN_y}\right) + C_{d\perp_{(i+1,4-i)}}\left(X^H_{mni} - X^H_{(m+1)(n-1)(3-i)}\right)^2\left(1-\delta_{1m}\right)\left(1-\delta_{mN_y}\right)\\
&\left.+\begin{pmatrix} K_t\left(V^H_{mni}\right)^2 + K_r\left(\Psi^H_{z_{mni}}\right)^2 \\ K_t\left(W^H_{mni}\right)^2 + K_r\left(\Psi^H_{y_{mni}}\right)^2 \end{pmatrix}\begin{pmatrix} \delta_{1n} + \delta_{1m} + \delta_{nN_z} + \delta_{mN_y} - \delta_{1m}\delta_{1n} \\ -\delta_{1m}\delta_{nN_z} - \delta_{1n}\delta_{mN_y} - \delta_{nN_z}\delta_{mN_y} \end{pmatrix}\left(1-\delta_{1i}\right)\right\}\mathrm{d}x,
\end{aligned}
\tag{7}
$$

where $(Q^{nl}_{by_{mni}})^H + \alpha_i \partial (P^{nl}_{by_{mni}})^H/\partial x$ and $(Q^{nl}_{bz_{mni}})^H + \alpha_i \partial (P^{nl}_{bz_{mni}})^H/\partial x$ in order are the total resultant shear forces in the (m,n,i)th tube of the DWCNTs along the y and z axes, $(M^{nl}_{by_{mni}})^H$

and $(M^{nl}_{bz_{mni}})^H$ represent the nonlocal flexural moments of the (m,n,i)th nanotube of the DWCNTs about the y-axis and the z-axis, respectively.

In the context of a simplified version of nonlocal elasticity theory of Eringen (Kiani 2015, 2018a), the nonlocal shear forces as well as the flexural moments of the ECS modeled by the NHOBT could be related to their corresponding local values by:

$$\begin{aligned}&\left(Q^H_{by_{mni}}+\alpha_i\frac{\partial P^H_{by_{mni}}}{\partial x}\right)-(e_0a)^2\,\frac{\partial^2}{\partial x^2}\left(Q^H_{by_{mni}}+\alpha_i\frac{\partial P^H_{by_{mni}}}{\partial x}\right)=\\&\kappa_i\left(\Psi^H_{bz_{mni}}+\frac{\partial V^H_{mni}}{\partial x}\right)+\alpha_i J_{4_i}\frac{\partial^2\Psi^H_{z_{mni}}}{\partial x^2}-\alpha_i^2J_{6_i}\left(\frac{\partial^2\Psi^H_{z_{mni}}}{\partial x^2}+\frac{\partial^3V^H_{mni}}{\partial x^3}\right),\end{aligned}\tag{8a}$$

$$\begin{aligned}&\left(Q^H_{bz_{mni}}+\alpha_i\frac{\partial P^H_{bz_{mni}}}{\partial x}\right)-(e_0a)^2\,\frac{\partial^2}{\partial x^2}\left(Q^H_{bz_{mni}}+\alpha_i\frac{\partial P^H_{bz_{mni}}}{\partial x}\right)=\\&\kappa_i\left(\Psi^H_{by_{mni}}+\frac{\partial W^H_{mni}}{\partial x}\right)+\alpha_i J_{4_i}\frac{\partial^2\Psi^H_{y_{mni}}}{\partial x^2}-\alpha_i^2J_{6_i}\left(\frac{\partial^2\Psi^H_{y_{mni}}}{\partial x^2}+\frac{\partial^3W^H_{mni}}{\partial x^3}\right),\end{aligned}\tag{8b}$$

$$M^H_{by_{mni}}-(e_0a)^2\,\frac{\partial^2M^H_{by_{mni}}}{\partial x^2}=J_{2_i}\frac{\partial\Psi^H_{y_{mni}}}{\partial x}-\alpha_iJ_{4_i}\left(\frac{\partial\Psi^H_{y_{mni}}}{\partial x}+\frac{\partial^2W^H_{mni}}{\partial x^2}\right),\tag{8c}$$

$$M^H_{bz_{mni}}-(e_0a)^2\,\frac{\partial^2M^H_{bz_{mni}}}{\partial x^2}=J_{2_i}\frac{\partial\Psi^H_{z_{mni}}}{\partial x}-\alpha_iJ_{4_i}\left(\frac{\partial\Psi^H_{z_{mni}}}{\partial x}+\frac{\partial^2V^H_{mni}}{\partial x^2}\right),\tag{8d}$$

where $\kappa_i=\int_{A_{b_i}}G_{b_i}(1-3\alpha_iz^2)\mathrm{d}A$ and $J_{n_i}=\int_{A_{b_i}}E_{b_i}z^n\mathrm{d}A$. To derive the nonlocal continuum-based equations of motion, the Hamilton's principle is implemented: $\int\left(\delta T^H(t)-\delta U^H(t)\right)\mathrm{d}t=0$. By taking into account the following dimensionless parameters:

$$\begin{aligned}&\overline{V}^H_{mni}=\frac{V^H_{mni}}{l_b},\ \overline{W}^H_{mni}=\frac{W^H_{mni}}{l_b},\ \overline{\Psi}^H_{y_{mni}}=\Psi^H_{y_{mni}},\ \overline{\Psi}^H_{z_{mni}}=\Psi^H_{z_{mni}},\ \tau=\frac{\alpha_1}{l_b^2}\sqrt{\frac{J_{6_1}}{I_{0_1}}}\,t,\\&\gamma_1^2=\frac{\alpha_1J_{4_1}-\alpha_1^2J_{6_1}}{I_{0_1}l_b^2},\ \gamma_2^2=\frac{\alpha_1^2I_{6_1}}{I_{0_1}l_b^2},\ \gamma_3^2=\frac{\kappa_1l_b^2}{\alpha_1^2J_{6_1}},\ \gamma_4^2=\frac{\alpha_1J_{4_1}-\alpha_1^2J_{6_1}}{\alpha_1^2J_{6_1}},\ \gamma_6^2=\frac{\alpha_1I_{4_1}-\alpha_1^2I_{6_1}}{I_{2_1}-2\alpha_1I_{4_1}+\alpha_1^2I_{6_1}},\\&\gamma_7^2=\frac{\kappa_1I_{0_1}l_b^4}{I_{2_1}-2\alpha_1I_{4_1}+\alpha_1^2I_{6_1}\alpha_1^2J_{6_1}},\ \gamma_8^2=\frac{\left(J_{2_1}-2\alpha_1J_{4_1}+\alpha_1^2J_{6_1}\right)I_{0_1}l_b^2}{\left(I_{2_1}-2\alpha_1I_{4_1}+\alpha_1^2I_{6_1}\right)\alpha_1^2J_{6_1}},\ \gamma_9^2=\frac{\left(\alpha_1J_{4_1}-\alpha_1^2J_{6_1}\right)I_{0_1}l_b^2}{\left(I_{2_1}-2\alpha_1I_{4_1}+\alpha_1^2I_{6_1}\right)\alpha_1^2J_{6_1}},\\&\overline{C}^H_{v[\bullet]_{(i,j)}}=\frac{C_{v[\bullet]_{ij}}l_b^4}{\alpha_1^2J_{6_1}},\ \overline{C}^H_{d[\bullet]_{(i,j)}}=\frac{C_{d[\bullet]_{ij}}l_b^4}{\alpha_1^2J_{6_1}},\ \overline{K}^H_r=\frac{K_rI_{0_1}l_b^4}{\alpha_1^2J_{6_1}\left(I_{2_1}-2\alpha_1I_{4_1}+\alpha_1^2I_{6_1}\right)},\ \overline{K}^H_t=\frac{K_tl_b^4}{\alpha_1^2J_{6_1}},\\&\vartheta_1^2=\frac{I_{0_2}}{I_{0_1}},\ \vartheta_2^2=\frac{\alpha_2I_{4_2}-\alpha_2^2I_{6_2}}{\alpha_1I_{4_1}-\alpha_1^2I_{6_1}},\ \vartheta_3^2=\frac{\alpha_2^2I_{6_2}}{\alpha_1^2I_{6_1}},\ \vartheta_4^2=\frac{\kappa_2}{\kappa_1},\ \vartheta_5^2=\frac{\alpha_2J_{4_2}-\alpha_2^2J_{6_2}}{\alpha_1J_{4_1}-\alpha_1^2J_{6_1}},\\&\vartheta_6^2=\frac{\alpha_2^2J_{6_2}}{\alpha_1^2J_{6_1}},\ \vartheta_7^2=\frac{I_{2_2}-2\alpha_2I_{4_2}+\alpha_2^2I_{6_2}}{I_{2_1}-2\alpha_1I_{4_1}+\alpha_1^2I_{6_1}},\ \vartheta_8^2=\frac{J_{2_2}-2\alpha_2J_{4_2}+\alpha_2^2J_{6_2}}{J_{2_1}-2\alpha_1J_{4_1}+\alpha_1^2J_{6_1}},\ [\bullet]=\parallel\text{ or }\perp,\end{aligned}\tag{9}$$

after some manipulations, the dimensionless governing equations that describe lateral vibrations of vertically aligned jungles of DWCNTs on the basis of the discrete form of the NHOBT are obtained as provided in Appendix C.

For frequency analysis of the problem, we discretize the dimensionless deformation fields of the simply supported nanosystem as follows:

$$\overline{V}^{H}_{mni}(\xi,\tau) = \sum_{j=1}^{NM} \overline{V}^{H}_{mnij}(\tau)\sin(j\pi\xi)\,, \tag{10a}$$

$$\overline{\Psi}^{H}_{z_{mni}}(\xi,\tau) = \sum_{j=1}^{NM} \overline{\Psi}^{H}_{z_{mnij}}(\tau)\cos(j\pi\xi)\,, \tag{10b}$$

$$\overline{W}^{H}_{mni}(\xi,\tau) = \sum_{j=1}^{NM} \overline{W}^{H}_{mnij}(\tau)\sin(j\pi\xi)\,, \tag{10c}$$

$$\overline{\Psi}^{H}_{y_{mni}}(\xi,\tau) = \sum_{j=1}^{NM} \overline{\Psi}^{H}_{y_{mnij}}(\tau)\cos(j\pi\xi)\,. \tag{10d}$$

By applying the Galerkin approach to the given equations of motion, namely Eqs. (C.1)-(C.4), using integration by part technique, and substituting Eqs. (10a)-(10d) into the resulted relation, it is derived: $\overline{\mathbf{M}}^{H}\dfrac{\mathrm{d}^2\overline{\boldsymbol{x}}^{H}}{\mathrm{d}\tau^2} + \overline{\mathbf{K}}^{H}\overline{\boldsymbol{x}}^{H} = \mathbf{0}$. Now the vector of the dimensionless time-dependent parameter is stated in the following harmonic form: $\overline{\boldsymbol{x}}^{H} = \overline{\boldsymbol{x}}^{H}_{0}\ \exp(\mathrm{i}\varpi\tau)$. By introducing such a form to the obtained set of discretized equations of motion, the natural frequencies of the vertically aligned jungles of DWCNTs embedded in an elastic matrix according to the NHOBT discrete-based model are evaluated from: $\det\left(-\varpi^2\overline{\mathbf{M}}^{H} + \overline{\mathbf{K}}^{H}\right) = 0$.

4. Continuous modeling of jungle-like configuration of vertically aligned DWCNTs

As it is seen for the case of the suggested discrete model based on the NRBT, each nanotube has its own doubly unknown transverse displacements while in the case of the proposed discrete model based on the NHOBT, each nanotube has its four individual unknown deformation fields (i.e., two unknown deflection fields plus to two angle of deflection fields). It implies that for a vertically aligned group of nanotubes with $N_y N_z$ DWCNTs, we would confront to $4N_y N_z$ and $8N_y N_z$ unknown fields when it has been modeled on the basis of the NRBT and the NHOBT, respectively. Therefore, the size of both mass and stiffness matrices of the discrete-based models would drastically grow by an increase of the population of the jungle-like nanostructure.

Since each two adjacent tubes could interact statically and dynamically because of the existing vdW forces, and in view of linear modeling of such distributed forces (i.e., elastic layers as a fairly rational replacement of such forces), perhaps one could establish the appropriate continuous version of the recently developed discrete models in the previous section. In other words, we are eagerly interested in constructing the governing equations of the continuous deflections, and then, we would proceed in finding continuous deflections as an appropriate representation of the discrete deflections.

4.1. Application of the NRBT for frequency analysis

For constructing continuous models, let us to approximate the continuous deformation fields (i.e., $[\cdot]$) in terms of their corresponding deformations of the suggested discrete-based-models (i.e., $[\bullet]$) as follows:

$$\begin{aligned}
&[\bullet]_{mni}(x,t) \approx [\cdot]_i(x, y_{mni}, z_{mni}, t), \quad [\bullet]_{(m-1)(n-1)i}(x,t) \approx [\cdot]_i(x, y_{mni}-d, z_{mni}-d, t), \\
&[\bullet]_{(m-1)(n+1)i}(x,t) \approx [\cdot]_i(x, y_{mni}-d, z_{mni}+d, t), \quad [\bullet]_{(m+1)(n-1)i}(x,t) \approx [\cdot]_i(x, y_{mni}+d, z_{mni}-d, t), \\
&[\bullet]_{(m+1)(n+1)i}(x,t) \approx [\cdot]_i(x, y_{mni}+d, z_{mni}+d, t),
\end{aligned} \tag{11}$$

where (y_{mni}, z_{mni}) represents the coordinates of the revolutionary axis of the mnith nanotube on the plane z=0, $[.]$=$v^{[\circ]}$ or $w^{[\circ]}$, and $[\bullet]$=$V^{[\circ]}$ or $W^{[\circ]}$ where $[\circ]$=R or H. In order to approximate the continuous fields at the neighboring tubes of the (mni)th tube, we use the Taylor's series of sixth-order:

$$[\cdot]_i(x, y_{mni} \pm d, z_{mni} \pm d, t) = \sum_{l=1}^{6} \sum_{k=0}^{l} \begin{pmatrix} l \\ l-k \end{pmatrix} \frac{\partial^l [\cdot]_i(x, y_{mni}, z_{mni}, t)}{\partial z^k \partial z^{l-k}} (\pm d)^k (\pm d)^{l-k}. \tag{12}$$

By introducing Eq. (12) to Eqs. (B.1) and (B.2) carefully by virtue of Eq. (11) carefully, the non-dimensional governing equations that display transverse vibrations of the vertically aligned jungle-like DWCNTs embedded in a matrix are derived as given in Appendix D1.

Let us express the dimensionless displacements of the continuous-NRBT-based model in terms of the vibrational modes of the nanosystem as follows:

$$\begin{aligned}
\overline{v}_i^R(\xi,\eta,\gamma,\tau) &= \sum_{m=1}^{N_{mv}}\sum_{n=1}^{N_{nv}}\sum_{p=1}^{N_{pv}} \overline{v}_{mnpi}^R(\tau)\,\phi_{mnpi}^{v_i}(\xi,\eta,\gamma)\,,\\
\overline{w}_i^R(\xi,\eta,\gamma,\tau) &= \sum_{m=1}^{N_{mw}}\sum_{n=1}^{N_{nw}}\sum_{p=1}^{N_{pw}} \overline{w}_{mnpi}^R(\tau)\,\phi_{mnpi}^{w_i}(\xi,\eta,\gamma)\,,
\end{aligned} \tag{13}$$

where $\phi_{mnpi}^{v_i}$ and $\phi_{mnpi}^{w_i}$ represent the (m,n,p)th mode of the ith tube associated with the deflections in the y and z directions, respectively, $\overline{v}_{mnpi}^R(\tau)$ and $\overline{w}_{mnpi}^R(\tau)$ denote their corresponding dimensionless time-dependent factors. For a vertically aligned jungle of DWCNTs whose the outermost tubes at the edges are fixed and the consisting nanotubes have simple ends, we consider the following mode shapes for dynamic deflections of the nanosystem:

$$\phi_{mnpi}^{v_i}(\xi,\eta,\gamma) = \phi_{mnpi}^{w_i}(\xi,\eta,\gamma) = \sin(m\pi\xi)\sin(n\pi\eta)\sin(p\pi\gamma)\,. \tag{14}$$

Now for free vibration analysis, the Galerkin method is implemented. For this purpose, we premultiply both sides of Eqs. (D.1) and (D.2) by $\delta\overline{v}^R$ and $\delta\overline{w}^R$, respectively, and then the resulted relations are integrated over the dimensionless spatial domain of the nanosystem. After successful application of the integration by parts technique, one could arrive at the following set of equations:

$$\begin{bmatrix} \left[\overline{\mathbf{M}}_b^R\right]^{v_1v_1} & \left[\overline{\mathbf{M}}_b^R\right]^{v_1v_2} & \left[\overline{\mathbf{M}}_b^R\right]^{v_1w_1} & \left[\overline{\mathbf{M}}_b^R\right]^{v_1w_2} \\ \left[\overline{\mathbf{M}}_b^R\right]^{v_2v_1} & \left[\overline{\mathbf{M}}_b^R\right]^{v_2v_2} & \left[\overline{\mathbf{M}}_b^R\right]^{v_2w_1} & \left[\overline{\mathbf{M}}_b^R\right]^{v_2w_2} \\ \left[\overline{\mathbf{M}}_b^R\right]^{w_1v_1} & \left[\overline{\mathbf{M}}_b^R\right]^{w_1v_2} & \left[\overline{\mathbf{M}}_b^R\right]^{w_1w_1} & \left[\overline{\mathbf{M}}_b^R\right]^{w_1w_2} \\ \left[\overline{\mathbf{M}}_b^R\right]^{w_2v_1} & \left[\overline{\mathbf{M}}_b^R\right]^{w_2v_2} & \left[\overline{\mathbf{M}}_b^R\right]^{w_2w_1} & \left[\overline{\mathbf{M}}_b^R\right]^{w_2w_2} \end{bmatrix} \begin{Bmatrix} \dfrac{\mathrm{d}^2\overline{\mathbf{v}}_1^R}{\mathrm{d}\tau^2} \\ \dfrac{\mathrm{d}^2\overline{\mathbf{v}}_2^R}{\mathrm{d}\tau^2} \\ \dfrac{\mathrm{d}^2\overline{\mathbf{w}}_1^R}{\mathrm{d}\tau^2} \\ \dfrac{\mathrm{d}^2\overline{\mathbf{w}}_2^R}{\mathrm{d}\tau^2} \end{Bmatrix} + \begin{bmatrix} \left[\overline{\mathbf{K}}_b^R\right]^{v_1v_1} & \left[\overline{\mathbf{K}}_b^R\right]^{v_1v_2} & \left[\overline{\mathbf{K}}_b^R\right]^{v_1w_1} & \left[\overline{\mathbf{K}}_b^R\right]^{v_1w_2} \\ \left[\overline{\mathbf{K}}_b^R\right]^{v_2v_1} & \left[\overline{\mathbf{K}}_b^R\right]^{v_2v_2} & \left[\overline{\mathbf{K}}_b^R\right]^{v_2w_1} & \left[\overline{\mathbf{K}}_b^R\right]^{v_2w_2} \\ \left[\overline{\mathbf{K}}_b^R\right]^{w_1v_1} & \left[\overline{\mathbf{K}}_b^R\right]^{w_1v_2} & \left[\overline{\mathbf{K}}_b^R\right]^{w_1w_1} & \left[\overline{\mathbf{K}}_b^R\right]^{w_1w_2} \\ \left[\overline{\mathbf{K}}_b^R\right]^{w_2v_1} & \left[\overline{\mathbf{K}}_b^R\right]^{w_2v_2} & \left[\overline{\mathbf{K}}_b^R\right]^{w_2w_1} & \left[\overline{\mathbf{K}}_b^R\right]^{w_2w_2} \end{bmatrix} \begin{Bmatrix} \overline{\mathbf{v}}_1^R \\ \overline{\mathbf{v}}_2^R \\ \overline{\mathbf{w}}_1^R \\ \overline{\mathbf{w}}_2^R \end{Bmatrix} = \begin{Bmatrix} \mathbf{0} \\ \mathbf{0} \\ \mathbf{0} \\ \mathbf{0} \end{Bmatrix}, \tag{15}$$

where the elements of the dimensionless mass and stiffness matrices of the nanosystem could be readily derived as provided in Eqs. (D.4)-(D.13). For frequency analysis of the problem at hand more specifically, the dimensionless time-dependent parameters in Eq. (15) are stated in the following form: $<\overline{\mathbf{v}}_i^R(\tau), \overline{\mathbf{w}}_i^R(\tau)> = <\overline{\mathbf{v}}_{0_i}^R, \overline{\mathbf{w}}_{0_i}^R> \exp(\mathrm{i}\varpi^R\tau)$, where ϖ^R are dimensionless natural frequencies of the nanosystem, and $\overline{\mathbf{v}}_{0_i}^R$ and $\overline{\mathbf{w}}_{0_i}^R$ denote the dimensionless amplitude vectors. By substituting the recently harmonic form of the dimensionless time-dependent parameters into Eq. (15), and solving the eigenvalue equations, the mth natural frequency of the vertically aligned jungle of DWCNTs based on the continuous-NRBT model are calculated from: $\omega_m^R = \dfrac{\varpi_m^R}{l_b^2}\sqrt{\dfrac{E_{b_1}I_{b_1}}{\rho_{b_1}A_{b_1}}}$.

4.2. Application of the NHOBT for frequency analysis

Let us approximate the continuous angle of deflections of the constitutive nanotubes of the vertically aligned jungles of DWCNTs as follows:

$$\psi_{y_i}^H(x, y_{mni}, z_{mni}, t) \approx \Psi_{y_{mni}}^H(x,t), \quad \psi_{z_i}^H(x, y_{mni}, z_{mni}, t) \approx \Psi_{z_{mni}}^H(x,t). \tag{16}$$

Now by introducing Eqs. (11) and (16) to the discrete-based equations of motion of the nanosystem via NHOBT (i.e., Eqs. (C.1)-(C.4)) in view of Eq. (12), the continuous-based governing equations that display transverse vibrations of vertically aligned jungles of DWC-NTs using NHOBT would be derived as given in Appendix E.1 (see Eqs. (E.1)-(E.4)).

By discretizing the continuous-based deformation fields of the ith tubes of the vertically aligned jungle of DWCNTs as a function of admissible mode shapes in the following form:

$$\begin{aligned}
\overline{v}_i^H(\xi,\eta,\gamma,\tau) &= \sum_{m=1}^{N_{mv}}\sum_{n=1}^{N_{nv}}\sum_{p=1}^{N_{pv}} \overline{v}_{mnpi}^H(\tau)\,\phi_{mnpi}^v(\xi,\eta,\gamma)\,,\\
\overline{w}_i^H(\xi,\eta,\gamma,\tau) &= \sum_{m=1}^{N_{mw}}\sum_{n=1}^{N_{nw}}\sum_{p=1}^{N_{pw}} \overline{w}_{mnpi}^H(\tau)\,\phi_{mnpi}^w(\xi,\eta,\gamma)\,,\\
\overline{\psi}_{y_i}^H(\xi,\eta,\gamma,\tau) &= \sum_{m=1}^{N_{m\psi_y}}\sum_{n=1}^{N_{n\psi_y}}\sum_{p=1}^{N_{p\psi_y}} \overline{\psi}_{y_{mnpi}}^H(\tau)\,\phi_{mnpi}^{\psi_y}(\xi,\eta,\gamma)\,,\\
\overline{\psi}_{z_i}^H(\xi,\eta,\gamma,\tau) &= \sum_{m=1}^{N_{m\psi_z}}\sum_{n=1}^{N_{n\psi_z}}\sum_{p=1}^{N_{p\psi_z}} \overline{\psi}_{z_{mnpi}}^H(\tau)\,\phi_{mnpi}^{\psi_z}(\xi,\eta,\gamma)\,,
\end{aligned} \tag{17}$$

where $\overline{v}_{mnpi}^H(\tau)$, $\overline{w}_{mnpi}^H(\tau)$, $\overline{\psi}_{y_{mnpi}}^H(\tau)$, and $\overline{\psi}_{z_{mnpi}}^H(\tau)$ are the time-dependent parameters, and ϕ_{mnpi}^v, ϕ_{mnpi}^w, $\phi_{mnpi}^{\psi_y}$, and $\phi_{mnpi}^{\psi_z}$ represent the appropriate (m,n,p)th vibration modes pertinent to the boundary conditions of the nonlocal-continuous-based nanosystem. For a vertically aligned forest of DWCNTs with simply supported ends whose the outermost tubes of the exterior DWCNTs have been fixed, we consider the following admissible modes:

$$\begin{aligned}
\phi_{mnpi}^v(\xi,\eta,\gamma) = \phi_{mnpi}^w(\eta,\gamma,\tau) &= \sin(m\pi\xi)\sin(n\pi\eta)\sin(p\pi\gamma)\,,\\
\phi_{mnpi}^{\psi_y}(\xi,\eta,\gamma) = \phi_{mnpi}^{\psi_z}(\eta,\gamma,\tau) &= \cos(m\pi\xi)\sin(n\pi\eta)\sin(p\pi\gamma)\,.
\end{aligned} \tag{18}$$

In order to arrive at the appropriate ordinary differential equations, we premultiply both sides of Eqs. (E.1)-(E.4) by $\delta\overline{v}_i^H$, $\delta\overline{w}_i^H$, $\delta\overline{\psi}_{z_i}^H$, and $\delta\overline{\psi}_{y_i}^H$, respectively, and then, the resulted relations are integrated over the dimensionless spatial domain of the nanosystem. By using the integration by parts technique, it is obtainable:

$$
\begin{bmatrix}
\left[\overline{\mathbf{M}}_b^H\right]^{\psi_{z_1}\psi_{z_1}} & \left[\overline{\mathbf{M}}_b^H\right]^{\psi_{z_1}\psi_{z_2}} & \left[\overline{\mathbf{M}}_b^H\right]^{\psi_{z_1}v_1} & \left[\overline{\mathbf{M}}_b^H\right]^{\psi_{z_1}v_2} & \left[\overline{\mathbf{M}}_b^H\right]^{\psi_{z_1}\psi_{y_1}} & \left[\overline{\mathbf{M}}_b^H\right]^{\psi_{z_1}\psi_{y_2}} \\
\left[\overline{\mathbf{M}}_b^H\right]^{\psi_{z_2}\psi_{z_1}} & \left[\overline{\mathbf{M}}_b^H\right]^{\psi_2\psi_{z_2}} & \left[\overline{\mathbf{M}}_b^H\right]^{\psi_{z_2}v_1} & \left[\overline{\mathbf{M}}_b^H\right]^{\psi_{z_2}v_2} & \left[\overline{\mathbf{M}}_b^H\right]^{\psi_{z_2}\psi_{y_1}} & \left[\overline{\mathbf{M}}_b^H\right]^{\psi_{z_2}\psi_{y_2}} \\
\left[\overline{\mathbf{M}}_b^H\right]^{v_1\psi_{z_1}} & \left[\overline{\mathbf{M}}_b^H\right]^{v_1\psi_{z_2}} & \left[\overline{\mathbf{M}}_b^H\right]^{v_1v_1} & \left[\overline{\mathbf{M}}_b^H\right]^{v_1v_2} & \left[\overline{\mathbf{M}}_b^H\right]^{v_1\psi_{y_1}} & \left[\overline{\mathbf{M}}_b^H\right]^{v_1\psi_{y_2}} \\
\left[\overline{\mathbf{M}}_b^H\right]^{v_2\psi_{z_1}} & \left[\overline{\mathbf{M}}_b^H\right]^{v_2\psi_{z_2}} & \left[\overline{\mathbf{M}}_b^H\right]^{v_2v_1} & \left[\overline{\mathbf{M}}_b^H\right]^{v_2v_2} & \left[\overline{\mathbf{M}}_b^H\right]^{v_2\psi_{y_1}} & \left[\overline{\mathbf{M}}_b^H\right]^{v_2\psi_{y_2}} \\
\left[\overline{\mathbf{M}}_b^H\right]^{\psi_{y_1}\psi_{z_1}} & \left[\overline{\mathbf{M}}_b^H\right]^{\psi_{y_1}\psi_{z_2}} & \left[\overline{\mathbf{M}}_b^H\right]^{\psi_{y_1}v_1} & \left[\overline{\mathbf{M}}_b^H\right]^{\psi_{y_1}v_2} & \left[\overline{\mathbf{M}}_b^H\right]^{\psi_{y_1}\psi_{y_1}} & \left[\overline{\mathbf{M}}_b^H\right]^{\psi_{y_1}\psi_{y_2}} \\
\left[\overline{\mathbf{M}}_b^H\right]^{\psi_{y_2}\psi_{z_1}} & \left[\overline{\mathbf{M}}_b^H\right]^{\psi_{y_2}\psi_{z_2}} & \left[\overline{\mathbf{M}}_b^H\right]^{\psi_{y_2}v_1} & \left[\overline{\mathbf{M}}_b^H\right]^{\psi_{y_2}v_2} & \left[\overline{\mathbf{M}}_b^H\right]^{\psi_{y_2}\psi_{y_1}} & \left[\overline{\mathbf{M}}_b^H\right]^{\psi_{y_2}\psi_{y_2}} \\
\left[\overline{\mathbf{M}}_b^H\right]^{w_1\psi_{z_1}} & \left[\overline{\mathbf{M}}_b^H\right]^{w_1\psi_{z_2}} & \left[\overline{\mathbf{M}}_b^H\right]^{w_1v_1} & \left[\overline{\mathbf{M}}_b^H\right]^{w_1v_2} & \left[\overline{\mathbf{M}}_b^H\right]^{w_1\psi_{y_1}} & \left[\overline{\mathbf{M}}_b^H\right]^{w_1\psi_{y_2}} \\
\left[\overline{\mathbf{M}}_b^H\right]^{w_2\psi_{z_1}} & \left[\overline{\mathbf{M}}_b^H\right]^{w_2\psi_{z_2}} & \left[\overline{\mathbf{M}}_b^H\right]^{w_2v_1} & \left[\overline{\mathbf{M}}_b^H\right]^{w_2v_2} & \left[\overline{\mathbf{M}}_b^H\right]^{w_2\psi_{y_1}} & \left[\overline{\mathbf{M}}_b^H\right]^{w_2\psi_{y_2}}
\end{bmatrix}
\begin{Bmatrix}
\dfrac{\mathrm{d}^2\overline{\mathbf{\Psi}}^H_{z_1}}{\mathrm{d}\tau^2} \\
\dfrac{\mathrm{d}^2\overline{\mathbf{\Psi}}^H_{z_2}}{\mathrm{d}\tau^2} \\
\dfrac{\mathrm{d}^2\overline{\mathbf{v}}^H_{1}}{\mathrm{d}\tau^2} \\
\dfrac{\mathrm{d}^2\overline{\mathbf{v}}^H_{2}}{\mathrm{d}\tau^2} \\
\dfrac{\mathrm{d}^2\overline{\mathbf{\Psi}}^H_{y_1}}{\mathrm{d}\tau^2} \\
\dfrac{\mathrm{d}^2\overline{\mathbf{\Psi}}^H_{y_2}}{\mathrm{d}\tau^2} \\
\dfrac{\mathrm{d}^2\overline{\mathbf{w}}^H_{1}}{\mathrm{d}\tau^2} \\
\dfrac{\mathrm{d}^2\overline{\mathbf{w}}^H_{2}}{\mathrm{d}\tau^2}
\end{Bmatrix} +
$$

$$
\begin{bmatrix}
\left[\overline{\mathbf{K}}_b^H\right]^{\psi_{z_1}v_2} & \left[\overline{\mathbf{K}}_b^H\right]^{\psi_{z_1}\psi_{y_1}} & \left[\overline{\mathbf{K}}_b^H\right]^{\psi_{z_1}\psi_2} & \left[\overline{\mathbf{K}}_b^H\right]^{\psi_{z_1}w_1} & \left[\overline{\mathbf{K}}_b^H\right]^{\psi_{z_1}w_2} \\
\left[\overline{\mathbf{K}}_b^H\right]^{\psi_{z_2}v_2} & \left[\overline{\mathbf{K}}_b^H\right]^{\psi_{z_2}\psi_{y_1}} & \left[\overline{\mathbf{K}}_b^H\right]^{\psi_{z_2}\psi_{y_2}} & \left[\overline{\mathbf{K}}_b^H\right]^{\psi_{z_2}w_1} & \left[\overline{\mathbf{K}}_b^H\right]^{\psi_{z_2}w_2} \\
\left[\overline{\mathbf{K}}_b^H\right]^{v_1v_2} & \left[\overline{\mathbf{K}}_b^H\right]^{v_1\psi_{y_1}} & \left[\overline{\mathbf{K}}_b^H\right]^{v_1\psi_{y_2}} & \left[\overline{\mathbf{K}}_b^H\right]^{v_1w_1} & \left[\overline{\mathbf{K}}_b^H\right]^{v_1w_2} \\
\left[\overline{\mathbf{K}}_b^H\right]^{v_2v_2} & \left[\overline{\mathbf{K}}_b^H\right]^{v_2\psi_{y_1}} & \left[\overline{\mathbf{K}}_b^H\right]^{v_2\psi_{y_2}} & \left[\overline{\mathbf{K}}_b^H\right]^{v_2w_1} & \left[\overline{\mathbf{K}}_b^H\right]^{v_2w_2} \\
\left[\overline{\mathbf{K}}_b^H\right]^{\psi_{y_1}v_2} & \left[\overline{\mathbf{K}}_b^H\right]^{\psi_{y_1}\psi_{y_1}} & \left[\overline{\mathbf{K}}_b^H\right]^{\psi_{y_1}\psi_{y_2}} & \left[\overline{\mathbf{K}}_b^H\right]^{\psi_{y_1}w_1} & \left[\overline{\mathbf{K}}_b^H\right]^{\psi_{y_1}w_2} \\
\left[\overline{\mathbf{K}}_b^H\right]^{\psi_{y_2}v_2} & \left[\overline{\mathbf{K}}_b^H\right]^{\psi_{y_2}\psi_{y_1}} & \left[\overline{\mathbf{K}}_b^H\right]^{\psi_{y_2}\psi_{y_2}} & \left[\overline{\mathbf{K}}_b^H\right]^{\psi_{y_2}w_1} & \left[\overline{\mathbf{K}}_b^H\right]^{\psi_{y_2}w_2} \\
\left[\overline{\mathbf{K}}_b^H\right]^{w_1v_2} & \left[\overline{\mathbf{K}}_b^H\right]^{w_1\psi_{y_1}} & \left[\overline{\mathbf{K}}_b^H\right]^{w_1\psi_{y_2}} & \left[\overline{\mathbf{K}}_b^H\right]^{w_1w_1} & \left[\overline{\mathbf{K}}_b^H\right]^{w_1w_2} \\
\left[\overline{\mathbf{K}}_b^H\right]^{w_2v_2} & \left[\overline{\mathbf{K}}_b^H\right]^{w_2\psi_{y_1}} & \left[\overline{\mathbf{K}}_b^H\right]^{w_2\psi_{y_2}} & \left[\overline{\mathbf{K}}_b^H\right]^{w_2w_1} & \left[\overline{\mathbf{K}}_b^H\right]^{w_2w_2}
\end{bmatrix}
\begin{Bmatrix}
\overline{\mathbf{\Psi}}^H_{z_1} \\ \overline{\mathbf{\Psi}}^H_{z_2} \\ \overline{\mathbf{v}}^H_1 \\ \overline{\mathbf{v}}^H_2 \\ \overline{\mathbf{\Psi}}^H_{y_1} \\ \overline{\mathbf{\Psi}}^H_{y_2} \\ \overline{\mathbf{w}}^H_1 \\ \overline{\mathbf{w}}^H_2
\end{Bmatrix} =
\begin{Bmatrix}
\mathbf{0} \\ \mathbf{0} \\ \mathbf{0} \\ \mathbf{0} \\ \mathbf{0} \\ \mathbf{0} \\ \mathbf{0} \\ \mathbf{0}
\end{Bmatrix}, \tag{19}
$$

where the dimensionless mass and stiffness matrices of the continuous-NHOBT-based model for free vibration analysis of vertically aligned jungles of DWCNTs have been given in Appendix E.2. By taking into account the deformation field as follows: $< \overline{\mathbf{v}}_i^H(\tau), \overline{\mathbf{w}}_i^H(\tau), \overline{\mathbf{\Psi}}_{z_i}^H(\tau), \overline{\mathbf{\Psi}}_{y_i}^H(\tau) >$ $= < \overline{\mathbf{v}}_{0_i}^H, \overline{\mathbf{w}}_{0_i}^H, \overline{\mathbf{\Psi}}_{z0_i}^H, \overline{\mathbf{\Psi}}_{y0_i}^H >\ \exp(\mathrm{i}\varpi^H\tau)$, where ϖ^H denote the dimensionless natural frequencies of the nanosystem based on the NHOBT, and $\overline{\mathbf{v}}_{0_i}^H$, $\overline{\mathbf{w}}_{0_i}^H$, $\overline{\mathbf{\Psi}}_{z0_i}^H$, and $\overline{\mathbf{\Psi}}_{y0_i}^H$ are the amplitudes of the nanosystem. Finally, by following up the given procedure in section 2.2, the natural frequencies of the nanosystem could be readily evaluated by: $\omega_m^H = \dfrac{\alpha_1\varpi^H}{l_b^2}\sqrt{\dfrac{J_{6_1}}{I_{0_1}}}$.

5. Results and discussion

In this section, a roughly comprehensive parametric study is presented to examine free transverse vibrations of vertically aligned DWCNTs with forest configuration. Using suggested discrete and continuous models, geometric effects, the nonlocal parameter, and the lateral stiffness of the matrix on the fundamental frequency of the nanosystem are investigated. The mechanical and geometry data of the constitutive DWCNTs are considered to be: t_b=0.34 nm, r_{m_1}=1 nm, e_0a=2 nm, ρ_b=2300 kg/m^3, and E_b=1000 GPa. For all provided parametric studies, the outermost tubes of the exterior DWCNTs have been fixed unless explicitly referred to.

5.1. Natural frequencies of the nanosystem for two boundary conditions

In Table 1, the results of the discrete models for a group of DWCNTs based on the NRBT and the NHOBT are presented for two different boundary conditions. In the first boundary condition, denoted by BC1, all the exterior DWCNTs have been fixed while in the case of the second boundary condition-represented by BC2-only those DWCNTs at the corners are fixed. For six slenderness ratios as well as three small-scale parameters, the predicted fundamental frequencies of the nanosystem under the above-mentioned conditions for the case of N_y=N_z=20 are given in Table 1. A brief comparison of the results of these two boundary conditions shows that in all proposed nonlocal models, the natural frequencies of the BC1 are greater than those of the BC2. This issue is more obvious for nanosystems with higher slender nanotubes. Since the lateral constrains of the nanosystem with BC1 are higher than that with BC2, the above-mentioned conclusion is rational. A more detailed investigation of the results of both boundary conditions indicates that an increase in the slenderness ratio would result in a decrease of the fundamental frequencies. The rate of reduction is more apparent for lower values of the slenderness ratio. Additionally, an increase of the nonlocal parameter yields decreasing of the fundamental frequencies via both theories. Another important point is the moderate increase of the fundamental frequency at slenderness ratios higher than 100 due to the strong increase in the tightly interactional vdW forces between the different walls, particularly those of the internal and external walls of consisting DWCNTs.

It should be noted that the small-scale factor for a DWCNTs with given geometry and boundary conditions has a constant value; however, herein we explore the role of the small-scale factor in the frequencies of the nanosystem for two reasons: (i) to examine the difference between the classical models' results and those of the novel nonlocal models, (ii) to reveal the influence of the nonlocality on the trends of the natural frequencies' plots.

5.2. Natural frequencies based on the discrete and continuous models

In Table 2, the results of discrete and continuous models in the case of fixed exterior DWCNTs have been provided for three slenderness ratios (i.e., λ_1=14, 24, and 34) as well as five levels of the population of the nanosystem (i.e., N_y=N_z=4, 8, 12, 16, and 20). A close survey of the predicted results by the continuous models with those of the discrete models demonstrates that the continuous model could successfully capture the results of the discrete models for various values of the slenderness ratio and the populations. The importance of the continuous models in predicting free vibrational behavior of the nanosystem becomes apparent for nanosystems with a large number of DWCNTs. For such a case, application of the discrete models would compromise with a high computational effort. More scrutiny of the obtained results reveals that an increase of the number of DWCNTs would result in a reduction of the fundamental frequency. Such a decrease is more obvious for a nanosystem with a higher slenderness ratio. Furthermore, the rate of reduction of fundamental frequencies as a function of the slenderness ratio is more obvious for nanosystems with a higher number of DWCNTs. A detailed comparison of the results of the NRBT and those of the NHOBT displays that the predicted results by the continuous models are in a fairly good agreement with those of the discrete models. Regarding the shear deformation effect, the presented results in Table 2 show that the results of the NRBT and those of the NHOBT are generally close to each other, particularly for nanosystems with high levels of the slenderness ratio. In most of the cases, the predicted results by the NHOBT are lower than those of the NRBT and their relative discrepancies would commonly increase by reducing the slenderness ratio of the nanosystem.

5.3. Influence of the matrix's stiffness on frequencies

The surrounding medium of the nanosystem was modeled by continuous lateral and rotational springs that have been attached to the outermost tubes of the exterior DWCNTs. The constants of these springs could be readily evaluated by considering the geometry and mechanical properties of such an elastic medium as well as their lateral interactional of atoms of the exterior DWCNTs with the neighboring atoms of the elastic medium. However, it is anticipated that the later interaction would not contribute into the constant of the continuous rotational springs. Since the main focus of the authors in the present work is on the free transverse vibrations of vertically aligned groups of DWCNTs, more details on evaluation of the above-mentioned constants of springs have not been provided.

In Fig. 3, the fundamental frequencies of the elastically embedded of the nanosystems of various populations as a function of the lateral stiffness and rotational stiffness of the surrounding elastic medium are demonstrated. The plotted results have been extracted from the developed continuous models based on the NRBT and the NHOBT for three levels of the population of nanosystem (i.e., N_y=N_z=5, 8, and 15). Based on the proposed nonlocal continuous models, an increase of the elastic medium parameters (i.e., rotational stiffness or transverse stiffness) leads to increasing of the fundamental frequency of the nanosystem. The increase of the fundamental frequency of the nanosystem due to stiffening of the surrounding medium is more apparent for those nanosystems with lower numbers of DWCNTs. For a given transverse stiffness or rotational stiffness of the surrounding medium, by increasing the population of the nanosystem, the fundamental frequency would reduce. Such a trend will be discussed in the next part with a more detail. Further studies indicate that the rate of the increase of the fundamental frequency of the nanosystem in terms of the rotational stiffness for low values of such a parameter is very high in compare to the case of very stiff surrounding elastic medium. This issue becomes more apparent for lowly populated nanosystems. For instance, in the case of N_y=N_z=5, by increasing the dimensionless rotational stiffness from 500 to 700, the variation of the fundamental frequency as a function of rotational stiffness would be obviously reduced. For $\overline{K}_r^R > 1000$, variation of the rotation stiffness has a trivial influence on the variation of the fundamental frequency. For all considered levels of the transverse and rotational stiffness of the surrounding elastic medium, the graphical results demonstrate that the results of the NHOBT are lower than the results of the NRBT. In addition, the relative differences between the results of these two nonlocal models would lessen as the nanosystem's population grows.

5.4. Influence of the number of DWCNTs on frequencies

Figure 4 shows the variation of the fundamental frequency in terms of the number of DWCNTs for two distinct boundary conditions as well as three slenderness ratios. The results of Figs. 4(a) and (b) in order are corresponding to the nanosystems whose the outermost tubes of all the exterior tubes and the four cornered DWCNTs have been fully prevented from any transverse motion. By increasing the number of DWCNTs, the fundamental frequencies of the nanosystem for both boundary conditions would decrease. In other words, with the increase of the number of DWCNTs, the nanosystem dimensions in y and z directions would increase, which reduces the lateral stiffness of the nanosystem. A closer examination of the obtained results shows that increasing the slenderness ratio not only reduces the fundamental frequencies but also increases the rate of variation of the fundamental frequency in terms of the number of DWCNTs. Also, the increase in the slenderness ratio makes the results of the two nonlocal theories become closer to each other, so that in the case of λ_1=32, the plotted results are almost overlapping. This means that the effect of the shear deformation becomes negligible for nanosystems whose slenderness ratios of the constitutive nanotubes are high enough. According to the results of two proposed models, the results of the continuous-based NHOBT, especially for lower slenderness ratios, are lower than those of the continuous-based NRBT. It means that the transverse stiffness of stocky nanosystems based on the NRBT is usually overestimated due to not consideration of the shear effect in its formulations. A comparison study of the demonstrated results in Figs. 4(a) and (b) reveals that the fundamental frequencies of the nanosystem with BC1 are commonly greater than those of the nanosystem with BC2. In addition, the rate of variation of the frequency as a function of the number of DWCNTs in the case of BC1 is greater than that for the case of BC2.

5.5. Influence of the slenderness ratio on frequencies

Figure 5 shows the variation of the fundamental frequency in terms of the slenderness ratio for different numbers of DWCNTs. For nanosystems with a low number of DWCNTs, the plots consist of two obvious branches: the descending branch and the ascending branch. In the first branch, the reduction rate of fundamental frequency is notable such that the plots take their relative minimum points at the end of the branch. Thereafter, the ascending branch is started, and the fundamental frequencies would increase with a fairly mild slope. Such an odd behavior is attributed to a combination of the decreasing effect of the slenderness ration and the increasing effect of the coefficients of vdW forces. Actually, in the descending branch, the role of decreasing effect of the slenderness ratio in the transverse stiffness of the nanosystem is more obvious with respect to the increasing effect of the coefficients of vdW forces. However, in the second branch, the increasing of the transverse stiffness is mainly dedicated to the increasing of the vdW forces' coefficients. It should be noted that the location of the aforementioned extremum points essentially depends on the population of the nanosystem. For example, a nanosystem with a higher population has a minimum point with a higher slenderness ratio. In the descending branch, the transverse stiffness of the nanosystem would reduce by increasing the slenderness ratio. The predicted rate of reduction by the NRBT is fairly greater than that by the NHOBT. As it is seen, by increasing the slenderness ratio, the results of the NHOBT become closer to those of the NRBT and the role of shear deformation on the free transverse vibration of the vertically aligned groups of DWCNTs would decrease. For instance, for nanosystems with λ_1=10 and 100 in the case of N_y=N_z=500, the NRBT could overestimate the results of the NHOBT with relative error lower than 17 and 0.5 percent, respectively.

5.6. Influence of the intertube distance of DWCNTs on frequencies

The dependency of the transverse frequency of the nanosystem to the intertube distance is one of the major factors that could be paid attention to in their structural mechanics design. In Fig. 6, the plots of the fundamental frequency as a function of the normalized intertube distance have been provided for three levels of the population of the nanosystem (i.e., N_y=N_z=5, 8, and 28). The demonstrated results indicate that with the increase in the distance between the nanotubes, the fundamental frequency initially decreases sharply. For example, in a group of DWCNTs with N_y=N_z=5, the fundamental frequency would reduce from 1.1 THz to 0.15 THz (minimum value), and in a group with N_y=N_z=8, the reduction of fundamental frequency from 0.85 THz to 0.5 THz(minimum value) is observed. These changes reflect further influence of the intertube distance on the results of the low-population nanosystems. By increasing the intertube distance, contrary to the previous branch of the frequency variation, the incremental process is followed by the normalized distance of 4 and then remains almost constant. That means for $d_N > 4$, transverse vibrations of each DWCNTs are independent from its neighboring ones. The reason for such a mechanical behavior of the nanosystem is chiefly attributed to the variation of the coefficients of vdW forces, which initially decreases to a certain distance, and then, it will take an ascending trend. A close comparison of the obtained results shows that the relative difference between the proposed models reaches its maximum value when the frequency of the nanosystem is the minimum. This issue is more apparent for nanosystems with lower numbers of DWCNTs.

For example, in the case of N_y=N_z=5, the NRBT could predict the results of the NHOBT with the relative error lower about 44% while in the case of N_y=N_z=28, the aforementioned relative error reaches 5%.

6. Concluding remarks

Due to the importance of vibration of clusters made from carbon nanotubes, herein, free vibrations of elastically confined forests of vertically aligned DWCNTs with three-dimensional configuration were investigated using nonlocal beam models. The crucially obtained results of this research are as follows:

1. The vibrating frequency of the nanosystem when all the exterior DWCNTs have been restrained is more than that of the case whose cornered nanotubes have been restrained. Such a fact is much less pronounced in nanosystems with a high slenderness ratio. Also, with the increase in the number of DWCNTs, the difference between the fundamental frequencies in these two boundary conditions decreases.

2. The fundamental frequency of the nanosystem decreases with the increase of the small-scale factor. The effect of this parameter on vibrational behavior of nanosystems with a lower slenderness ratio is greater. In general, the reduction of the fundamental frequency is attributed to the reduction of the lateral stiffness to the mass ratio.

3. The increase in the slenderness ratio initially leads to the reduction of the fundamental frequency, but in high slender nanosystems, it yields growing of the fundamental frequency, which is more pronounced for nanosystems with a low population. Furthermore, as the slenderness ratio becomes greater than 30, the shear deformation of the higher-order beam-based model would reduce; as a result, the results of the two suggested models approach each other.

4. With increasing the number of DWCNTs, the fundamental frequency decreases. This reduction for nanosystems whose all the exterior tubes are tied represents a higher rate than the case when only the cornered nanotubes are kept fixed.

5. Using continuous models, it is easy to analyze the free vibrations of nanosystems with an arbitrary number of DWCNTs, although discrete models require high computational efforts.

6. With increasing the rigidity of the surrounding elastic matrix (i.e., increasing the rotational and transverse stiffness of the attached springs), the fundamental frequencies increase. In addition, the relative difference in the results of the NRBT with the results of the NHOBT increases with the growing the rotational stiffness of the adjacent environment. The increase in the population of DWCNTs also leads to a decrease in the rate of change of the fundamental frequency with respect to the increase in the adjacent environment stiffness.

7. An increasing the intertube distance of the DWCNTs initially leads to reduce the fundamental frequency of the nanosystem. Similarly, with an increasing distance, the use of a nanosystem with a lower population causes a further decrease of the frequency. As the distance increases further, the frequency increases up to a certain distance, and at greater intertube distances, the frequency change becomes very low and fairly remains constant.

The suggested nonlocal models in this work could be appropriately extended to vibrational analysis of layer-by-layer assembly of vertically aligned multi-walled carbon nanotubes (MWCNTs) with some effort. Additionally, by realizing the dynamical interactional effects of doubly orthogonal DWCNTs, this work would be regarded as a good basis for examining vibrations of orthogonal layers consist of vertically aligned DWCNTs or even MWCNTs. The work on these scientific gaps should be paid attention to by investigators who are exploring the mechanical behaviors of ensembles of CNTs. Surely, by increasing our knowledge on various mechanical aspects of such tiny nanosystems (i.e., their statics, buckling, post-buckling, flexural and shear effects), we could then proceed in their optimal design under externally applied loads.

Appendix A. Introducing the coefficients of the vdW forces

Using Lennard-Jones potential function, the coefficients of the vdW forces between constitutive elastically deformable tubes of the doubly parallel DWCNTs system shown in Fig. A1 are calculated as follows:

$$C_{v\perp_{(j,i)}} = \frac{-256\varepsilon r_{m_j} r_{m_i}}{9a^4 l_b} \int_0^{l_b}\int_0^{l_b}\int_0^{2\pi}\int_0^{2\pi} \left\{ \begin{array}{l} \sigma^{12}\left[\chi^{-7} - 14\chi^{-8}\begin{pmatrix} r_{m_j}\cos(\varphi_j) - \\ r_{m_i}\cos(\varphi_i) \end{pmatrix}^2\right] \\ -\frac{\sigma^6}{2}\left[\chi^{-4} - 8\chi^{-5}\begin{pmatrix} r_{m_j}\cos(\varphi_j) - \\ r_{m_i}\cos(\varphi_i) \end{pmatrix}^2\right] \end{array} \right\} \tag{A.1}$$

$$\times \mathrm{d}\varphi_j \mathrm{d}\varphi_i \mathrm{d}x_j \mathrm{d}x_i,$$

$$C_{v\|_{(j,i)}} = \frac{-256\varepsilon r_{m_j} r_{m_i}}{9a^4 l_b} \int_0^{l_b}\int_0^{l_b}\int_0^{2\pi}\int_0^{2\pi} \left\{ \begin{array}{l} \sigma^{12}\left[\chi^{-7} - 14\chi^{-8}\begin{pmatrix} r_{m_j}\sin(\varphi_j) - \\ r_{m_i}\sin(\varphi_i) + d \end{pmatrix}^2\right] \\ -\frac{\sigma^6}{2}\left[\chi^{-4} - 8\chi^{-5}\begin{pmatrix} r_{m_j}\sin(\varphi_j) - \\ r_{m_i}\sin(\varphi_i) \\ +d(1-\delta_{j2}-\delta_{i3}) \end{pmatrix}^2\right] \end{array} \right\} \tag{A.2}$$

$$\times \mathrm{d}\varphi_j \mathrm{d}\varphi_i \mathrm{d}x_j \mathrm{d}x_i,$$

where

$$\begin{aligned} \chi\left(x_j, x_i, \varphi_j, \varphi_i; r_{m_j}, r_{m_i}, d\right) = \; & (x_j - x_i)^2 + \left(r_{m_j}\cos(\varphi_j) - r_{m_i}\cos(\varphi_i)\right)^2 + \\ & \left(r_{m_j}\sin(\varphi_j) - r_{m_i}\sin(\varphi_i) + d(1-\delta_{j2}-\delta_{i3})\right)^2, \end{aligned} \tag{A.3}$$

in which $(j,i) = (3,1), (3,2), (4,1), (4,2), (2,1), (4,3)$, $0 \le x_i, x_j \le l_b$, $0 \le \varphi_i, \varphi_j \le 2\pi$, $C_{d\perp_{(j,i)}} = C_{v\perp_{(j,i)}}\left(\sqrt{2}d, l_b, r_{m_j}, r_{m_i}\right)$, $C_{d\|_{(j,i)}} = C_{v\|_{(j,i)}}\left(\sqrt{2}d, l_b, r_{m_j}, r_{m_i}\right)$, r_{m_i} and r_{m_j} are the mean radii of the constitutive tubes of DWCNTs, a is the length of the C-C bond, ϵ is the potential well's depth, and σ is the distance corresponds to the zero potential function.

Appendix B. Nonlocal equations of motion on the basis of the discrete-based-NRBT

$$
\begin{aligned}
&\varrho_3^{2i-2}\frac{\partial^4\overline{V}^R_{mni}}{\partial\xi^4}+\Xi\Bigg\{\varrho_1^{2i-2}\frac{\partial^2\overline{V}^R_{mni}}{\partial\tau^2}-\frac{\varrho_2^{2i-2}}{\lambda_1^2}\frac{\partial^4\overline{V}^R_{mni}}{\partial\tau^2\partial\xi^2}+\overline{C}^R_{v\|_{(i+2,i)}}\Big[\Big(\overline{V}^R_{mni}-\overline{V}^R_{(m+1)ni}\Big)\left(1-\delta_{mN_y}\right)+\\
&\Big(\overline{V}^R_{mni}-\overline{V}^R_{(m-1)ni}\Big)\left(1-\delta_{1m}\right)\Big]+\overline{C}^R_{v\|_{(i,3-i)}}\Big(\overline{V}^R_{mni}-\overline{V}^R_{mn(3-i)}\Big)+\overline{C}^R_{v\|_{(i+1,4-i)}}\Big[\Big(\overline{V}^R_{mni}-\overline{V}^R_{(m+1)n(3-i)}\Big)\\
&\left(1-\delta_{mN_y}\right)+\Big(\overline{V}^R_{mni}-\overline{V}^R_{(m-1)n(3-i)}\Big)\left(1-\delta_{1m}\right)\Big]+\overline{C}^R_{v\perp_{(i+2,i)}}\Big[\Big(\overline{V}^R_{mni}-\overline{V}^R_{m(n-1)i}\Big)\left(1-\delta_{1n}\right)\\
&+\Big(\overline{V}^R_{mni}-\overline{V}^R_{m(n+1)i}\Big)\left(1-\delta_{nN_z}\right)\Big]+\overline{C}^R_{v\perp_{(i,3-i)}}\Big(\overline{V}^R_{mni}-\overline{V}^R_{mn(3-i)}\Big)+\overline{C}^R_{v\perp_{(i+1,4-i)}}\Big[\Big(\overline{V}^R_{mni}-\overline{V}^R_{m(n-1)(3-i)}\Big)\\
&\times\left(1-\delta_{1n}\right)+\Big(\overline{V}^R_{mni}-\overline{V}^R_{m(n+1)(3-i)}\Big)\left(1-\delta_{nN_z}\right)\Big]+0.5\overline{C}^R_{d\|_{(i+2,i)}}\Big(\overline{W}^R_{mni}+\overline{V}^R_{mni}-\overline{W}^R_{(m-1)(n-1)i}-\overline{V}^R_{(m-1)(n-1)i}\Big)\\
&\times\left(1-\delta_{1n}\right)\left(1-\delta_{1m}\right)+0.5\overline{C}^R_{d\|_{(i,3-i)}}\Big(\overline{W}^R_{mni}+\overline{V}^R_{mni}-\overline{W}^R_{mn(3-i)}-\overline{V}^R_{mn(3-i)}\Big)+0.5\overline{C}^R_{d_{\|(i+1,4-i)}}\\
&\times\Big(\overline{W}^R_{mni}+\overline{V}^R_{mni}-\overline{W}^R_{(m-1)(n-1)(3-i)}-\overline{V}^R_{(m-1)(n-1)(3-i)}\Big)\left(1-\delta_{1m}\right)\left(1-\delta_{1n}\right)+0.5\overline{C}^R_{d\|_{(i+2,i)}}\\
&\Big(\overline{W}^R_{mni}+\overline{V}^R_{mni}-\overline{W}^R_{(m+1)(n+1)i}-\overline{V}^R_{(m+1)(n+1)i}\Big)\left(1-\delta_{nN_z}\right)\left(1-\delta_{mN_y}\right)+0.5\overline{C}^R_{d_{\|(i+1,4-i)}}\\
&\Big(\overline{W}^R_{mni}+\overline{V}^R_{mni}-\overline{W}^R_{(m+1)(n+1)(3-i)}-\overline{V}^R_{(m+1)(n+1)(3-i)}\Big)\left(1-\delta_{nN_z}\right)\left(1-\delta_{mN_y}\right)+0.5\overline{C}^R_{d\|_{(i+2,i)}}\\
&\Big(\overline{V}^R_{mni}-\overline{W}^R_{mni}-\overline{V}^R_{(m+1)(n-1)i}+\overline{W}^R_{(m+1)(n-1)i}\Big)\left(1-\delta_{1n}\right)\left(1-\delta_{mN_y}\right)+0.5\overline{C}^R_{d\|_{(i,3-i)}}\\
&\Big(\overline{V}^R_{mni}-\overline{W}^R_{mni}-\overline{V}^R_{mn(3-i)}+\overline{W}^R_{mn(3-i)}\Big)+0.5\overline{C}^R_{d_{\|(i+1,4-i)}}\Big(\overline{V}^R_{mni}-\overline{W}^R_{mni}-\overline{V}^R_{(m+1)(n-1)(3-i)}+\\
&\overline{W}^R_{(m+1)(n-1)(3-i)}\Big)\left(1-\delta_{1n}\right)\left(1-\delta_{mN_y}\right)+0.5\overline{C}^R_{d\|_{(i+2,i)}}\Big(\overline{V}^R_{mni}-\overline{W}^R_{mni}-\overline{V}^R_{(m-1)(n+1)i}+\overline{W}^R_{(m-1)(n+1)i}\Big)\\
&\left(1-\delta_{nN_z}\right)\left(1-\delta_{1m}\right)+0.5\overline{C}^R_{d_{\|(i+1,4-i)}}\Big(\overline{V}^R_{mni}-\overline{W}^R_{mni}-\overline{V}^R_{(m-1)(n+1)(3-i)}+\overline{W}^R_{(m-1)(n+1)(3-i)}\Big)\left(1-\delta_{nN_z}\right)\left(1-\delta_{1m}\right)\\
&+0.5\overline{C}^R_{d\perp_{(i+2,i)}}\Big(\overline{V}^R_{mni}-\overline{W}^R_{mni}+\overline{W}^R_{(m-1)(n-1)i}-\overline{V}^R_{(m-1)(n-1)i}\Big)\left(1-\delta_{1n}\right)\left(1-\delta_{1m}\right)+0.5\overline{C}^R_{d\perp_{(i,3-i)}}\\
&\times\Big(\overline{V}^R_{mni}-\overline{W}^R_{mni}+\overline{W}^R_{mn(3-i)}-\overline{V}^R_{mn(3-i)}\Big)+0.5\overline{C}^R_{d\perp_{(i+1,4-i)}}\Big(\overline{V}^R_{mni}-\overline{W}^R_{mni}+\overline{W}^R_{(m-1)(n-1)(3-i)}-\\
&\overline{V}^R_{(m-1)(n-1)(3-i)}\Big)\left(1-\delta_{1n}\right)\left(1-\delta_{1m}\right)+0.5\overline{C}^R_{d\perp_{(i+2,i)}}\Big(\overline{V}^R_{mni}-\overline{W}^R_{mni}+\overline{W}^R_{(m+1)(n+1)i}-\overline{V}^R_{(m+1)(n+1)i}\Big)\\
&\times\left(1-\delta_{nN_z}\right)\left(1-\delta_{mN_y}\right)+0.5\overline{C}^R_{d\perp_{(i+1,4-i)}}\Big(\overline{V}^R_{mni}-\overline{W}^R_{mni}+\overline{W}^R_{(m+1)(n+1)(3-i)}-\overline{V}^R_{(m+1)(n+1)(3-i)}\Big)\\
&\times\left(1-\delta_{nN_z}\right)\left(1-\delta_{mN_y}\right)+0.5\overline{C}^R_{d\perp_{(i+2,i)}}\Big(\overline{V}^R_{mni}+\overline{W}^R_{mni}-\overline{V}^R_{(m-1)(n+1)i}-\overline{W}^R_{(m-1)(n+1)i}\Big)\left(1-\delta_{nN_z}\right)\left(1-\delta_{1m}\right)\\
&+0.5\overline{C}^R_{d\perp_{(i,3-i)}}\Big(\overline{V}^R_{mni}+\overline{W}^R_{mni}-\overline{V}^R_{mn(3-i)}-\overline{W}^R_{mn(3-i)}\Big)+0.5\overline{C}^R_{d\perp_{(i+1,4-i)}}\Big(\overline{V}^R_{mni}+\overline{W}^R_{mni}-\overline{V}^R_{(m-1)(n+1)(3-i)}-\\
&\overline{W}^R_{(m-1)(n+1)(3-i)}\Big)\left(1-\delta_{nN_z}\right)\left(1-\delta_{1m}\right)+0.5\overline{C}^R_{d\perp_{(i+2,i)}}\Big(\overline{V}^R_{mni}+\overline{W}^R_{mni}-\overline{V}^R_{(m+1)(n-1)i}-\overline{W}^R_{(m+1)(n-1)i}\Big)\\
&\times\left(1-\delta_{1n}\right)\left(1-\delta_{mN_y}\right)+0.5\overline{C}^R_{d\perp_{(i+1,4-i)}}\Big(\overline{V}^R_{mni}+\overline{W}^R_{mni}-\overline{V}^R_{(m+1)(n-1)(3-i)}-\overline{W}^R_{(m+1)(n-1)(3-i)}\Big)\left(1-\delta_{1m}\right)\left(1-\delta_{mN_y}\right)\\
&+\left(\overline{K}^R_t\overline{V}^R_{mni}-\overline{K}^R_r\frac{\partial^2\overline{V}^R_{mni}}{\partial\xi^2}\right)\begin{pmatrix}\delta_{1n}+\delta_{1m}+\delta_{nN_z}+\delta_{mN_y}\\ -\delta_{1m}\delta_{1n}-\delta_{1m}\delta_{nN_z}-\delta_{1n}\delta_{mN_y}-\delta_{nN_z}\delta_{mN_y}\end{pmatrix}\left(1-\delta_{1i}\right)\Bigg\}=0,
\end{aligned}
\tag{B.1}
$$

$$
\begin{aligned}
&\varrho_3^{2i-2}\frac{\partial^4\overline{W}^R_{mni}}{\partial\xi^4}+\Xi\left\{\varrho_1^{2i-2}\frac{\partial^2\overline{W}^R_{mni}}{\partial\tau^2}-\frac{\varrho_2^{2i-2}}{\lambda_1^2}\frac{\partial^4\overline{W}^R_{mni}}{\partial\tau^2\partial\xi^2}+\overline{C}^R_{v\|_{(i+2,i)}}\left[\left(\overline{W}^R_{mni}-\overline{W}^R_{m(n+1)i}\right)(1-\delta_{nN_z})\right.\right.\\
&+\left.\left(\overline{W}^R_{mni}-\overline{W}^R_{m(n-1)i}\right)(1-\delta_{1n})\right]+\overline{C}^R_{v\|_{(i,3-i)}}\left(\overline{W}^R_{mni}-\overline{W}^R_{mn(3-i)}\right)+\overline{C}^R_{v\|_{(i+1,4-i)}}\left[\left(\overline{W}^R_{mni}-\overline{W}^R_{m(n+1)(3-i)}\right)\right.\\
&\left.(1-\delta_{nN_z})+\left(\overline{W}^R_{mni}-\overline{W}^R_{m(n-1)(3-i)}\right)(1-\delta_{1n})\right]+\overline{C}^R_{v\perp_{(i+2,i)i}}\left[\left(\overline{W}^R_{mni}-\overline{W}^R_{(m-1)ni}\right)(1-\delta_{1m})\right.\\
&+\left.\left(\overline{W}^R_{mni}-\overline{W}^R_{(m+1)ni}\right)\left(1-\delta_{mN_y}\right)\right]+\overline{C}^R_{v\perp_{(i,3-i)}}\left(\overline{W}^R_{mni}-\overline{W}^R_{mn(3-i)}\right)+\overline{C}^R_{v\perp_{(i+1,4-i)}}\left[\left(\overline{W}^R_{mni}-\overline{W}^R_{(m-1)n(3-i)}\right)\right.\\
&\times(1-\delta_{1m})+\left.\left(\overline{W}^R_{mni}-\overline{W}^R_{(m+1)n(3-i)}\right)\left(1-\delta_{mN_y}\right)\right]+0.5\overline{C}^R_{d\|_{(i+2,i)}}\left(\overline{W}^R_{mni}+\overline{V}^R_{mni}-\overline{W}^R_{(m-1)(n-1)i}-\overline{V}^R_{(m-1)(n-1)i}\right)\\
&\times(1-\delta_{1n})(1-\delta_{1m})+0.5\overline{C}^R_{d\|_{(i,3-i)}}\left(\overline{W}^R_{mni}+\overline{V}^R_{mni}-\overline{W}^R_{mn(3-i)}-\overline{V}^R_{mn(3-i)}\right)\\
&+0.5\overline{C}^R_{d\|_{(i+1,4-i)}}\left(\overline{W}^R_{mni}+\overline{V}^R_{mni}-\overline{W}^R_{(m-1)(n-1)(3-i)}-\overline{V}^R_{(m-1)(n-1)(3-i)}\right)(1-\delta_{1m})(1-\delta_{1n})\\
&+0.5\overline{C}^R_{d\|_{(i+2,i)}}\left(\overline{W}^R_{mni}+\overline{V}^R_{mni}-\overline{W}^R_{(m+1)(n+1)i}-\overline{V}^R_{(m+1)(n+1)i}\right)(1-\delta_{nN_z})\left(1-\delta_{mN_y}\right)\\
&+0.5\overline{C}^R_{d\|_{(i+1,4-i)}}\left(\overline{W}^R_{mni}+\overline{V}^R_{mni}-\overline{W}^R_{(m+1)(n+1)(3-i)}-\overline{V}^R_{(m+1)(n+1)(3-i)}\right)(1-\delta_{nN_z})\left(1-\delta_{mN_y}\right)\\
&+0.5\overline{C}^R_{d\|_{(i+2,i)}}\left(\overline{W}^R_{mni}-\overline{V}^R_{mni}-\overline{W}^R_{(m-1)(n+1)i}+\overline{V}^R_{(m-1)(n+1)i}\right)(1-\delta_{1m})(1-\delta_{nN_z})\\
&+0.5\overline{C}^R_{d\|_{(i,3-i)}}\left(\overline{W}^R_{mni}-\overline{V}^R_{mni}-\overline{W}^R_{mn(3-i)}+\overline{V}^R_{mn(3-i)}\right)+0.5\overline{C}^R_{d\|_{(i+1,4-i)}}\left(\overline{W}^R_{mni}-\overline{V}^R_{mni}-\overline{W}^R_{(m-1)(n+1)(3-i)}+\right.\\
&\left.\overline{V}^R_{(m-1)(n+1)(3-i)}\right)(1-\delta_{1m})(1-\delta_{nN_z})+0.5\overline{C}^R_{d\|_{(i+2,i)}}\left(\overline{W}^R_{mni}-\overline{V}^R_{mni}-\overline{W}^R_{(m+1)(n-1)i}+\overline{V}^R_{(m+1)(n-1)i}\right)\left(1-\delta_{mN_y}\right)\\
&\times(1-\delta_{1n})+0.5\overline{C}^R_{d\|_{(i+1,4-i)}}\left(\overline{W}^R_{mni}-\overline{V}^R_{mni}-\overline{W}^R_{(m+1)(n-1)(3-i)}+\overline{V}^R_{(m+1)(n-1)(3-i)}\right)\left(1-\delta_{mN_y}\right)(1-\delta_{1n})\\
&+0.5\overline{C}^R_{d\perp_{(i+2,i)}}\left(\overline{W}^R_{mni}-\overline{V}^R_{mni}-\overline{W}^R_{(m-1)(n-1)i}+\overline{V}^R_{(m-1)(n-1)i}\right)(1-\delta_{1n})(1-\delta_{1m})+0.5\overline{C}^R_{d\perp_{(i,3-i)}}\\
&\times\left(\overline{W}^R_{mni}-\overline{V}^R_{mni}-\overline{W}^R_{mn(3-i)}+\overline{V}^R_{mn(3-i)}\right)+0.5\overline{C}^R_{d\perp_{(i+1,4-i)}}\left(\overline{W}^R_{mni}-\overline{V}^R_{mni}-\overline{W}^R_{(m-1)(n-1)(3-i)}\right.\\
&\left.+\overline{V}^R_{(m-1)(n-1)(3-i)}\right)(1-\delta_{1m})(1-\delta_{1n})+0.5\overline{C}^R_{d\perp_{(i+2,i)}}\left(\overline{W}^R_{mni}-\overline{V}^R_{mni}-\overline{W}^R_{(m+1)(n+1)i}+\overline{V}^R_{(m+1)(n+1)i}\right)\\
&\times(1-\delta_{nN_z})\left(1-\delta_{mN_y}\right)+0.5\overline{C}^R_{d\perp_{(i+1,4-i)}}\left(\overline{W}^R_{mni}-\overline{V}^R_{mni}-\overline{W}^R_{(m+1)(n+1)(3-i)}+\overline{V}^R_{(m+1)(n+1)(3-i)}\right)(1-\delta_{nN_z})\\
&\times\left(1-\delta_{mN_y}\right)+0.5\overline{C}^R_{d\perp_{(i+2,i)}}\left(\overline{W}^R_{mni}+\overline{V}^R_{mni}-\overline{W}^R_{(m-1)(n+1)i}-\overline{V}^R_{(m-1)(n+1)i}\right)(1-\delta_{1m})(1-\delta_{nN_z})\\
&+0.5\overline{C}^R_{d\perp_{(i,3-i)}}\left(\overline{W}^R_{mni}+\overline{V}^R_{mni}-\overline{W}^R_{mn(3-i)}-\overline{V}^R_{mn(3-i)}\right)+0.5\overline{C}^R_{d\perp_{(i+1,4-i)}}\left(\overline{W}^R_{mni}+\overline{V}^R_{mni}-\overline{W}^R_{(m-1)(n+1)(3-i)}-\right.\\
&\left.\overline{V}^R_{(m-1)(n+1)(3-i)}\right)(1-\delta_{1m})(1-\delta_{nN_z})+0.5\overline{C}^R_{d\perp_{(i+2,i)}}\left(\overline{W}^R_{mni}+\overline{V}^R_{mni}-\overline{W}^R_{(m+1)(n-1)i}-\overline{V}^R_{(m+1)(n-1)i}\right)\\
&\times\left(1-\delta_{mN_y}\right)(1-\delta_{1n})+0.5\overline{C}^R_{d\perp_{(i+1,4-i)}}\left(\overline{W}^R_{mni}+\overline{V}^R_{mni}-\overline{W}^R_{(m+1)(n-1)(3-i)}-\overline{V}^R_{(m+1)(n-1)(3-i)}\right)\\
&\left.\times\left(1-\delta_{mN_y}\right)(1-\delta_{1n})+\left(\overline{K}^R_t\overline{W}^R_{mni}-\overline{K}^R_r\frac{\partial^2\overline{W}^R_{mni}}{\partial\xi^2}\right)\begin{pmatrix}\delta_{1n}+\delta_{1m}+\delta_{nN_z}+\delta_{mN_y}-\delta_{1m}\delta_{1n}-\\ \delta_{1m}\delta_{nN_z}-\delta_{1n}\delta_{mN_y}-\delta_{nN_z}\delta_{mN_y}\end{pmatrix}(1-\delta_{1i})\right\}=0,
\end{aligned}
\tag{B.2}
$$

where $\Xi[.]=[.]-\mu^2\dfrac{\partial^2[.]}{\partial\xi^2}$.

Appendix C. Nonlocal equations of motion on the basis of the discrete-based-NHOBT

$$\Xi\left\{\begin{array}{l}\vartheta_7^{2i-2}\frac{\partial^2\overline{\Psi}^H_{z_{mni}}}{\partial\tau^2}-\vartheta_2^{2i-2}\gamma_6^2\frac{\partial^3\overline{V}^H_{mni}}{\partial\tau^2\partial\xi}+\overline{K}^H_r\overline{\Psi}^H_{z_{mni}}\left(1-\delta_{1i}\right)\times\\ \left(\begin{array}{l}\delta_{1n}+\delta_{1m}+\delta_{nN_z}+\delta_{mN_y}-\delta_{1m}\delta_{1n}\\ -\delta_{1m}\delta_{nN_z}-\delta_{1n}\delta_{mN_y}-\delta_{nN_z}\delta_{mN_y}\end{array}\right)\end{array}\right\}$$
$$+\vartheta_4^{2i-2}\gamma_7^2\left(\overline{\Psi}^H_{z_{mni}}+\frac{\partial\overline{V}^H_{mni}}{\partial\xi}\right)-\vartheta_8^{2i-2}\gamma_8^2\frac{\partial^2\overline{\Psi}^H_{z_{mni}}}{\partial\xi^2}+\vartheta_5^{2i-2}\gamma_9^2\frac{\partial^3\overline{V}^H_{mni}}{\partial\xi^3}=0, \tag{C.1}$$

$$-\vartheta_4^{2i-2}\gamma_3^2\left(\frac{\partial\overline{\Psi}^H_{z_{mni}}}{\partial\varrho}+\frac{\partial^2\overline{V}^H_{mni}}{\partial\varrho^2}\right)-\vartheta_5^{2i-2}\gamma_4^2\frac{\partial^3\overline{\Psi}^H_{z_{mni}}}{\partial\xi^3}+\vartheta_6^{2i-2}\frac{\partial^4\overline{V}^H_{mni}}{\partial\xi^4}+\Xi\{\vartheta_1^{2i-2}\frac{\partial^2\overline{V}^H_{mni}}{\partial\tau^2}+\vartheta_2^{2i-2}\gamma_1^2\frac{\partial^3\overline{\Psi}^H_{z_{mni}}}{\partial\tau^2\partial\xi}-$$
$$\vartheta_3^{2i-2}\gamma_2^2\frac{\partial^4\overline{V}^H_{mni}}{\partial\tau^2\partial\xi^2}+\overline{C}^H_{v\|_{(i+2,i)}}$$
$$\times\left[\left(\overline{V}^H_{mni}-\overline{V}^H_{(m+1)ni}\right)\left(1-\delta_{mN_y}\right)+\left(\overline{V}^H_{mni}-\overline{V}^H_{(m-1)ni}\right)\left(1-\delta_{1m}\right)\right]+\overline{C}^H_{v\|_{(i,3-i)}}\left(\overline{V}^H_{mni}-\overline{V}^H_{mn(3-i)}\right)+$$
$$\overline{C}^H_{v\|_{(i+1,4-i)}}\left[\left(\overline{V}^H_{mni}-\overline{V}^H_{(m+1)n(3-i)}\right)\left(1-\delta_{mN_y}\right)+\left(\overline{V}^H_{mni}-\overline{V}^H_{(m-1)n(3-i)}\right)\left(1-\delta_{1m}\right)\right]+$$
$$\overline{C}^H_{v\perp_{(i+2,i)}}\left[\left(\overline{V}^H_{mni}-\overline{V}^H_{m(n-1)i}\right)\left(1-\delta_{1n}\right)+\left(\overline{V}^H_{mni}-\overline{V}^H_{m(n+1)i}\right)\left(1-\delta_{nN_z}\right)\right]+$$
$$\overline{C}^H_{v\perp_{(i,3-i)}}\left(\overline{V}^H_{mni}-\overline{V}^H_{mn(3-i)}\right)+$$
$$\overline{C}^H_{v\perp_{(i+1,4-i)}}\left[\left(\overline{V}^H_{mni}-\overline{V}^H_{m(n-1)(3-i)}\right)\left(1-\delta_{1n}\right)+\left(\overline{V}^H_{mni}-\overline{V}^H_{m(n+1)(3-i)}\right)\left(1-\delta_{nN_z}\right)\right]+$$
$$0.5\overline{C}^H_{d\|_{(i+2,i)}}\left(\overline{W}^H_{mni}+\overline{V}^H_{mni}-\overline{W}^H_{(m-1)(n-1)i}-\overline{V}^H_{(m-1)(n-1)i}\right)\left(1-\delta_{1n}\right)\left(1-\delta_{1m}\right)+$$
$$0.5\overline{C}^H_{d\|_{(i,3-i)}}\left(\overline{W}^H_{mni}+\overline{V}^H_{mni}-\overline{W}^H_{mn(3-i)}-\overline{V}^H_{mn(3-i)}\right)+$$
$$0.5\overline{C}^H_{d\|_{(i+1,4-i)}}\left(\overline{W}^H_{mni}+\overline{V}^H_{mni}-\overline{W}^H_{(m-1)(n-1)(3-i)}-\overline{V}^H_{(m-1)(n-1)(3-i)}\right)\left(1-\delta_{1m}\right)\left(1-\delta_{1n}\right)+$$
$$0.5\overline{C}^H_{d\|_{(i+2,i)}}\left(\overline{W}^H_{mni}+\overline{V}^H_{mni}-\overline{W}^H_{(m+1)(n+1)i}-\overline{V}^H_{(m+1)(n+1)i}\right)\left(1-\delta_{nN_z}\right)\left(1-\delta_{mN_y}\right)+$$
$$0.5\overline{C}^H_{d\|_{(i+1,4-i)}}\left(\overline{W}^H_{mni}+\overline{V}^H_{mni}-\overline{W}^H_{(m+1)(n+1)(3-i)}-\overline{V}^H_{(m+1)(n+1)(3-i)}\right)\left(1-\delta_{nN_z}\right)\left(1-\delta_{mN_y}\right)+$$
$$0.5\overline{C}^H_{d\|_{(i+2,i)}}\left(\overline{V}^H_{mni}-\overline{W}^H_{mni}-\overline{V}^H_{(m+1)(n-1)i}+\overline{W}^H_{(m+1)(n-1)i}\right)\left(1-\delta_{1n}\right)\left(1-\delta_{mN_y}\right)+$$
$$0.5\overline{C}^H_{d\|_{(i,3-i)}}\left(\overline{V}^H_{mni}-\overline{W}^H_{mni}-\overline{V}^H_{mn(3-i)}+\overline{W}^H_{mn(3-i)}\right)+$$
$$0.5\overline{C}^H_{d\|_{(i+1,4-i)}}\left(\overline{V}^H_{mni}-\overline{W}^H_{mni}-\overline{V}^H_{(m+1)(n-1)(3-i)}+\overline{W}^H_{(m+1)(n-1)(3-i)}\right)\left(1-\delta_{1n}\right)\left(1-\delta_{mN_y}\right)+$$
$$0.5\overline{C}^H_{d\|_{(i+2,i)}}\left(\overline{V}^H_{mni}-\overline{W}^H_{mni}-\overline{V}^H_{(m-1)(n+1)i}+\overline{W}^H_{(m-1)(n+1)i}\right)\left(1-\delta_{nN_z}\right)\left(1-\delta_{1m}\right)+$$
$$0.5\overline{C}^H_{d\|_{(i+1,4-i)}}\left(\overline{V}^H_{mni}-\overline{W}^H_{mni}-\overline{V}^H_{(m-1)(n+1)(3-i)}+\overline{W}^H_{(m-1)(n+1)(3-i)}\right)\left(1-\delta_{nN_z}\right)\left(1-\delta_{1m}\right)+$$
$$0.5\overline{C}^H_{d\perp_{(i+2,i)}}\left(\overline{V}^H_{mni}-\overline{W}^H_{mni}+\overline{W}^H_{(m-1)(n-1)i}-\overline{V}^H_{(m-1)(n-1)i}\right)\left(1-\delta_{1n}\right)\left(1-\delta_{1m}\right)+$$
$$0.5\overline{C}^H_{d\perp_{(i,3-i)}}\left(\overline{V}^H_{mni}-\overline{W}^H_{mni}+\overline{W}^H_{mn(3-i)}-\overline{V}^H_{mn(3-i)}\right)+$$

$$0.5\overline{C}^H_{d\perp_{(i+1,4-i)}}\left(\overline{V}^H_{mni}-\overline{W}^H_{mni}+\overline{W}^H_{(m-1)(n-1)(3-i)}-\overline{V}^H_{(m-1)(n-1)(3-i)}\right)(1-\delta_{1n})(1-\delta_{1m})+$$
$$0.5\overline{C}^H_{d\perp_{(i+2,i)}}\left(\overline{V}^H_{mni}-\overline{W}^H_{mni}+\overline{W}^H_{(m+1)(n+1)i}-\overline{V}^H_{(m+1)(n+1)i}\right)(1-\delta_{nN_z})\left(1-\delta_{mN_y}\right)+$$
$$0.5\overline{C}^H_{d\perp_{(i+1,4-i)}}\left(\overline{V}^H_{mni}-\overline{W}^H_{mni}+\overline{W}^H_{(m+1)(n+1)(3-i)}-\overline{V}^H_{(m+1)(n+1)(3-i)}\right)(1-\delta_{nN_z})\left(1-\delta_{mN_y}\right)+$$
$$0.5\overline{C}^H_{d\perp_{(i+2,i)}}\left(\overline{V}^H_{mni}+\overline{W}^H_{mni}-\overline{V}^H_{(m-1)(n+1)i}-\overline{W}^H_{(m-1)(n+1)i}\right)(1-\delta_{nN_z})(1-\delta_{1m})+$$
$$0.5\overline{C}^H_{d\perp_{(i,3-i)}}\left(\overline{V}^H_{mni}+\overline{W}^H_{mni}-\overline{V}^H_{mn(3-i)}-\overline{W}^H_{mn(3-i)}\right)+$$
$$0.5\overline{C}^H_{d\perp_{(i+1,4-i)}}\left(\overline{V}^H_{mni}+\overline{W}^H_{mni}-\overline{V}^H_{(m-1)(n+1)(3-i)}-\overline{W}^H_{(m-1)(n+1)(3-i)}\right)(1-\delta_{nN_z})(1-\delta_{1m})+$$
$$0.5\overline{C}^H_{d\perp_{(i+2,i)}}\left(\overline{V}^H_{mni}+\overline{W}^H_{mni}-\overline{V}^H_{(m+1)(n-1)i}-\overline{W}^H_{(m+1)(n-1)i}\right)(1-\delta_{1n})\left(1-\delta_{mN_y}\right)+$$
$$0.5\overline{C}^H_{d\perp_{(i+1,4-i)}}\left(\overline{V}^H_{mni}+\overline{W}^H_{mni}-\overline{V}^H_{(m+1)(n-1)(3-i)}-\overline{W}^H_{(m+1)(n-1)(3-i)}\right)(1-\delta_{1m})\left(1-\delta_{mN_y}\right)+$$
$$\overline{K}^H_t\overline{V}^H_{mni}\left(\delta_{1n}+\delta_{1m}+\delta_{nN_z}+\delta_{mN_y}-\delta_{1m}\delta_{1n}-\delta_{1m}\delta_{nN_z}-\delta_{1n}\delta_{mN_y}-\delta_{nN_z}\delta_{mN_y}\right)(1-\delta_{1i})\}=0,$$

(C.2)

$$\Xi\left\{\begin{array}{l}\vartheta_7^{2i-2}\frac{\partial^2\overline{\Psi}^H_{y_{mni}}}{\partial\tau^2}-\vartheta_2^{2i-2}\gamma_6^2\frac{\partial^3\overline{W}^H_{mni}}{\partial\tau^2\partial\xi}+\overline{K}^H_r\overline{\Psi}^H_{y_{mni}}(1-\delta_{1i})\times\\ \left(\begin{array}{l}\delta_{1n}+\delta_{1m}+\delta_{nN_z}+\delta_{mN_y}-\delta_{1m}\delta_{1n}-\delta_{1m}\delta_{nN_z}-\\ \delta_{1n}\delta_{mN_y}-\delta_{nN_z}\delta_{mN_y}\end{array}\right)\end{array}\right\}$$
$$+\vartheta_4^{2i-2}\gamma_7^2\left(\overline{\Psi}^H_{y_{mni}}+\frac{\partial\overline{W}^H_{mni}}{\partial\xi}\right)-\vartheta_8^{2i-2}\gamma_8^2\frac{\partial^2\overline{\Psi}^H_{y_{mni}}}{\partial\xi^2}+\vartheta_5^{2i-2}\gamma_9^2\frac{\partial^3\overline{W}^H_{mni}}{\partial\xi^3}=0,$$

(C.3)

$$-\vartheta_4^{2i-2}\gamma_3^2\left(\frac{\partial\overline{\Psi}^H_{y_{mni}}}{\partial\xi}+\frac{\partial^2\overline{W}^H_{mni}}{\partial\xi^2}\right)-\vartheta_5^{2i-2}\gamma_4^2\frac{\partial^3\overline{\Psi}^H_{y_{mni}}}{\partial\xi^3}+\vartheta_6^{2i-2}\frac{\partial^4\overline{W}^H_{mni}}{\partial\xi^4}+\Xi\{\vartheta_1^{2i-2}\frac{\partial^2\overline{W}^H_{mni}}{\partial\tau^2}+\vartheta_2^{2i-2}\gamma_1^2\frac{\partial^3\overline{\Psi}^H_{y_{mni}}}{\partial\tau^2\partial\xi}-$$
$$\vartheta_3^{2i-2}\gamma_2^2\frac{\partial^4\overline{W}^H_{mni}}{\partial\tau^2\partial\xi^2}+\overline{C}^H_{v\|_{(i+2,i)}}$$
$$\times\left[\left(\overline{W}^H_{mni}-\overline{W}^H_{m(n+1)i}\right)(1-\delta_{nN_z})+\left(\overline{W}^H_{mni}-\overline{W}^H_{m(n-1)i}\right)(1-\delta_{1n})\right]+\overline{C}^H_{v\|_{(i,3-i)}}\left(\overline{W}^H_{mni}-\overline{W}^H_{mn(3-i)}\right)+$$
$$\overline{C}^H_{v\|_{(i+1,4-i)}}\left[\left(\overline{W}^H_{mni}-\overline{W}^H_{m(n+1)(3-i)}\right)(1-\delta_{nN_z})+\left(\overline{W}^H_{mni}-\overline{W}^H_{m(n-1)(3-i)}\right)(1-\delta_{1n})\right]+$$
$$\overline{C}^H_{v\perp_{(i+2,i)}}\left[\left(\overline{W}^H_{mni}-\overline{W}^H_{(m-1)ni}\right)(1-\delta_{1m})+\left(\overline{W}^H_{mni}-\overline{W}^H_{(m+1)ni}\right)\left(1-\delta_{mN_y}\right)\right]+$$
$$\overline{C}^H_{v\perp_{(i,3-i)}}\left(\overline{W}^H_{mni}-\overline{W}^H_{mn(3-i)}\right)+$$
$$\overline{C}^H_{v\perp_{(i+1,4-i)}}\left[\left(\overline{W}^H_{mni}-\overline{W}^H_{(m-1)n(3-i)}\right)(1-\delta_{1m})+\left(\overline{W}^H_{mni}-\overline{W}^H_{(m+1)n(3-i)}\right)\left(1-\delta_{mN_y}\right)\right]+$$
$$0.5\overline{C}^H_{d\|_{(i+2,i)}}\left(\overline{W}^H_{mni}+\overline{V}^H_{mni}-\overline{W}^H_{(m-1)(n-1)i}-\overline{V}^H_{(m-1)(n-1)i}\right)(1-\delta_{1n})(1-\delta_{1m})+$$
$$0.5\overline{C}^H_{d\|_{(i,3-i)}}\left(\overline{W}^H_{mni}+\overline{V}^H_{mni}-\overline{W}^H_{mn(3-i)}-\overline{V}^H_{mn(3-i)}\right)+$$
$$0.5\overline{C}^H_{d\|_{(i+1,4-i)}}\left(\overline{W}^H_{mni}+\overline{V}^H_{mni}-\overline{W}^H_{(m-1)(n-1)(3-i)}-\overline{V}^H_{(m-1)(n-1)(3-i)}\right)(1-\delta_{1m})(1-\delta_{1n})+$$
$$0.5\overline{C}^H_{d\|_{(i+2,i)}}\left(\overline{W}^H_{mni}+\overline{V}^H_{mni}-\overline{W}^H_{(m+1)(n+1)i}-\overline{V}^H_{(m+1)(n+1)i}\right)(1-\delta_{nN_z})\left(1-\delta_{mN_y}\right)+$$

$$
\begin{aligned}
&0.5\overline{C}^H_{d\|_{(i+1,4-i)}}\left(\overline{W}^H_{mni}+\overline{V}^H_{mni}-\overline{W}^H_{(m+1)(n+1)(3-i)}-\overline{V}^H_{(m+1)(n+1)(3-i)}\right)(1-\delta_{nN_z})\left(1-\delta_{mN_y}\right)+\\
&0.5\overline{C}^H_{d\|_{(i+2,i)}}\left(\overline{W}^H_{mni}-\overline{V}^H_{mni}-\overline{W}^H_{(m-1)(n+1)i}+\overline{V}^H_{(m-1)(n+1)i}\right)(1-\delta_{1m})(1-\delta_{nN_z})+\\
&0.5\overline{C}^H_{d\|_{(i,3-i)}}\left(\overline{W}^H_{mni}-\overline{V}^H_{mni}-\overline{W}^H_{mn(3-i)}+\overline{V}^H_{mn(3-i)}\right)+\\
&0.5\overline{C}^H_{d\|_{(i+1,4-i)}}\left(\overline{W}^H_{mni}-\overline{V}^H_{mni}-\overline{W}^H_{(m-1)(n+1)(3-i)}+\overline{V}^H_{(m-1)(n+1)(3-i)}\right)(1-\delta_{1m})(1-\delta_{nN_z})+\\
&0.5\overline{C}^H_{d\|_{(i+2,i)}}\left(\overline{W}^H_{mni}-\overline{V}^H_{mni}-\overline{W}^H_{(m+1)(n-1)i}+\overline{V}^H_{(m+1)(n-1)i}\right)\left(1-\delta_{mN_y}\right)(1-\delta_{1n})+\\
&0.5\overline{C}^H_{d\|_{(i+1,4-i)}}\left(\overline{W}^H_{mni}-\overline{V}^H_{mni}-\overline{W}^H_{(m+1)(n-1)(3-i)}+\overline{V}^H_{(m+1)(n-1)(3-i)}\right)\left(1-\delta_{mN_y}\right)(1-\delta_{1n})+\\
&0.5\overline{C}^H_{d\perp_{(i+2,i)}}\left(\overline{W}^H_{mni}-\overline{V}^H_{mni}-\overline{W}^H_{(m-1)(n-1)i}+\overline{V}^H_{(m-1)(n-1)i}\right)(1-\delta_{1n})(1-\delta_{1m})+\\
&0.5\overline{C}^H_{d\perp_{(i,3-i)}}\left(\overline{W}^H_{mni}-\overline{V}^H_{mni}-\overline{W}^H_{mn(3-i)}+\overline{V}^H_{mn(3-i)}\right)+\\
&0.5\overline{C}^H_{d\perp_{(i+1,4-i)}}\left(\overline{W}^H_{mni}-\overline{V}^H_{mni}-\overline{W}^H_{(m-1)(n-1)(3-i)}+\overline{V}^H_{(m-1)(n-1)(3-i)}\right)(1-\delta_{1m})(1-\delta_{1n})+\\
&0.5\overline{C}^H_{d\perp_{(i+2,i)}}\left(\overline{W}^H_{mni}-\overline{V}^H_{mni}-\overline{W}^H_{(m+1)(n+1)i}+\overline{V}^H_{(m+1)(n+1)i}\right)(1-\delta_{nN_z})\left(1-\delta_{mN_y}\right)+\\
&0.5\overline{C}^H_{d\perp_{(i+1,4-i)}}\left(\overline{W}^H_{mni}-\overline{V}^H_{mni}-\overline{W}^H_{(m+1)(n+1)(3-i)}+\overline{V}^H_{(m+1)(n+1)(3-i)}\right)(1-\delta_{nN_z})\left(1-\delta_{mN_y}\right)+\\
&0.5\overline{C}^H_{d\perp_{(i+2,i)}}\left(\overline{W}^H_{mni}+\overline{V}^H_{mni}-\overline{W}^H_{(m-1)(n+1)i}-\overline{V}^H_{(m-1)(n+1)i}\right)(1-\delta_{1m})(1-\delta_{nN_z})+\\
&0.5\overline{C}^H_{d\perp_{(i,3-i)}}\left(\overline{W}^H_{mni}+\overline{V}^H_{mni}-\overline{W}^H_{mn(3-i)}-\overline{V}^H_{mn(3-i)}\right)+\\
&0.5\overline{C}^H_{d\perp_{(i+1,4-i)}}\left(\overline{W}^H_{mni}+\overline{V}^H_{mni}-\overline{W}^H_{(m-1)(n+1)(3-i)}-\overline{V}^H_{(m-1)(n+1)(3-i)}\right)(1-\delta_{1m})(1-\delta_{nN_z})+\\
&0.5\overline{C}^H_{d\perp_{(i+2,i)}}\left(\overline{W}^H_{mni}+\overline{V}^H_{mni}-\overline{W}^H_{(m+1)(n-1)i}-\overline{V}^H_{(m+1)(n-1)i}\right)\left(1-\delta_{mN_y}\right)(1-\delta_{1n})+\\
&0.5\overline{C}^H_{d\perp_{(i+1,4-i)}}\left(\overline{W}^H_{mni}+\overline{V}^H_{mni}-\overline{W}^H_{(m+1)(n-1)(3-i)}-\overline{V}^H_{(m+1)(n-1)(3-i)}\right)\left(1-\delta_{mN_y}\right)(1-\delta_{1n})+\\
&\overline{K}^H_t\overline{W}^H_{mni}\left(\delta_{1n}+\delta_{1m}+\delta_{nN_z}+\delta_{mN_y}-\delta_{1m}\delta_{1n}-\delta_{1m}\delta_{nN_z}-\delta_{1n}\delta_{mN_y}-\delta_{nN_z}\delta_{mN_y}\right)(1-\delta_{1i})\}=0,
\end{aligned}
\tag{C.4}
$$

Appendix D. Formulations of the continuous model based on the NRBT

Appendix D.1. Nonlocal governing equations

$$
\begin{aligned}
&\varrho_3^{2i-2}\frac{\partial^4\overline{v}_i^R}{\partial\xi^4}+\Xi\Bigg\{\varrho_1^{2i-2}\frac{\partial^2\overline{v}_i^R}{\partial\tau^2}-\frac{\varrho_2^{2i-2}}{\lambda_1^2}\frac{\partial^4\overline{v}_i^R}{\partial\tau^2\partial\xi^2}-\left(k\overline{d}\right)^2\overline{C}^R_{v\parallel_{(i+2,i)}}\Bigg(\frac{\partial^2\overline{v}_i^R}{\partial\eta^2}+\frac{\left(k\overline{d}\right)^2}{12}\frac{\partial^4\overline{v}_i^R}{\partial\eta^4}+\frac{\left(k\overline{d}\right)^4}{360}\frac{\partial^6\overline{v}_i^R}{\partial\eta^6}+\\
&\frac{\left(k\overline{d}\right)^6}{20160}\frac{\partial^8\overline{v}_i^R}{\partial\eta^8}\Bigg)+\overline{C}^R_{v\parallel_{(i,3-i)}}\left(\overline{v}_i^R-\overline{v}_{3-i}^R\right)+\overline{C}^R_{v\parallel_{(i+1,4-i)}}\Bigg(2\left(\overline{v}_i^R-\overline{v}_{3-i}^R\right)-\left(k\overline{d}\right)^2\frac{\partial^2\overline{v}_{3-i}^R}{\partial\eta^2}-\frac{\left(k\overline{d}\right)^4}{12}\frac{\partial^4\overline{v}_{3-i}^R}{\partial\eta^4}\\
&-\frac{\left(k\overline{d}\right)^6}{360}\frac{\partial^6\overline{v}_{3-i}^R}{\partial\eta^6}-\frac{\left(k\overline{d}\right)^8}{20160}\frac{\partial^8\overline{v}_{3-i}^R}{\partial\eta^8}\Bigg)-\overline{C}^R_{v\perp_{(i+2,i)}}\overline{d}^2\Bigg(\frac{\partial^2\overline{v}_i^R}{\partial\gamma^2}+\frac{\overline{d}^2}{12}\frac{\partial^4\overline{v}_i^R}{\partial\gamma^4}+\frac{\overline{d}^4}{360}\frac{\partial^6\overline{v}_i^R}{\partial\gamma^6}+\frac{\overline{d}^6}{20160}\frac{\partial^8\overline{v}_i^R}{\partial\gamma^8}\Bigg)\\
&+\overline{C}^R_{v\perp_{(i,3-i)}}\left(\overline{v}_i^R-\overline{v}_{3-i}^R\right)+\overline{C}^R_{v\perp_{(i+1,4-i)}}\Bigg(2\left(\overline{v}_i^R-\overline{v}_{3-i}^R\right)-\overline{d}^2\frac{\partial^2\overline{v}_{3-i}^R}{\partial\gamma^2}-\frac{\overline{d}^4}{12}\frac{\partial^4\overline{v}_{3-i}^R}{\partial\gamma^4}-\frac{\overline{d}^6}{360}\frac{\partial^6\overline{v}_{3-i}^R}{\partial\gamma^6}\\
&-\frac{\overline{d}^8}{20160}\frac{\partial^8\overline{v}_{3-i}^R}{\partial\gamma^8}\Bigg)-\left(\overline{C}^R_{d\parallel_{(i+2,i)}}+\overline{C}^R_{d\perp_{(i+2,i)}}\right)\overline{d}^2\Bigg[k^2\frac{\partial^2\overline{v}_i^R}{\partial\eta^2}+\frac{\partial^2\overline{v}_i^R}{\partial\gamma^2}+\frac{\overline{d}^2}{12}\left(\frac{\partial^4\overline{v}_i^R}{\partial\gamma^4}+6k^2\frac{\partial^4\overline{v}_i^R}{\partial\gamma^2\partial\eta^2}+k^4\frac{\partial^4\overline{v}_i^R}{\partial\eta^4}\right)\\
&+\frac{\overline{d}^4}{360}\left(\frac{\partial^6\overline{v}_i^R}{\partial\gamma^6}+15k^2\frac{\partial^6\overline{v}_i^R}{\partial\gamma^4\partial\eta^2}+15k^4\frac{\partial^6\overline{v}_i^R}{\partial\gamma^2\partial\eta^4}+k^6\frac{\partial^6\overline{v}_i^R}{\partial\eta^6}\right)\Bigg]+\left(\overline{C}^R_{d\parallel_{(i,3-i)}}+\overline{C}^R_{d\perp_{(i,3-i)}}\right)\left(\overline{v}_i^R-\overline{v}_{3-i}^R\right)\\
&+\left(\overline{C}^R_{d\parallel_{(i+1,4-i)}}+\overline{C}^R_{d\perp_{(i+1,4-i)}}\right)\Bigg[2\left(\overline{v}_i^R-\overline{v}_{3-i}^R\right)+\overline{d}^2\Bigg(-k^2\frac{\partial^2\overline{v}_{3-i}^R}{\partial\eta^2}-\frac{\partial^2\overline{v}_{3-i}^R}{\partial\gamma^2}-\frac{\overline{d}^2}{12}\Bigg(\frac{\partial^4\overline{v}_{3-i}^R}{\partial\gamma^4}+6k^2\frac{\partial^4\overline{v}_{3-i}^R}{\partial\gamma^2\partial\eta^2}\\
&+k^4\frac{\partial^4\overline{v}_{3-i}^R}{\partial\eta^4}\Bigg)-\frac{\overline{d}^4}{360}\Bigg(\frac{\partial^6\overline{v}_{3-i}^R}{\partial\gamma^6}+15k^2\frac{\partial^6\overline{v}_{3-i}^R}{\partial\gamma^4\partial\eta^2}+15k^4\frac{\partial^6\overline{v}_{3-i}^R}{\partial\gamma^2\partial\eta^4}+k^6\frac{\partial^6\overline{v}_{3-i}^R}{\partial\eta^6}\Bigg)\Bigg)\Bigg]-\left(\overline{C}^R_{d\parallel_{(i+2,i)}}-\overline{C}^R_{d\perp_{(i+2,i)}}\right)\times\\
&\overline{d}^2k\Bigg[2\frac{\partial^2\overline{w}_i^R}{\partial\eta\partial\gamma}+\frac{\overline{d}^2}{3}\left(\frac{\partial^4\overline{w}_i^R}{\partial\eta\partial\gamma^3}+k^2\frac{\partial^4\overline{w}_i^R}{\partial\eta^3\partial\gamma}\right)+\frac{\overline{d}^4}{180}\left(3k^4\frac{\partial^6\overline{w}_i^R}{\partial\eta^5\partial\gamma}+10k^2\frac{\partial^6\overline{w}_i^R}{\partial\eta^6\partial\gamma^6}+3\frac{\partial^6\overline{w}_i^R}{\partial\eta\partial\gamma^5}\right)\Bigg]\\
&-\left(\overline{C}^R_{d\parallel_{(i+1,4-i)}}-\overline{C}^R_{d\perp_{(i+1,4-i)}}\right)\overline{d}^2k\Bigg[2\frac{\partial^2\overline{w}_{3-i}^R}{\partial\eta\partial\gamma}+\frac{\overline{d}^2}{3}\left(\frac{\partial^4\overline{w}_{3-i}^R}{\partial\eta\partial\gamma^3}+k^2\frac{\partial^4\overline{w}_{3-i}^R}{\partial\eta^3\partial\gamma}\right)+\frac{\overline{d}^4}{180}\Bigg(3k^4\frac{\partial^6\overline{w}_{3-i}^R}{\partial\eta^5\partial\gamma}\\
&+10k^2\frac{\partial^6\overline{w}_{3-i}^R}{\partial\eta^6\partial\gamma^6}+3\frac{\partial^6\overline{w}_{3-i}^R}{\partial\eta\partial\gamma^5}\Bigg)\Bigg]+\left(\overline{K}_t^R\overline{v}_i^R-\overline{K}_r^R\left(\frac{\partial^2\overline{v}_i^R}{\partial\xi^2}\right)\right)\begin{pmatrix}\delta_{1n}+\delta_{1m}+\delta_{nN_z}+\delta_{mN_y}-\delta_{1m}\delta_{1n}\\-\delta_{1m}\delta_{nN_z}-\delta_{1n}\delta_{mN_y}-\delta_{nN_z}\delta_{mN_y}\end{pmatrix}\left(1-\delta_{1i}\right)\Bigg\}=0,
\end{aligned}
\tag{D.1}
$$

$$\varrho_3^{2i-2}\frac{\partial^4\overline{w}_i^R}{\partial\xi^4}+\Xi\left\{\varrho_1^{2i-2}\frac{\partial^2\overline{w}_i^R}{\partial\tau^2}-\frac{\varrho_2^{2i-2}}{\lambda_1^2}\frac{\partial^4\overline{w}_i^R}{\partial\tau^2\partial\xi^2}-\overline{C}_{v\|_{(i+2,i)}}^R\overline{d}^2\left(\frac{\partial^2\overline{w}_i^R}{\partial\gamma^2}+\frac{\overline{d}^2}{12}\frac{\partial^4\overline{w}_i^R}{\partial\gamma^4}+\frac{\overline{d}^4}{360}\frac{\partial^6\overline{w}_i^R}{\partial\gamma^6}\right.\right.$$
$$\left.+\frac{\overline{d}^6}{20160}\frac{\partial^8\overline{w}_i^R}{\partial\gamma^8}\right)+\overline{C}_{v\|_{i(3-i)}}^R\left(\overline{v}_i^R-\overline{v}_{3-i}^R\right)+\overline{C}_{v\|_{(i+1,4-i)}}^R\left(2\left(\overline{w}_i^R-\overline{w}_{3-i}^R\right)-\overline{d}^2\frac{\partial^2\overline{w}_{3-i}^R}{\partial\gamma^2}-\frac{\overline{d}^4}{12}\frac{\partial^4\overline{w}_{3-i}^R}{\partial\gamma^4}\right.$$
$$\left.-\frac{\overline{d}^6}{360}\frac{\partial^6\overline{w}_{3-i}^R}{\partial\gamma^6}-\frac{\overline{d}^8}{20160}\frac{\partial^8\overline{w}_{3-i}^R}{\partial\gamma^8}\right)-\overline{C}_{v\perp_{(i+2,i)}}^R(k\overline{d})^2\left(\frac{\partial^2\overline{w}_i^R}{\partial\eta^2}+\frac{(k\overline{d})^2}{12}\frac{\partial^4\overline{w}_i^R}{\partial\eta^4}+\frac{(k\overline{d})^4}{360}\frac{\partial^6\overline{w}_i^R}{\partial\eta^6}+\frac{(k\overline{d})^6}{20160}\frac{\partial^8\overline{w}_i^R}{\partial\eta^8}\right)$$
$$+\overline{C}_{v\perp_{(i,3-i)}}^R\left(\overline{w}_i^R-\overline{w}_{3-i}^R\right)+\overline{C}_{v\perp_{(i+1,4-i)}}^R\left(2\left(\overline{w}_i^R-\overline{w}_{3-i}^R\right)-(k\overline{d})^2\frac{\partial^2\overline{w}_{3-i}^R}{\partial\eta^2}-\frac{(k\overline{d})^4}{12}\frac{\partial^4\overline{w}_{3-i}^R}{\partial\eta^4}-\frac{(k\overline{d})^6}{360}\frac{\partial^6\overline{w}_{3-i}^R}{\partial\eta^6}\right.$$
$$\left.-\frac{(k\overline{d})^8}{20160}\frac{\partial^8\overline{w}_{3-i}^R}{\partial\eta^8}\right)-\left(\overline{C}_{d\|_{(i+2,i)}}^R+\overline{C}_{d\perp_{(i+2,i)}}^R\right)\overline{d}^2\left[k^2\frac{\partial^2\overline{w}_i^R}{\partial\eta^2}+\frac{\partial^2\overline{w}_i^R}{\partial\gamma^2}+\frac{\overline{d}^2}{12}\left(\frac{\partial^4\overline{w}_i^R}{\partial\gamma^4}+6k^2\frac{\partial^4\overline{w}_i^R}{\partial\gamma^2\partial\eta^2}+k^4\frac{\partial^4\overline{w}_i^R}{\partial\eta^4}\right)\right.$$
$$\left.+\frac{\overline{d}^4}{360}\left(\frac{\partial^6\overline{w}_i^R}{\partial\gamma^6}+15k^2\frac{\partial^6\overline{w}_i^R}{\partial\gamma^4\partial\eta^2}+15k^4\frac{\partial^6\overline{w}_i^R}{\partial\gamma^2\partial\eta^4}+k^6\frac{\partial^6\overline{w}_i^R}{\partial\eta^6}\right)\right]+\left(\overline{C}_{d\|_{(i,3-i)}}^R+\overline{C}_{d\perp_{(i,3-i)}}^R\right)\left(\overline{w}_i^R-\overline{w}_{3-i}^R\right)$$
$$+\left(\overline{C}_{d\|_{(i+1,4-i)}}^R+\overline{C}_{d\perp_{(i+1,4-i)}}^R\right)\left[2\left(\overline{w}_i^R-\overline{w}_{3-i}^R\right)+\overline{d}^2\left(-k^2\frac{\partial^2\overline{w}_{3-i}^R}{\partial\eta^2}-\frac{\partial^2\overline{w}_{3-i}^R}{\partial\gamma^2}-\frac{\overline{d}^2}{12}\left(\frac{\partial^4\overline{w}_{3-i}^R}{\partial\gamma^4}+6k^2\frac{\partial^4\overline{w}_{3-i}^R}{\partial\gamma^2\partial\eta^2}\right.\right.\right.$$
$$\left.\left.\left.+k^4\frac{\partial^4\overline{w}_{3-i}^R}{\partial\eta^4}\right)-\frac{\overline{d}^4}{360}\left(\frac{\partial^6\overline{w}_{3-i}^R}{\partial\gamma^6}+15k^2\frac{\partial^6\overline{w}_{3-i}^R}{\partial\gamma^4\partial\eta^2}+15k^4\frac{\partial^6\overline{w}_{3-i}^R}{\partial\gamma^2\partial\eta^4}+k^6\frac{\partial^6\overline{w}_{3-i}^R}{\partial\eta^6}\right)\right)\right]-\left(\overline{C}_{d\|_{(i+2,i)}}^R-\overline{C}_{d\perp_{(i+2,i)}}^R\right)\times$$
$$\overline{d}^2k\left[2\frac{\partial^2\overline{v}_i^R}{\partial\eta\partial\gamma}+\frac{\overline{d}^2}{3}\left(\frac{\partial^4\overline{v}_i^R}{\partial\eta\partial\gamma^3}+k^2\frac{\partial^4\overline{v}_i^R}{\partial\eta^3\partial\gamma}\right)+\frac{\overline{d}^4}{180}\left(3k^4\frac{\partial^6\overline{v}_i^R}{\partial\eta^5\partial\gamma}+10k^2\frac{\partial^6\overline{v}_i^R}{\partial\eta^6\partial\gamma^6}+3\frac{\partial^6\overline{v}_i^R}{\partial\eta\partial\gamma^5}\right)\right]$$
$$-\left(\overline{C}_{d\|_{(i+1,4-i)}}^R-\overline{C}_{d\perp_{(i+1,4-i)}}^R\right)\overline{d}^2k\left[2\frac{\partial^2\overline{v}_{3-i}^R}{\partial\eta\partial\gamma}+\frac{\overline{d}^2}{3}\left(\frac{\partial^4\overline{v}_{3-i}^R}{\partial\eta\partial\gamma^3}+k^2\frac{\partial^4\overline{v}_{3-i}^R}{\partial\eta^3\partial\gamma}\right)+\frac{\overline{d}^4}{180}\left(3k^4\frac{\partial^6\overline{v}_{3-i}^R}{\partial\eta^5\partial\gamma}\right.\right.$$
$$\left.\left.\left.+10k^2\frac{\partial^6\overline{v}_{3-i}^R}{\partial\eta^6\partial\gamma^6}+3\frac{\partial^6\overline{v}_{3-i}^R}{\partial\eta\partial\gamma^5}\right)\right]+\left(\overline{K}_t^R\overline{w}_i^R-\overline{K}_r^R\frac{\partial^2\overline{w}_i^R}{\partial\xi^2}\right)\left(\begin{array}{c}\delta_{1n}+\delta_{1m}+\delta_{nN_z}+\delta_{mN_y}-\delta_{1m}\delta_{1n}\\-\delta_{1m}\delta_{nN_z}-\delta_{1n}\delta_{mN_y}-\delta_{nN_z}\delta_{mN_y}\end{array}\right)(1-\delta_{1i})\right\}=0, \tag{D.2}$$

where

$$\eta=\frac{y}{l_y},\ k=\frac{l_z}{l_y},\ \overline{v}_i^R=\frac{v_i^R}{l_b},\ \overline{w}_i^R=\frac{w_i^R}{l_b}. \tag{D.3}$$

Appendix D.2. Nonlocal mass and stiffness matrices

The non-dimensional mass and stiffness matrices associated with the vertically aligned jungles of DWCNTs surrounded by an elastic matrix which is modeled by the continuous-based-NRBT are provided by:

$$\left[\overline{\mathbf{M}}_b^R\right]_{mnpqrs}^{v_iv_i}=\int_0^1\int_0^1\int_0^1\left[\begin{array}{l}\varrho_1^{2i-2}\left(\phi_{mnp}^{v_i}\phi_{qrs}^{v_i}+\mu^2\phi_{mnp,\varrho}^{v_i}\phi_{qrs,\varrho}^{v_i}\right)\\+\varrho_2^{2i-2}\lambda_1^{-2}\left(\phi_{mnp,\xi}^{v_i}\phi_{qrs,\xi}^{v_i}+\mu^2\phi_{mnp,\xi\xi}^{v_i}\phi_{qrs,\xi\xi}^{v_i}\right)\end{array}\right]\mathrm{d}\xi\mathrm{d}\eta\mathrm{d}\gamma, \tag{D.4}$$

$$
\begin{aligned}
&\left[\overline{\mathbf{K}}_b^R\right]_{mnpqrs}^{v_i v_i} = \int_0^1\int_0^1\int_0^1 \Big\{ \varrho_3^{2i-2}\phi_{mnp,\xi\xi}^{v_i}\phi_{qrs,\xi\xi}^{v_i} + \overline{C}_{v\|_{(i+2,i)}}^R \left(\kappa\overline{d}\right)^2 \Big[\phi_{mnp,\eta}^{v_i}\phi_{qrs,\eta}^{v_i} + \mu^2\phi_{mnp,\xi\eta}^{v_i}\phi_{qrs,\xi\eta}^{v_i} \\
&-\frac{\left(\kappa\overline{d}\right)^2}{12}\left(\phi_{mnp,\eta\eta}^{v_i}\phi_{qrs,\eta\eta}^{v_i} + \mu^2\phi_{mnp,\xi\eta\eta}^{v_i}\phi_{qrs,\xi\eta\eta}^{v_i}\right) + \frac{\left(\kappa\overline{d}\right)^4}{360}\left(\phi_{mnp,\eta\eta\eta}^{v_i}\phi_{qrs,\eta\eta\eta}^{v_i} + \mu^2\phi_{mnp,\xi\eta\eta\eta}^{v_i}\phi_{qrs,\xi\eta\eta\eta}^{v_i}\right) \\
&-\frac{\left(\kappa\overline{d}\right)^6}{20160}\left(\phi_{mnp,\eta\eta\eta\eta}^{v_i}\phi_{qrs,\eta\eta\eta\eta}^{v_i} + \mu^2\phi_{mnp,\xi\eta\eta\eta\eta}^{v_i}\phi_{qrs,\xi\eta\eta\eta\eta}^{v_i}\right)\Big] + \overline{C}_{v\|_{(i,3-i)}}^R\left(\phi_{mnp}^{v_i}\phi_{qrs}^{v_i}\right) + 2\overline{C}_{v\|_{(i+1,4-i)}}^R\left(\phi_{mnp}^{v_i}\phi_{qrs}^{v_i}\right) \\
&+\overline{C}_{v\perp_{(i+2,i)}}^R\overline{d}^2\Big[\phi_{mnp,\gamma}^{v_i}\phi_{qrs,\gamma}^{v_i} + \mu^2\phi_{mnp,\xi\gamma}^{v_i}\phi_{qrs,\xi\gamma}^{v_i} - \frac{\overline{d}^2}{12}\left(\phi_{mnp,\gamma\gamma}^{v_i}\phi_{qrs,\gamma\gamma}^{v_i} + \mu^2\phi_{mnp,\xi\gamma\gamma}^{v_i}\phi_{qrs,\xi\gamma\gamma}^{v_i}\right) \\
&+\frac{\overline{d}^4}{360}\left(\phi_{mnp,\gamma\gamma\gamma}^{v_i}\phi_{qrs,\gamma\gamma\gamma}^{v_i} + \mu^2\phi_{mnp,\xi\gamma\gamma\gamma}^{v_i}\phi_{qrs,\xi\gamma\gamma\gamma}^{v_i}\right) - \frac{\overline{d}^6}{20160}\left(\phi_{mnp,\gamma\gamma\gamma\gamma}^{v_i}\phi_{qrs,\gamma\gamma\gamma\gamma}^{v_i} + \mu^2\phi_{mnp,\xi\gamma\gamma\gamma\gamma}^{v_i}\phi_{qrs,\xi\gamma\gamma\gamma\gamma}^{v_i}\right)\Big] \\
&+\overline{C}_{v\|_{(i,3-i)}}^R\left(\phi_{mnp}^{v_i}\phi_{qrs}^{v_i}\right) + 2\overline{C}_{v\|_{(i+1,4-i)}}^R\left(\phi_{mnp}^{v_i}\phi_{qrs}^{v_i}\right) + \left(\overline{C}_{d\|_{(i+2,i)}}^R + \overline{C}_{d\perp_{(i+2,i)}}^R\right)\overline{d}^2\Big[\phi_{mnp,\gamma}^{v_i}\phi_{qrs,\gamma}^{v_i} + \\
&\mu^2\phi_{mnp,\xi\gamma}^{v_i}\phi_{qrs,\xi\gamma}^{v_i} + \kappa^2\left(\phi_{mnp,\eta}^{v_i}\phi_{qrs,\eta}^{v_i} + \mu^2\phi_{mnp,\xi\eta}^{v_i}\phi_{qrs,\xi\eta}^{v_i}\right) - \frac{\overline{d}^2}{12}\Big(\phi_{mnp,\gamma\gamma}^{v_i}\phi_{qrs,\gamma\gamma}^{v_i} + \mu^2\phi_{mnp,\xi\gamma\gamma}^{v_i}\phi_{qrs,\xi\gamma\gamma}^{v_i} \\
&+6\kappa^2\left(\phi_{mnp,\eta\gamma}^{v_i}\phi_{qrs,\eta\gamma}^{v_i} + \mu^2\phi_{mnp,\xi\eta\gamma}^{v_i}\phi_{qrs,\xi\eta\gamma}^{v_i}\right) + \kappa^4\left(\phi_{mnp,\eta\eta}^{v_i}\phi_{qrs,\eta\eta}^{v_i} + \mu^2\phi_{mnp,\xi\eta\eta}^{v_i}\phi_{qrs,\xi\eta\eta}^{v_i}\right)\Big) \\
&+\frac{\overline{d}^4}{360}\Big[\left(\phi_{mnp,\gamma\gamma\gamma}^{v_i}\phi_{qrs,\gamma\gamma\gamma}^{v_i} + \mu^2\phi_{mnp,\xi\gamma\gamma\gamma}^{v_i}\phi_{qrs,\xi\gamma\gamma\gamma}^{v_i}\right) + 15\kappa^2\left(\phi_{mnp,\eta\gamma\gamma}^{v_i}\phi_{qrs,\eta\gamma\gamma}^{v_i} + \mu^2\phi_{mnp,\xi\eta\gamma\gamma}^{v_i}\phi_{qrs,\xi\eta\gamma\gamma}^{v_i}\right) \\
&+15\kappa^4\left(\phi_{mnp,\eta\eta\gamma}^{v_i}\phi_{qrs,\eta\eta\gamma}^{v_i} + \mu^2\phi_{mnp,\xi\eta\eta\gamma}^{v_i}\phi_{qrs,\xi\eta\eta\gamma}^{v_i}\right) + \kappa^6\left(\phi_{mnp,\eta\eta\eta}^{v_i}\phi_{qrs,\eta\eta\eta}^{v_i} + \mu^2\phi_{mnp,\xi\eta\eta\eta}^{v_i}\phi_{qrs,\xi\eta\eta\eta}^{v_i}\right)\Big] \\
&+\left(\overline{C}_{d\|_{(i,3-i)}}^R + \overline{C}_{d\perp_{(i,3-i)}}^R\right)\left(\phi_{mnp}^{v_i}\phi_{qrs}^{v_i}\right) + 2\left(\overline{C}_{d\|_{(i+1,4-i)}}^R + \overline{C}_{d\perp_{(i+1,4-i)}}^R\right)\left(\phi_{mnp}^{v_i}\phi_{qrs}^{v_i}\right)\Big\}\,\mathrm{d}\xi\mathrm{d}\eta\mathrm{d}\gamma,
\end{aligned}
\tag{D.5}
$$

$$
\begin{aligned}
&\left[\overline{\mathbf{K}}_b^R\right]_{mnpqrs}^{v_i v_{3-i}} = \int_0^1\int_0^1\int_0^1 \Big\{ -\overline{C}_{v\|_{(i,3-i)}}^R\left(\phi_{mnp}^{v_i}\phi_{qrs}^{v_i}\right) - 2\overline{C}_{v\|_{(i+1,4-i)}}^R\left(\phi_{mnp}^{v_i}\phi_{qrs}^{v_i}\right) + \overline{C}_{v\|_{(i+1,4-i)}}^R\left(\kappa\overline{d}\right)^2 \\
&\Big[\phi_{mnp,\eta}^{v_i}\phi_{qrs,\eta}^{v_i} + \mu^2\phi_{mnp,\xi\eta}^{v_i}\phi_{qrs,\xi\eta}^{v_i} - \frac{\left(\kappa\overline{d}\right)^2}{12}\left(\phi_{mnp,\eta\eta}^{v_i}\phi_{qrs,\eta\eta}^{v_i} + \mu^2\phi_{mnp,\xi\eta\eta}^{v_i}\phi_{qrs,\xi\eta\eta}^{v_i}\right) + \frac{\left(\kappa\overline{d}\right)^4}{360}\Big(\phi_{mnp,\eta\eta\eta}^{v_i}\phi_{qrs,\eta\eta\eta}^{v_i} \\
&+\mu^2\phi_{mnp,\xi\eta\eta\eta}^{v_i}\phi_{qrs,\xi\eta\eta\eta}^{v_i}\Big) - \frac{\left(\kappa\overline{d}\right)^6}{20160}\left(\phi_{mnp,\eta\eta\eta\eta}^{v_i}\phi_{qrs,\eta\eta\eta\eta}^{v_i} + \mu^2\phi_{mnp,\xi\eta\eta\eta\eta}^{v_i}\phi_{qrs,\xi\eta\eta\eta\eta}^{v_i}\right)\Big] - \overline{C}_{v\perp_{(i,3-i)}}^R\left(\phi_{mnp}^{v_i}\phi_{qrs}^{v_i}\right) \\
&-2\overline{C}_{v\perp_{(i+1,4-i)}}^R\left(\phi_{mnp}^{v_i}\phi_{qrs}^{v_i}\right) + \overline{C}_{v\perp_{(i+1,4-i)}}^R\overline{d}^2\Big[\phi_{mnp,\gamma}^{v_i}\phi_{qrs,\gamma}^{v_i} + \mu^2\phi_{mnp,\xi\gamma}^{v_i}\phi_{qrs,\xi\gamma}^{v_i} - \frac{\overline{d}^2}{12}\Big(\phi_{mnp,\gamma\gamma}^{v_i}\phi_{qrs,\gamma\gamma}^{v_i} \\
&+\mu^2\phi_{mnp,\xi\gamma\gamma}^{v_i}\phi_{qrs,\xi\gamma\gamma}^{v_i}\Big) + \frac{\overline{d}^4}{360}\left(\phi_{mnp,\gamma\gamma\gamma}^{v_i}\phi_{qrs,\gamma\gamma\gamma}^{v_i} + \mu^2\phi_{mnp,\xi\gamma\gamma\gamma}^{v_i}\phi_{qrs,\xi\gamma\gamma\gamma}^{v_i}\right) - \frac{\overline{d}^6}{20160}\Big(\phi_{mnp,\gamma\gamma\gamma\gamma}^{v_i}\phi_{qrs,\gamma\gamma\gamma\gamma}^{v_i} \\
&+\mu^2\phi_{mnp,\xi\gamma\gamma\gamma\gamma}^{v_i}\phi_{qrs,\xi\gamma\gamma\gamma\gamma}^{v_i}\Big)\Big] - \left(\overline{C}_{d\|_{(i,3-i)}}^R + \overline{C}_{d\perp_{(i,3-i)}}^R\right)\left(\phi_{mnp}^{v_i}\phi_{qrs}^{v_i}\right) - 2\left(\overline{C}_{d\|_{(i+1,4-i)}}^R + \overline{C}_{d\perp_{(i+1,4-i)}}^R\right)\left(\phi_{mnp}^{v_i}\phi_{qrs}^{v_i}\right) \\
&+\left(\overline{C}_{d\|_{(i+1,4-i)}}^R + \overline{C}_{d\perp_{(i+1,4-i)}}^R\right)\overline{d}^2\Big[\phi_{mnp,\gamma}^{v_i}\phi_{qrs,\gamma}^{v_i} + \mu^2\phi_{mnp,\xi\gamma}^{v_i}\phi_{qrs,\xi\gamma}^{v_i} + \kappa^2\left(\phi_{mnp,\eta}^{v_i}\phi_{qrs,\eta}^{v_i} + \mu^2\phi_{mnp,\xi\eta}^{v_i}\phi_{qrs,\xi\eta}^{v_i}\right) \\
&-\frac{\overline{d}^2}{12}\Big(\phi_{mnp,\gamma\gamma}^{v_i}\phi_{qrs,\gamma\gamma}^{v_i} + \mu^2\phi_{mnp,\xi\gamma\gamma}^{v_i}\phi_{qrs,\xi\gamma\gamma}^{v_i} + 6\kappa^2\left(\phi_{mnp,\eta\gamma}^{v_i}\phi_{qrs,\eta\gamma}^{v_i} + \mu^2\phi_{mnp,\xi\eta\gamma}^{v_i}\phi_{qrs,\xi\eta\gamma}^{v_i}\right) \\
&+\kappa^4\left(\phi_{mnp,\eta\eta}^{v_i}\phi_{qrs,\eta\eta}^{v_i} + \mu^2\phi_{mnp,\xi\eta\eta}^{v_i}\phi_{qrs,\xi\eta\eta}^{v_i}\right)\Big) + \frac{\overline{d}^4}{360}\Big(\phi_{mnp,\gamma\gamma\gamma}^{v_i}\phi_{qrs,\gamma\gamma\gamma}^{v_i} + \mu^2\phi_{mnp,\xi\gamma\gamma\gamma}^{v_i}\phi_{qrs,\xi\gamma\gamma\gamma}^{v_i} + \\
&15\kappa^2\left(\phi_{mnp,\eta\gamma\gamma}^{v_i}\phi_{qrs,\eta\gamma\gamma}^{v_i} + \mu^2\phi_{mnp,\xi\eta\gamma\gamma}^{v_i}\phi_{qrs,\xi\eta\gamma\gamma}^{v_i}\right) + 15\kappa^4\left(\phi_{mnp,\eta\eta\gamma}^{v_i}\phi_{qrs,\eta\eta\gamma}^{v_i} + \mu^2\phi_{mnp,\xi\eta\eta\gamma}^{v_i}\phi_{qrs,\xi\eta\eta\gamma}^{v_i}\right) \\
&+\kappa^6\left(\phi_{mnp,\eta\eta\eta}^{v_i}\phi_{qrs,\eta\eta\eta}^{v_i} + \mu^2\phi_{mnp,\xi\eta\eta\eta}^{v_i}\phi_{qrs,\xi\eta\eta\eta}^{v_i}\right)\Big)\Big]\Big\}\,\mathrm{d}\xi\mathrm{d}\eta\mathrm{d}\gamma,
\end{aligned}
\tag{D.6}
$$

$$\left[\overline{\mathbf{K}}_b^R\right]_{mnpqrs}^{v_i w_1} = \left(\overline{C}^R_{d\|_{(i+2,i)}} - \overline{C}^R_{d\perp_{(i+2,i)}}\right) \kappa \overline{d}^2 \int_0^1 \int_0^1 \int_0^1 \Big\{ \phi^{v_i}_{mnp,\eta} \phi^{w_i}_{qrs,\gamma} + \phi^{v_i}_{mnp,\gamma} \phi^{w_i}_{qrs,\eta} + \mu^2 \Big(\phi^{v_i}_{mnp,\xi\eta} \phi^{w_i}_{qrs,\xi\gamma} + \phi^{v_i}_{mnp,\xi\gamma} \phi^{w_i}_{qrs,\xi\eta} \Big) - \frac{\overline{d}^2}{6} \Big[\overline{\nabla}_{\eta\gamma} \left\{ \phi^{v_i}_{mnp,\eta} \right\} \cdot \overline{\nabla}_{\eta\gamma} \left\{ \phi^{w_i}_{qrs,\gamma} \right\} + \overline{\nabla}_{\eta\gamma} \left\{ \phi^{v_i}_{mnp,\gamma} \right\} \cdot \overline{\nabla}_{\eta\gamma} \left\{ \phi^{w_i}_{qrs,\eta} \right\} + \mu^2 \Big(\overline{\nabla}_{\eta\gamma} \left\{ \phi^{v_i}_{mnp,\xi\eta} \right\} \cdot \overline{\nabla}_{\eta\gamma} \left\{ \phi^{w_i}_{qrs,\xi\gamma} \right\} + \overline{\nabla}_{\eta\gamma} \left\{ \phi^{v_i}_{mnp,\xi\gamma} \right\} \cdot \overline{\nabla}_{\eta\gamma} \left\{ \phi^{w_i}_{qrs,\xi\eta} \right\} \Big) \Big] + \frac{\overline{d}^4}{360} \Big[3\kappa^4 \Big(\phi^{v_i}_{mnp,\gamma\eta\eta} \phi^{w_i}_{qrs,\eta\eta\eta} + \phi^{v_i}_{mnp,\eta\eta\eta} \phi^{w_i}_{qrs,\gamma\eta\eta} + \mu^2 \Big(\phi^{v_i}_{mnp,\xi\eta\eta\gamma} \phi^{w_i}_{qrs,\xi\eta\eta\eta} + \phi^{v_i}_{mnp,\xi\eta\eta\eta} \phi^{w_i}_{qrs,\xi\eta\eta\gamma} \Big) \Big) + 10\kappa^2 \Big(\phi^{v_i}_{mnp,\eta\eta\eta} \phi^{w_i}_{qrs,\gamma\gamma\gamma} + \phi^{v_i}_{mnp,\gamma\gamma\gamma} \phi^{w_i}_{qrs,\eta\eta\eta} + \mu^2 \Big(\phi^{v_i}_{mnp,\xi\eta\eta\eta} \phi^{w_i}_{qrs,\xi\gamma\gamma\gamma} + \phi^{v_i}_{mnp,\xi\gamma\gamma\gamma} \phi^{w_i}_{qrs,\xi\eta\eta\eta} \Big) \Big) + 3 \Big(\phi^{v_i}_{mnp,\eta\gamma\gamma} \phi^{w_i}_{qrs,\gamma\gamma\gamma} + \phi^{v_i}_{mnp,\gamma\gamma\gamma} \phi^{w_i}_{qrs,\eta\gamma\gamma} + \mu^2 \Big(\phi^{v_i}_{mnp,\xi\eta\gamma\gamma} \phi^{w_i}_{qrs,\xi\gamma\gamma\gamma} + \phi^{v_i}_{mnp,\xi\gamma\gamma\gamma} \phi^{w_i}_{qrs,\xi\eta\gamma\gamma} \Big) \Big) \Big] \Big\} \mathrm{d}\xi \mathrm{d}\eta \mathrm{d}\gamma, \tag{D.7}$$

$$\left[\overline{\mathbf{K}}_b^R\right]_{mnpqrs}^{v_i w_2} = \left(\overline{C}^R_{d\|_{(i+1,4-i)}} - \overline{C}^R_{d\perp_{(i+1,4-i)}}\right) \kappa \overline{d}^2 \int_0^1 \int_0^1 \int_0^1 \Big\{ \phi^{v_i}_{mnp,\eta} \phi^{w_i}_{qrs,\gamma} + \phi^{v_i}_{mnp,\gamma} \phi^{w_i}_{qrs,\eta} + \mu^2 \Big(\phi^{v_i}_{mnp,\xi\eta} \phi^{w_i}_{qrs,\xi\gamma} + \phi^{v_i}_{mnp,\xi\gamma} \phi^{w_i}_{qrs,\xi\eta} \Big) - \frac{\overline{d}^2}{6} \Big[\overline{\nabla}_{\eta\gamma} \left\{ \phi^{v_i}_{mnp,\eta} \right\} \cdot \overline{\nabla}_{\eta\gamma} \left\{ \phi^{w_i}_{qrs,\gamma} \right\} + \overline{\nabla}_{\eta\gamma} \left\{ \phi^{v_i}_{mnp,\gamma} \right\} \cdot \overline{\nabla}_{\eta\gamma} \left\{ \phi^{w_i}_{qrs,\eta} \right\} + \mu^2 \Big(\overline{\nabla}_{\eta\gamma} \left\{ \phi^{v_i}_{mnp,\xi\eta} \right\} \cdot \overline{\nabla}_{\eta\gamma} \left\{ \phi^{w_i}_{qrs,\xi\gamma} \right\} + \overline{\nabla}_{\eta\gamma} \left\{ \phi^{v_i}_{mnp,\xi\gamma} \right\} \cdot \overline{\nabla}_{\eta\gamma} \left\{ \phi^{w_i}_{qrs,\xi\eta} \right\} \Big) \Big] + \frac{\overline{d}^4}{360} \Big[3\kappa^4 \Big(\phi^{v_i}_{mnp,\gamma\eta\eta} \phi^{w_i}_{qrs,\eta\eta\eta} + \phi^{v_i}_{mnp,\eta\eta\eta} \phi^{w_i}_{qrs,\gamma\eta\eta} + \mu^2 \Big(\phi^{v_i}_{mnp,\xi\eta\eta\gamma} \phi^{w_i}_{qrs,\xi\eta\eta\eta} + \phi^{v_i}_{mnp,\xi\eta\eta\eta} \phi^{w_i}_{qrs,\xi\eta\eta\gamma} \Big) \Big) + 10\kappa^2 \Big(\phi^{v_i}_{mnp,\eta\eta\eta} \phi^{w_i}_{qrs,\gamma\gamma\gamma} + \phi^{v_i}_{mnp,\gamma\gamma\gamma} \phi^{w_i}_{qrs,\eta\eta\eta} + \mu^2 \Big(\phi^{v_i}_{mnp,\xi\eta\eta\eta} \phi^{w_i}_{qrs,\xi\gamma\gamma\gamma} + \phi^{v_i}_{mnp,\xi\gamma\gamma\gamma} \phi^{w_i}_{qrs,\xi\eta\eta\eta} \Big) \Big) + 3 \Big(\phi^{v_i}_{mnp,\eta\gamma\gamma} \phi^{w_i}_{qrs,\gamma\gamma\gamma} + \phi^{v_i}_{mnp,\gamma\gamma\gamma} \phi^{w_i}_{qrs,\eta\gamma\gamma} + \mu^2 \Big(\phi^{v_i}_{mnp,\xi\eta\gamma\gamma} \phi^{w_i}_{qrs,\xi\gamma\gamma\gamma} + \phi^{v_i}_{mnp,\xi\gamma\gamma\gamma} \phi^{w_i}_{qrs,\xi\eta\gamma\gamma} \Big) \Big) \Big] \Big\} \mathrm{d}\xi \mathrm{d}\eta \mathrm{d}\gamma, \tag{D.8}$$

$$\left[\overline{\mathbf{M}}_b^R\right]_{mnpqrs}^{w_i w_i} = \int_0^1 \int_0^1 \int_0^1 \left[\begin{array}{l} \varrho_1^{2i-2} \left(\phi^{w_i}_{mnp} \phi^{w_i}_{qrs} + \mu^2 \phi^{w_i}_{mnp,\xi} \phi^{w_i}_{qrs,\xi} \right) \\ + \varrho_2^{2i-2} \lambda_1^{-2} \left(\phi^{w_i}_{mnp,\xi} \phi^{w_i}_{qrs,\xi} + \mu^2 \phi^{w_i}_{mnp,\xi\xi} \phi^{w_i}_{qrs,\xi\xi} \right) \end{array} \right] \mathrm{d}\xi \mathrm{d}\eta \mathrm{d}\gamma, \tag{D.9}$$

$$
\begin{aligned}
&\left[\overline{\mathbf{K}}_b^R\right]^{w_i w_i}_{mnpqrs} = \int_0^1\int_0^1\int_0^1 \Big\{ \varrho_3^{2i-2}\phi^{w_i}_{mnp,\xi\xi}\phi^{w_i}_{qrs,\xi\xi} + \overline{C}^R_{v\_i\|_{(i+2,i)}}\overline{d}^2 \Big[\phi^{w_i}_{mnp,\gamma}\phi^{w_i}_{qrs,\gamma} + \mu^2\phi^{w_i}_{mnp,\xi\gamma}\phi^{w_i}_{qrs,\xi\gamma} \\
&-\frac{\overline{d}^2}{12}\left(\phi^{w_i}_{mnp,\gamma\gamma}\phi^{w_i}_{qrs,\gamma\gamma} + \mu^2\phi^{w_i}_{mnp,\xi\gamma\gamma}\phi^{w_i}_{qrs,\xi\gamma\gamma}\right) + \frac{\overline{d}^4}{360}\left(\phi^{w_i}_{mnp,\gamma\gamma\gamma}\phi^{w_i}_{qrs,\gamma\gamma\gamma} + \mu^2\phi^{w_i}_{mnp,\xi\gamma\gamma\gamma}\phi^{w_i}_{qrs,\xi\gamma\gamma\gamma}\right) \\
&-\frac{\overline{d}^6}{20160}\left(\phi^{w_i}_{mnp,\gamma\gamma\gamma\gamma}\phi^{w_i}_{qrs,\gamma\gamma\gamma\gamma} + \mu^2\phi^{w_i}_{mnp,\xi\gamma\gamma\gamma\gamma}\phi^{w_i}_{qrs,\xi\gamma\gamma\gamma\gamma}\right)\Big] + \overline{C}^R_{v\|_{(i,3-i)}}\left(\phi^{w_i}_{mnp}\phi^{w_i}_{qrs}\right) + 2\overline{C}^R_{v\|_{(i+1,4-i)}}\left(\phi^{w_i}_{mnp}\phi^{w_i}_{qrs}\right) \\
&+\overline{C}^R_{v\perp_{(i+2,i)}}\overline{d}^2\Big[\phi^{w_i}_{mnp,\eta}\phi^{w_i}_{qrs,\eta} + \mu^2\phi^{w_i}_{mnp,\xi\eta}\phi^{w_i}_{qrs,\xi\eta} - \frac{\overline{d}^2}{12}\left(\phi^{w_i}_{mnp,\eta\eta}\phi^{w_i}_{qrs,\eta\eta} + \mu^2\phi^{w_i}_{mnp,\xi\eta\eta}\phi^{w_i}_{qrs,\xi\eta\eta}\right) \\
&+\frac{\overline{d}^4}{360}\left(\phi^{w_i}_{mnp,\eta\eta\eta}\phi^{w_i}_{qrs,\eta\eta\eta} + \mu^2\phi^{w_i}_{mnp,\xi\eta\eta\eta}\phi^{w_i}_{qrs,\xi\eta\eta\eta}\right) - \frac{\overline{d}^6}{20160}\left(\phi^{w_i}_{mnp,\eta\eta\eta\eta}\phi^{w_i}_{qrs,\eta\eta\eta\eta} + \mu^2\phi^{w_i}_{mnp,\xi\eta\eta\eta\eta}\phi^{w_i}_{qrs,\xi\eta\eta\eta\eta}\right)\Big] \\
&+\overline{C}^R_{v\|_{(i,3-i)}}\left(\phi^{w_i}_{mnp}\phi^{w_i}_{qrs}\right) + 2\overline{C}^R_{v\|_{(i+1,4-i)}}\left(\phi^{w_i}_{mnp}\phi^{w_i}_{qrs}\right) + \left(\overline{C}^R_{d\|_{(i+2,i)}} + \overline{C}^R_{d\perp_{(i+2,i)}}\right)\overline{d}^2\Big[\phi^{w_i}_{mnp,\gamma}\phi^{w_i}_{qrs,\gamma} \\
&+\mu^2\phi^{w_i}_{mnp,\xi\gamma}\phi^{w_i}_{qrs,\xi\gamma} + \kappa^2\left(\phi^{w_i}_{mnp,\eta}\phi^{w_i}_{qrs,\eta} + \mu^2\phi^{w_i}_{mnp,\xi\eta}\phi^{w_i}_{qrs,\xi\eta}\right) - \frac{\overline{d}^2}{12}\Big(\phi^{w_i}_{mnp,\gamma\gamma}\phi^{w_i}_{qrs,\gamma\gamma} + \mu^2\phi^{w_i}_{mnp,\xi\gamma\gamma}\phi^{w_i}_{qrs,\xi\gamma\gamma} \\
&+6\kappa^2\left(\phi^{w_i}_{mnp,\eta\gamma}\phi^{w_i}_{qrs,\eta\gamma} + \mu^2\phi^{w_i}_{mnp,\xi\eta\gamma}\phi^{w_i}_{qrs,\xi\eta\gamma}\right) + \kappa^4\left(\phi^{w_i}_{mnp,\eta\eta}\phi^{w_i}_{qrs,\eta\eta} + \mu^2\phi^{w_i}_{mnp,\xi\eta\eta}\phi^{w_i}_{qrs,\xi\eta\eta}\right)\Big) \\
&+\frac{\overline{d}^4}{360}\Big(\phi^{w_i}_{mnp,\gamma\gamma\gamma}\phi^{w_i}_{qrs,\gamma\gamma\gamma} + \mu^2\phi^{w_i}_{mnp,\xi\gamma\gamma\gamma}\phi^{w_i}_{qrs,\xi\gamma\gamma\gamma} + 15\kappa^2\left(\phi^{w_i}_{mnp,\eta\gamma\gamma}\phi^{w_i}_{qrs,\eta\gamma\gamma} + \mu^2\phi^{w_i}_{mnp,\xi\eta\gamma\gamma}\phi^{w_i}_{qrs,\xi\eta\gamma\gamma}\right) \\
&+15\kappa^4\left(\phi^{w_i}_{mnp,\eta\eta\gamma}\phi^{w_i}_{qrs,\eta\eta\gamma} + \mu^2\phi^{w_i}_{mnp,\xi\eta\eta\gamma}\phi^{w_i}_{qrs,\xi\eta\eta\gamma}\right) + \kappa^6\left(\phi^{w_i}_{mnp,\eta\eta\eta}\phi^{w_i}_{qrs,\eta\eta\eta} + \mu^2\phi^{w_i}_{mnp,\xi\eta\eta\eta}\phi^{w_i}_{qrs,\xi\eta\eta\eta}\right)\Big)\Big] \\
&+\left(\overline{C}^R_{d\|_{(i,3-i)}} + \overline{C}^R_{d\perp_{(i,3-i)}}\right)\left(\phi^{w_i}_{mnp}\phi^{w_i}_{qrs}\right) + 2\left(\overline{C}^R_{d\|_{(i+1,4-i)}} + \overline{C}^R_{d\perp_{(i+1,4-i)}}\right)\left(\phi^{w_i}_{mnp}\phi^{w_i}_{qrs}\right)\Big\}\,\mathrm{d}\xi\mathrm{d}\eta\mathrm{d}\gamma,
\end{aligned}
\tag{D.10}
$$

$$
\begin{aligned}
&\left[\overline{\mathbf{K}}_b^R\right]^{w_i w_{3-i}}_{mnpqrs} = \int_0^1\int_0^1\int_0^1 \Big\{ -\overline{C}^R_{v\|_{(i,3-i)}}\left(\phi^{w_i}_{mnp}\phi^{w_i}_{qrs}\right) - 2\overline{C}^R_{v\|_{(i+1,4-i)}}\left(\phi^{w_i}_{mnp}\phi^{w_i}_{qrs}\right) + \overline{C}^R_{v_i\perp_{(i+1,4-i)}}\overline{d}^2 \\
&\Big[\phi^{w_i}_{mnp,\gamma}\phi^{w_i}_{qrs,\gamma} + \mu^2\phi^{w_i}_{mnp,\xi\gamma}\phi^{w_i}_{qrs,\xi\gamma} - \frac{\overline{d}^2}{12}\left(\phi^{w_i}_{mnp,\gamma\gamma}\phi^{w_i}_{qrs,\gamma\gamma} + \mu^2\phi^{w_i}_{mnp,\xi\gamma\gamma}\phi^{w_i}_{qrs,\xi\gamma\gamma}\right) + \frac{\overline{d}^4}{360}\Big(\phi^{w_i}_{mnp,\gamma\gamma\gamma}\phi^{w_i}_{qrs,\gamma\gamma\gamma} \\
&+\mu^2\phi^{w_i}_{mnp,\xi\gamma\gamma\gamma}\phi^{w_i}_{qrs,\xi\gamma\gamma\gamma}\Big) - \frac{\overline{d}^6}{20160}\left(\phi^{w_i}_{mnp,\gamma\gamma\gamma\gamma}\phi^{w_i}_{qrs,\gamma\gamma\gamma\gamma} + \mu^2\phi^{w_i}_{mnp,\xi\gamma\gamma\gamma\gamma}\phi^{w_i}_{qrs,\xi\gamma\gamma\gamma\gamma}\right)\Big] - \overline{C}^R_{v\perp_{(i,3-i)}}\left(\phi^{w_i}_{mnp}\phi^{w_i}_{qrs}\right) \\
&-2\overline{C}^R_{v\perp_{(i+1,4-i)}}\left(\phi^{w_i}_{mnp}\phi^{w_i}_{qrs}\right) + \overline{C}^R_{v\perp_{(i+1,4-i)}}\overline{d}^2\Big[\phi^{w_i}_{mnp,\eta}\phi^{w_i}_{qrs,\eta} + \mu^2\phi^{w_i}_{mnp,\xi\eta}\phi^{w_i}_{qrs,\xi\eta} - \frac{\overline{d}^2}{12}\Big(\phi^{w_i}_{mnp,\eta\eta}\phi^{w_i}_{qrs,\eta\eta} \\
&+\mu^2\phi^{w_i}_{mnp,\xi\eta\eta}\phi^{w_i}_{qrs,\xi\eta\eta}\Big) + \frac{\overline{d}^4}{360}\left(\phi^{w_i}_{mnp,\eta\eta\eta}\phi^{w_i}_{qrs,\eta\eta\eta} + \mu^2\phi^{w_i}_{mnp,\xi\eta\eta\eta}\phi^{w_i}_{qrs,\xi\eta\eta\eta}\right) - \frac{\overline{d}^6}{20160}\Big(\phi^{w_i}_{mnp,\eta\eta\eta\eta}\phi^{w_i}_{qrs,\eta\eta\eta\eta} \\
&+\mu^2\phi^{w_i}_{mnp,\xi\eta\eta\eta\eta}\phi^{w_i}_{qrs,\xi\eta\eta\eta\eta}\Big)\Big] - \left(\overline{C}^R_{d\|_{(i,3-i)}} + \overline{C}^R_{d\perp_{(i,3-i)}}\right)\left(\phi^{w_i}_{mnp}\phi^{w_i}_{qrs}\right) - 2\left(\overline{C}^R_{d\|_{(i+1,4-i)}} + \overline{C}^R_{d\perp_{(i+1,4-i)}}\right)\left(\phi^{w_i}_{mnp}\phi^{w_i}_{qrs}\right) \\
&+\left(\overline{C}^R_{d\|_{(i+1,4-i)}} + \overline{C}^R_{d\perp_{(i+1,4-i)}}\right)\overline{d}^2\Big[\phi^{w_i}_{mnp,\gamma}\phi^{w_i}_{qrs,\gamma} + \mu^2\phi^{w_i}_{mnp,\xi\gamma}\phi^{w_i}_{qrs,\xi\gamma} + \kappa^2\left(\phi^{w_i}_{mnp,\eta}\phi^{w_i}_{qrs,\eta} + \mu^2\phi^{w_i}_{mnp,\xi\eta}\phi^{w_i}_{qrs,\xi\eta}\right) \\
&-\frac{\overline{d}^2}{12}\Big(\phi^{w_i}_{mnp,\gamma\gamma}\phi^{w_i}_{qrs,\gamma\gamma} + \mu^2\phi^{w_i}_{mnp,\xi\gamma\gamma}\phi^{w_i}_{qrs,\xi\gamma\gamma} + 6\kappa^2\left(\phi^{w_i}_{mnp,\eta\gamma}\phi^{w_i}_{qrs,\eta\gamma} + \mu^2\phi^{w_i}_{mnp,\xi\eta\gamma}\phi^{w_i}_{qrs,\xi\eta\gamma}\right) \\
&+\kappa^4\left(\phi^{w_i}_{mnp,\eta\eta}\phi^{w_i}_{qrs,\eta\eta} + \mu^2\phi^{w_i}_{mnp,\xi\eta\eta}\phi^{w_i}_{qrs,\xi\eta\eta}\right)\Big) + \frac{\overline{d}^4}{360}\Big(\phi^{w_i}_{mnp,\gamma\gamma\gamma}\phi^{w_i}_{qrs,\gamma\gamma\gamma} + \mu^2\phi^{w_i}_{mnp,\xi\gamma\gamma\gamma}\phi^{w_i}_{qrs,\xi\gamma\gamma\gamma} \\
&+15\kappa^2\left(\phi^{w_i}_{mnp,\eta\gamma\gamma}\phi^{w_i}_{qrs,\eta\gamma\gamma} + \mu^2\phi^{w_i}_{mnp,\xi\eta\gamma\gamma}\phi^{w_i}_{qrs,\xi\eta\gamma\gamma}\right) + 15\kappa^4\left(\phi^{w_i}_{mnp,\eta\eta\gamma}\phi^{w_i}_{qrs,\eta\eta\gamma} + \mu^2\phi^{w_i}_{mnp,\xi\eta\eta\gamma}\phi^{w_i}_{qrs,\xi\eta\eta\gamma}\right) \\
&+\kappa^6\left(\phi^{w_i}_{mnp,\eta\eta\eta}\phi^{w_i}_{qrs,\eta\eta\eta} + \mu^2\phi^{w_i}_{mnp,\xi\eta\eta\eta}\phi^{w_i}_{qrs,\xi\eta\eta\eta}\right)\Big)\Big]\Big\}\,\mathrm{d}\xi\mathrm{d}\eta\mathrm{d}\gamma,
\end{aligned}
\tag{D.11}
$$

$$
\begin{aligned}
\left[\overline{\mathbf{K}}_b^R\right]^{w_i v_1}_{mnpqrs} &= \left(\overline{C}^R_{d\|_{(i+2,i)}} - \overline{C}^R_{d\perp_{(i+2,i)}}\right)\kappa\overline{d}^2 \int_0^1\int_0^1\int_0^1 \Big\{ \phi^{w_i}_{mnp,\eta}\phi^{v_i}_{qrs,\gamma} + \phi^{w_i}_{mnp,\gamma}\phi^{v_i}_{qrs,\eta} + \mu^2 \Big(\phi^{w_i}_{mnp,\xi\eta}\phi^{v_i}_{qrs,\xi\gamma} \\
&+\phi^{w_i}_{mnp,\xi\gamma}\phi^{v_i}_{qrs,\xi\eta}\Big) - \frac{\overline{d}^2}{6}\Big[\overline{\nabla}_{\eta\gamma}\left\{\phi^{w_i}_{mnp,\eta}\right\}\cdot\overline{\nabla}_{\eta\gamma}\left\{\phi^{v_i}_{qrs,\gamma}\right\} + \overline{\nabla}_{\eta\gamma}\left\{\phi^{w_i}_{mnp,\gamma}\right\}\cdot\overline{\nabla}_{\eta\gamma}\left\{\phi^{v_i}_{qrs,\eta}\right\} \\
&+\mu^2\Big(\overline{\nabla}_{\eta\gamma}\left\{\phi^{w_i}_{mnp,\xi\eta}\right\}\cdot\overline{\nabla}_{\eta\gamma}\left\{\phi^{v_i}_{qrs,\xi\gamma}\right\} + \overline{\nabla}_{\eta\gamma}\left\{\phi^{w_i}_{mnp,\xi\gamma}\right\}\cdot\overline{\nabla}_{\eta\gamma}\left\{\phi^{v_i}_{qrs,\xi\eta}\right\}\Big)\Big] + \frac{\overline{d}^4}{360}\Big[3\kappa^4\Big(\phi^{w_i}_{mnp,\gamma\eta\eta}\phi^{v_i}_{qrs,\eta\eta\eta} \\
&+\phi^{w_i}_{mnp,\eta\eta\eta}\phi^{v_i}_{qrs,\gamma\eta\eta} + \mu^2\Big(\phi^{w_i}_{mnp,\xi\eta\eta\gamma}\phi^{v_i}_{qrs,\xi\eta\eta\eta} + \phi^{w_i}_{mnp,\xi\eta\eta\eta}\phi^{v_i}_{qrs,\xi\eta\eta\gamma}\Big)\Big) + 10\kappa^2\Big(\phi^{w_i}_{mnp,\eta\eta\eta}\phi^{v_i}_{qrs,\gamma\gamma\gamma} \\
&+\phi^{w_i}_{mnp,\gamma\gamma\gamma}\phi^{v_i}_{qrs,\eta\eta\eta} + \mu^2\Big(\phi^{w_i}_{mnp,\xi\eta\eta\eta}\phi^{v_i}_{qrs,\xi\gamma\gamma\gamma} + \phi^{w_i}_{mnp,\xi\gamma\gamma\gamma}\phi^{v_i}_{qrs,\xi\eta\eta\eta}\Big)\Big) + 3\Big(\phi^{w_i}_{mnp,\eta\gamma\gamma}\phi^{v_i}_{qrs,\gamma\gamma\gamma} + \phi^{w_i}_{mnp,\gamma\gamma\gamma}\phi^{v_i}_{qrs,\eta\gamma\gamma} \\
&+\mu^2\Big(\phi^{w_i}_{mnp,\xi\eta\gamma\gamma}\phi^{v_i}_{qrs,\xi\gamma\gamma\gamma} + \phi^{w_i}_{mnp,\xi\gamma\gamma\gamma}\phi^{v_i}_{qrs,\xi\eta\gamma\gamma}\Big)\Big)\Big]\Big\}\,\mathrm{d}\xi\mathrm{d}\eta\mathrm{d}\gamma,
\end{aligned}
\tag{D.12}
$$

$$
\begin{aligned}
\left[\overline{\mathbf{K}}_b^R\right]^{w_i v_2}_{mnpqrs} &= \left(\overline{C}^R_{d\|_{(i+1,4-i)}} - \overline{C}^R_{d\perp_{(i+1,4-i)}}\right)\kappa\overline{d}^2 \int_0^1\int_0^1\int_0^1 \Big\{ \phi^{w_i}_{mnp,\eta}\phi^{v_i}_{qrs,\gamma} + \phi^{w_i}_{mnp,\gamma}\phi^{v_i}_{qrs,\eta} + \mu^2 \Big(\phi^{w_i}_{mnp,\xi\eta}\phi^{v_i}_{qrs,\xi\gamma} \\
&+\phi^{w_i}_{mnp,\xi\gamma}\phi^{v_i}_{qrs,\xi\eta}\Big) - \frac{\overline{d}^2}{6}\Big[\overline{\nabla}_{\eta\gamma}\left\{\phi^{w_i}_{mnp,\eta}\right\}\cdot\overline{\nabla}_{\eta\gamma}\left\{\phi^{v_i}_{qrs,\gamma}\right\} + \overline{\nabla}_{\eta\gamma}\left\{\phi^{w_i}_{mnp,\gamma}\right\}\cdot\overline{\nabla}_{\eta\gamma}\left\{\phi^{v_i}_{qrs,\eta}\right\} \\
&+\mu^2\Big(\overline{\nabla}_{\eta\gamma}\left\{\phi^{w_i}_{mnp,\xi\eta}\right\}\cdot\overline{\nabla}_{\eta\gamma}\left\{\phi^{v_i}_{qrs,\xi\gamma}\right\} + \overline{\nabla}_{\eta\gamma}\left\{\phi^{w_i}_{mnp,\xi\gamma}\right\}\cdot\overline{\nabla}_{\eta\gamma}\left\{\phi^{v_i}_{qrs,\xi\eta}\right\}\Big)\Big] + \frac{\overline{d}^4}{360}\Big[3\kappa^4\Big(\phi^{w_i}_{mnp,\gamma\eta\eta}\phi^{v_i}_{qrs,\eta\eta\eta} \\
&+\phi^{w_i}_{mnp,\eta\eta\eta}\phi^{v_i}_{qrs,\gamma\eta\eta} + \mu^2\Big(\phi^{w_i}_{mnp,\xi\eta\eta\gamma}\phi^{v_i}_{qrs,\xi\eta\eta\eta} + \phi^{w_i}_{mnp,\xi\eta\eta\eta}\phi^{v_i}_{qrs,\xi\eta\eta\gamma}\Big)\Big) + 10\kappa^2\Big(\phi^{w_i}_{mnp,\eta\eta\eta}\phi^{v_i}_{qrs,\gamma\gamma\gamma} \\
&+\phi^{w_i}_{mnp,\gamma\gamma\gamma}\phi^{v_i}_{qrs,\eta\eta\eta} + \mu^2\Big(\phi^{w_i}_{mnp,\xi\eta\eta\eta}\phi^{v_i}_{qrs,\xi\gamma\gamma\gamma} + \phi^{w_i}_{mnp,\xi\gamma\gamma\gamma}\phi^{v_i}_{qrs,\xi\eta\eta\eta}\Big)\Big) + 3\Big(\phi^{w_i}_{mnp,\eta\gamma\gamma}\phi^{v_i}_{qrs,\gamma\gamma\gamma} + \phi^{w_i}_{mnp,\gamma\gamma\gamma}\phi^{v_i}_{qrs,\eta\gamma\gamma} \\
&+\mu^2\Big(\phi^{w_i}_{mnp,\xi\eta\gamma\gamma}\phi^{v_i}_{qrs,\xi\gamma\gamma\gamma} + \phi^{w_i}_{mnp,\xi\gamma\gamma\gamma}\phi^{v_i}_{qrs,\xi\eta\gamma\gamma}\Big)\Big)\Big]\Big\}\,\mathrm{d}\xi\mathrm{d}\eta\mathrm{d}\gamma,
\end{aligned}
\tag{D.13}
$$

where $\overline{\nabla}_{\eta\gamma}[.] = \kappa\,[.]_{,\eta}\mathbf{e}_y + [.]_{,\gamma}\mathbf{e}_z$.

Appendix E. Formulations of the continuous model based on the NHOBT

Appendix E.1. Nonlocal governing equations

$$
\begin{aligned}
&\Xi\left\{ \vartheta_7^{2i-2}\frac{\partial^2\overline{\psi}^H_{z_i}}{\partial\tau^2} - \vartheta_2^{2i-2}\gamma_6^2\frac{\partial^3\overline{v}^H_i}{\partial\tau^2\partial\xi} + \overline{K}^H_r\overline{\psi}^H_{z_i}\left(1-\delta_{1i}\right)\begin{pmatrix} \delta_{1n}+\delta_{1m}+\delta_{nN_z}+\delta_{mN_y}-\delta_{1m}\delta_{1n} \\ -\delta_{1m}\delta_{nN_z}-\delta_{1n}\delta_{mN_y}-\delta_{nN_z}\delta_{mN_y} \end{pmatrix} \right\} \\
&+\vartheta_4^{2i-2}\gamma_7^2\left(\overline{\psi}^H_{z_i}+\frac{\partial\overline{v}^H_i}{\partial\xi}\right) - \vartheta_8^{2i-2}\gamma_8^2\frac{\partial^2\overline{\psi}^H_{z_i}}{\partial\xi^2} + \vartheta_5^{2i-2}\gamma_9^2\frac{\partial^3\overline{v}^H_i}{\partial\xi^3} = 0,
\end{aligned}
\tag{E.1}
$$

$$
\begin{aligned}
&-\vartheta_4^{2i-2}\gamma_3^2\left(\frac{\partial\overline{\psi}_{z_i}^H}{\partial\xi}+\frac{\partial^2\overline{v}_i^H}{\partial\xi^2}\right)-\vartheta_5^{2i-2}\gamma_4^2\frac{\partial^3\overline{\psi}_{z_i}^H}{\partial\xi^3}+\vartheta_6^{2i-2}\frac{\partial^4\overline{v}_i^H}{\partial\xi^4}+\Xi\left\{\vartheta_1^{2i-2}\frac{\partial^2\overline{v}_i^H}{\partial\tau^2}+\vartheta_2^{2i-2}\gamma_1^2\frac{\partial^3\overline{\psi}_{z_i}^H}{\partial\tau^2\partial\xi}\right.\\
&-\vartheta_3^{2i-2}\gamma_2^2\frac{\partial^4\overline{v}_i^H}{\partial\tau^2\partial\xi^2}-\left(k\overline{d}\right)^2\overline{C}_{v\|_{(i+2,i)}}^H\left(\frac{\partial^2\overline{v}_i^H}{\partial\eta^2}+\frac{\left(k\overline{d}\right)^2}{12}\frac{\partial^4\overline{v}_i^H}{\partial\eta^4}+\frac{\left(k\overline{d}\right)^4}{360}\frac{\partial^6\overline{v}_i^H}{\partial\eta^6}+\frac{\left(k\overline{d}\right)^6}{20160}\frac{\partial^8\overline{v}_i^H}{\partial\eta^8}\right)\\
&+\overline{C}_{v\|_{(i,3-i)}}^H\left(\overline{v}_i^H-\overline{v}_{3-i}^H\right)+\overline{C}_{v\|_{(i+1,4-i)}}^H\left(2\left(\overline{v}_i^H-\overline{v}_{3-i}^H\right)-\left(k\overline{d}\right)^2\frac{\partial^2\overline{v}_{3-i}^H}{\partial\eta^2}-\frac{\left(k\overline{d}\right)^4}{12}\frac{\partial^4\overline{v}_{3-i}^H}{\partial\eta^4}-\frac{\left(k\overline{d}\right)^6}{360}\frac{\partial^6\overline{v}_{3-i}^H}{\partial\eta^6}\right.\\
&\left.-\frac{\left(k\overline{d}\right)^8}{20160}\frac{\partial^8\overline{v}_{3-i}^H}{\partial\eta^8}\right)-\overline{C}_{v\perp_{(i+2,i)}}^H\overline{d}^2\left(\frac{\partial^2\overline{v}_i^H}{\partial\gamma^2}+\frac{\overline{d}^2}{12}\frac{\partial^4\overline{v}_i^H}{\partial\gamma^4}+\frac{\overline{d}^4}{360}\frac{\partial^6\overline{v}_i^H}{\partial\gamma^6}+\frac{\overline{d}^6}{20160}\frac{\partial^8\overline{v}_i^H}{\partial\gamma^8}\right)+\overline{C}_{v\perp_{(i,3-i)}}^H\left(\overline{v}_i^H-\overline{v}_{3-i}^H\right)\\
&+\overline{C}_{v\perp_{(i+1,4-i)}}^H\left(2\left(\overline{v}_i^H-\overline{v}_{3-i}^H\right)-\overline{d}^2\frac{\partial^2\overline{v}_{3-i}^H}{\partial\gamma^2}-\frac{\overline{d}^4}{12}\frac{\partial^4\overline{v}_{3-i}^H}{\partial\gamma^4}-\frac{\overline{d}^6}{360}\frac{\partial^6\overline{v}_{3-i}^H}{\partial\gamma^6}-\frac{\overline{d}^8}{20160}\frac{\partial^8\overline{v}_{3-i}^H}{\partial\gamma^8}\right)\\
&-\left(\overline{C}_{d\|_{(i+2,i)}}^H+\overline{C}_{d\perp_{(i+2,i)}}^H\right)\overline{d}^2\left[k^2\frac{\partial^2\overline{v}_i^H}{\partial\eta^2}+\frac{\partial^2\overline{v}_i^H}{\partial\gamma^2}+\frac{\overline{d}^2}{12}\left(\frac{\partial^4\overline{v}_i^H}{\partial\gamma^4}+6k^2\frac{\partial^4\overline{v}_i^H}{\partial\gamma^2\partial\eta^2}+k^4\frac{\partial^4\overline{v}_i^H}{\partial\eta^4}\right)\right.\\
&\left.+\frac{\overline{d}^4}{360}\left(\frac{\partial^6\overline{v}_i^H}{\partial\gamma^6}+15k^2\frac{\partial^6\overline{v}_i^H}{\partial\gamma^4\partial\eta^2}+15k^4\frac{\partial^6\overline{v}_i^H}{\partial\gamma^2\partial\eta^4}+k^6\frac{\partial^6\overline{v}_i^H}{\partial\eta^6}\right)\right]+\left(\overline{C}_{d\|_{(i,3-i)}}^H+\overline{C}_{d\perp_{(i,3-i)}}^H\right)\left(\overline{v}_i^H-\overline{v}_{3-i}^H\right)\\
&+\left(\overline{C}_{d\|_{(i+1,4-i)}}^H+\overline{C}_{d\perp_{(i+1,4-i)}}^H\right)\left[2\left(\overline{v}_i^H-\overline{v}_{3-i}^H\right)+\overline{d}^2\left(-k^2\frac{\partial^2\overline{v}_{3-i}^H}{\partial\eta^2}-\frac{\partial^2\overline{v}_{3-i}^H}{\partial\gamma^2}-\frac{\overline{d}^2}{12}\left(\frac{\partial^4\overline{v}_{3-i}^H}{\partial\gamma^4}+6k^2\frac{\partial^4\overline{v}_{3-i}^H}{\partial\gamma^2\partial\eta^2}\right.\right.\right.\\
&\left.\left.\left.+k^4\frac{\partial^4\overline{v}_{3-i}^H}{\partial\eta^4}\right)-\frac{\overline{d}^4}{360}\left(\frac{\partial^6\overline{v}_{3-i}^H}{\partial\gamma^6}+15k^2\frac{\partial^6\overline{v}_{3-i}^H}{\partial\gamma^4\partial\eta^2}+15k^4\frac{\partial^6\overline{v}_{3-i}^H}{\partial\gamma^2\partial\eta^4}+k^6\frac{\partial^6\overline{v}_{3-i}^H}{\partial\eta^6}\right)\right)\right]-\left(\overline{C}_{d\|_{(i+2,i)}}^H-\overline{C}_{d\perp_{(i+2,i)}}^H\right)\overline{d}^2k\\
&\times\left[2\frac{\partial^2\overline{w}_i^H}{\partial\eta\partial\gamma}+\frac{\overline{d}^2}{3}\left(\frac{\partial^4\overline{w}_i^H}{\partial\eta\partial\gamma^3}+k^2\frac{\partial^4\overline{w}_i^H}{\partial\eta^3\partial\gamma}\right)+\frac{\overline{d}^4}{180}\left(3k^4\frac{\partial^6\overline{w}_i^H}{\partial\eta^5\partial\gamma}+10k^2\frac{\partial^6\overline{w}_i^H}{\partial\eta^6\partial\gamma^6}+3\frac{\partial^6\overline{w}_i^H}{\partial\eta\partial\gamma^5}\right)\right]\\
&-\left(\overline{C}_{d\|_{(i+1,4-i)}}^H-\overline{C}_{d\perp_{(i+1,4-i)}}^H\right)\overline{d}^2k\left[2\frac{\partial^2\overline{w}_{3-i}^H}{\partial\eta\partial\gamma}+\frac{\overline{d}^2}{3}\left(\frac{\partial^4\overline{w}_{3-i}^H}{\partial\eta\partial\gamma^3}+k^2\frac{\partial^4\overline{w}_{3-i}^H}{\partial\eta^3\partial\gamma}\right)+\frac{\overline{d}^4}{180}\left(3k^4\frac{\partial^6\overline{w}_{3-i}^H}{\partial\eta^5\partial\gamma}\right.\right.\\
&\left.\left.\left.+10k^2\frac{\partial^6\overline{w}_{3-i}^H}{\partial\eta^6\partial\gamma^6}+3\frac{\partial^6\overline{w}_{3-i}^H}{\partial\eta\partial\gamma^5}\right)\right]+\overline{K}_t^H\overline{v}_i^H\begin{pmatrix}\delta_{1n}+\delta_{1m}+\delta_{nN_z}+\delta_{mN_y}-\delta_{1m}\delta_{1n}\\-\delta_{1m}\delta_{nN_z}-\delta_{1n}\delta_{mN_y}-\delta_{nN_z}\delta_{mN_y}\end{pmatrix}\left(1-\delta_{1i}\right)\right\}=0,
\end{aligned}
\tag{E.2}
$$

$$
\begin{aligned}
&\Xi\left\{\vartheta_7^{2i-2}\frac{\partial^2\overline{\psi}_{y_i}^H}{\partial\tau^2}-\vartheta_2^{2i-2}\gamma_6^2\frac{\partial^3\overline{w}_i^H}{\partial\tau^2\partial\xi}+\overline{K}_r^H\overline{\psi}_{y_i}^H\left(1-\delta_{1i}\right)\begin{pmatrix}\delta_{1n}+\delta_{1m}+\delta_{nN_z}+\delta_{mN_y}-\delta_{1m}\delta_{1n}\\-\delta_{1m}\delta_{nN_z}-\delta_{1n}\delta_{mN_y}-\delta_{nN_z}\delta_{mN_y}\end{pmatrix}\right\}\\
&+\vartheta_4^{2i-2}\gamma_7^2\left(\overline{\psi}_{y_i}^H+\frac{\partial\overline{w}_i^H}{\partial\xi}\right)-\vartheta_8^{2i-2}\gamma_8^2\frac{\partial^2\overline{\psi}_{y_i}^H}{\partial\xi^2}+\vartheta_5^{2i-2}\gamma_9^2\frac{\partial^3\overline{w}_i^H}{\partial\xi^3}=0,
\end{aligned}
\tag{E.3}
$$

$$
\begin{aligned}
&-\vartheta_4^{2i-2}\gamma_3^2\left(\frac{\partial\overline{\psi}_{y_i}^H}{\partial\xi}+\frac{\partial^2\overline{w}_i^H}{\partial\xi^2}\right)-\vartheta_5^{2i-2}\gamma_4^2\frac{\partial^3\overline{\psi}_{y_i}^H}{\partial\xi^3}+\vartheta_6^{2i-2}\frac{\partial^4\overline{w}_i^H}{\partial\xi^4}+\Xi\left\{\vartheta_1^{2i-2}\frac{\partial^2\overline{w}_i^H}{\partial\tau^2}+\vartheta_2^{2i-2}\gamma_1^2\frac{\partial^3\overline{\psi}_{y_i}^H}{\partial\tau^2\partial\xi}\right.\\
&-\vartheta_3^{2i-2}\gamma_2^2\frac{\partial^4\overline{w}_i^H}{\partial\tau^2\partial\xi^2}-\overline{C}_{v\|_{(i+2,i)}}^H\overline{d}^2\left(\frac{\partial^2\overline{w}_i^H}{\partial\gamma^2}+\frac{\overline{d}^2}{12}\frac{\partial^4\overline{w}_i^H}{\partial\gamma^4}+\frac{\overline{d}^4}{360}\frac{\partial^6\overline{w}_i^H}{\partial\gamma^6}+\frac{\overline{d}^6}{20160}\frac{\partial^8\overline{w}_i^H}{\partial\gamma^8}\right)\\
&+\overline{C}_{v\|_{(i,3-i)}}^H\left(\overline{v}_i^H-\overline{v}_{3-i}^H\right)+\overline{C}_{v\|_{(i+1,4-i)}}^H\left(2\left(\overline{w}_i^H-\overline{w}_{3-i}^H\right)-\overline{d}^2\frac{\partial^2\overline{w}_{3-i}^H}{\partial\gamma^2}-\frac{\overline{d}^4}{12}\frac{\partial^4\overline{w}_{3-i}^H}{\partial\gamma^4}-\frac{\overline{d}^6}{360}\frac{\partial^6\overline{w}_{3-i}^H}{\partial\gamma^6}-\frac{\overline{d}^8}{20160}\frac{\partial^8\overline{w}_{3-i}^H}{\partial\gamma^8}\right)\\
&-\overline{C}_{v\perp_{(i+2,i)}}^H\left(k\overline{d}\right)^2\left(\frac{\partial^2\overline{w}_i^H}{\partial\eta^2}+\frac{\left(k\overline{d}\right)^2}{12}\frac{\partial^4\overline{w}_i^H}{\partial\eta^4}+\frac{\left(k\overline{d}\right)^4}{360}\frac{\partial^6\overline{w}_i^H}{\partial\eta^6}+\frac{\left(k\overline{d}\right)^6}{20160}\frac{\partial^8\overline{w}_i^H}{\partial\eta^8}\right)+\overline{C}_{v\perp_{(i,3-i)}}^H\left(\overline{w}_i^H-\overline{w}_{3-i}^H\right)\\
&+\overline{C}_{v\perp_{(i+1,4-i)}}^H\left(2\left(\overline{w}_i^H-\overline{w}_{3-i}^H\right)-\left(k\overline{d}\right)^2\frac{\partial^2\overline{w}_{3-i}^H}{\partial\eta^2}-\frac{\left(k\overline{d}\right)^4}{12}\frac{\partial^4\overline{w}_{3-i}^H}{\partial\eta^4}-\frac{\left(k\overline{d}\right)^6}{360}\frac{\partial^6\overline{w}_{3-i}^H}{\partial\eta^6}-\frac{\left(k\overline{d}\right)^8}{20160}\frac{\partial^8\overline{w}_{3-i}^H}{\partial\eta^8}\right)\\
&-\left(\overline{C}_{d\|_{(i+2,i)}}^H+\overline{C}_{d\perp_{(i+2,i)}}^H\right)\overline{d}^2\left[k^2\frac{\partial^2\overline{w}_i^H}{\partial\eta^2}+\frac{\partial^2\overline{w}_i^H}{\partial\gamma^2}+\frac{\overline{d}^2}{12}\left(\frac{\partial^4\overline{w}_i^H}{\partial\gamma^4}+6k^2\frac{\partial^4\overline{w}_i^H}{\partial\gamma^2\partial\eta^2}+k^4\frac{\partial^4\overline{w}_i^H}{\partial\eta^4}\right)\right.\\
&\left.+\frac{\overline{d}^4}{360}\left(\frac{\partial^6\overline{w}_i^H}{\partial\gamma^6}+15k^2\frac{\partial^6\overline{w}_i^H}{\partial\gamma^4\partial\eta^2}+15k^4\frac{\partial^6\overline{w}_i^H}{\partial\gamma^2\partial\eta^4}+k^6\frac{\partial^6\overline{w}_i^H}{\partial\eta^6}\right)\right]+\left(\overline{C}_{d\|_{(i,3-i)}}^H+\overline{C}_{d\perp_{(i,3-i)}}^H\right)\left(\overline{w}_i^H-\overline{w}_{3-i}^H\right)\\
&+\left(\overline{C}_{d\|_{(i+1,4-i)}}^H+\overline{C}_{d\perp_{(i+1,4-i)}}^H\right)\left[2\left(\overline{w}_i^H-\overline{w}_{3-i}^H\right)+\overline{d}^2\left(-k^2\frac{\partial^2\overline{w}_{3-i}^H}{\partial\eta^2}-\frac{\partial^2\overline{w}_{3-i}^H}{\partial\gamma^2}-\frac{\overline{d}^2}{12}\left(\frac{\partial^4\overline{w}_{3-i}^H}{\partial\gamma^4}+6k^2\frac{\partial^4\overline{w}_{3-i}^H}{\partial\gamma^2\partial\eta^2}\right.\right.\right.\\
&\left.\left.\left.+k^4\frac{\partial^4\overline{w}_{3-i}^H}{\partial\eta^4}\right)-\frac{\overline{d}^4}{360}\left(\frac{\partial^6\overline{w}_{3-i}^H}{\partial\gamma^6}+15k^2\frac{\partial^6\overline{w}_{3-i}^H}{\partial\gamma^4\partial\eta^2}+15k^4\frac{\partial^6\overline{w}_{3-i}^H}{\partial\gamma^2\partial\eta^4}+k^6\frac{\partial^6\overline{w}_{3-i}^H}{\partial\eta^6}\right)\right)\right]-\left(\overline{C}_{d\|_{(i+2,i)}}^H-\overline{C}_{d\perp_{(i+2,i)}}^H\right)\overline{d}^2k\\
&\times\left[2\frac{\partial^2\overline{v}_i^H}{\partial\eta\partial\gamma}+\frac{\overline{d}^2}{3}\left(\frac{\partial^4\overline{v}_i^H}{\partial\eta\partial\gamma^3}+k^2\frac{\partial^4\overline{v}_i^H}{\partial\eta^3\partial\gamma}\right)+\frac{\overline{d}^4}{180}\left(3k^4\frac{\partial^6\overline{v}_i^H}{\partial\eta^5\partial\gamma}+10k^2\frac{\partial^6\overline{v}_i^H}{\partial\eta^6\partial\gamma^6}+3\frac{\partial^6\overline{v}_i^H}{\partial\eta\partial\gamma^5}\right)\right]\\
&-\left(\overline{C}_{d\|_{(i+1,4-i)}}^H-\overline{C}_{d\perp_{(i+1,4-i)}}^H\right)\overline{d}^2k\left[2\frac{\partial^2\overline{v}_{3-i}^H}{\partial\eta\partial\gamma}+\frac{\overline{d}^2}{3}\left(\frac{\partial^4\overline{v}_{3-i}^H}{\partial\eta\partial\gamma^3}+k^2\frac{\partial^4\overline{v}_{3-i}^H}{\partial\eta^3\partial\gamma}\right)+\frac{\overline{d}^4}{180}\left(3k^4\frac{\partial^6\overline{v}_{3-i}^H}{\partial\eta^5\partial\gamma}+10k^2\frac{\partial^6\overline{v}_{3-i}^H}{\partial\eta^6\partial\gamma^6}\right.\right.\\
&\left.\left.\left.+3\frac{\partial^6\overline{v}_{3-i}^H}{\partial\eta\partial\gamma^5}\right)\right]+\overline{K}_t^H\overline{w}_i^H\begin{pmatrix}\delta_{1n}+\delta_{1m}+\delta_{nN_z}+\delta_{mN_y}-\delta_{1m}\delta_{1n}\\-\delta_{1m}\delta_{nN_z}-\delta_{1n}\delta_{mN_y}-\delta_{nN_z}\delta_{mN_y}\end{pmatrix}\left(1-\delta_{1i}\right)\right\}=0.
\end{aligned}
\tag{E.4}
$$

Appendix E.2. Nonlocal mass and stiffness matrices

On the basis of the continuous-based-NHOBT, the non-dimensional mass and stiffness matrices of the vertically aligned jungles of DWCNTs embedded within an elastic matrix are obtained as:

$$\left[\overline{\mathbf{M}}_b^H\right]_{mnpqrs}^{\psi_{[\cdot]_i}\psi_{[\cdot]_i}}=\int_0^1\int_0^1\int_0^1\vartheta_7^{2i-2}\left(\phi_{mnp}^{\psi_{[\cdot]_i}}\phi_{qrs}^{\psi_{[\cdot]_i}}+\mu^2\phi_{mnp,\xi}^{\psi_{[\cdot]_i}}\phi_{qrs,\xi}^{\psi_{[\cdot]_i}}\right)\mathrm{d}\xi\mathrm{d}\eta\mathrm{d}\gamma, \tag{E.5}$$

$$\left[\overline{\mathbf{M}}_b^H\right]_{mnpqrs}^{\psi_{[\cdot]_i}[\bullet]_i}=\int_0^1\int_0^1\int_0^1\vartheta_2^{2i-2}\gamma_6^2\left(-\phi_{mnp,\xi}^{\psi_{[\cdot]_i}}\phi_{qrs}^{[\bullet]_i}-\mu^2\phi_{mnp,\xi\xi}^{\psi_{[\cdot]_i}}\phi_{qrs,\xi}^{[\bullet]_i}\right)\mathrm{d}\xi\mathrm{d}\eta\mathrm{d}\gamma, \tag{E.6}$$

$$\left[\overline{\mathbf{M}}_b^H\right]_{mnpqrs}^{[\bullet]_i[\bullet]_i}=\int_0^1\int_0^1\int_0^1\left[\begin{array}{l}\vartheta_1^{2i-2}\left(\phi_{mnp}^{[\bullet]_i}\phi_{qrs}^{[\bullet]_i}+\mu^2\phi_{mnp,\xi}^{[\bullet]_i}\phi_{qrs,\xi}^{[\bullet]_i}\right)\\+\vartheta_3^{2i-2}\gamma_2^2\left(\phi_{mnp,\xi}^{[\bullet]_i}\phi_{qrs,\xi}^{[\bullet]_i}+\mu^2\phi_{mnp,\xi\xi}^{[\bullet]_i}\phi_{qrs,\xi\xi}^{[\bullet]_i}\right)\end{array}\right]\mathrm{d}\xi\mathrm{d}\eta\mathrm{d}\gamma, \tag{E.7}$$

$$\left[\overline{\mathbf{M}}_b^H\right]_{mnpqrs}^{[\bullet]_i\psi_{[\cdot]_i}}=\int_0^1\int_0^1\int_0^1\vartheta_2^{2i-2}\gamma_1^2\left(\phi_{mnp,\xi}^{[\bullet]_i}\phi_{qrs}^{\psi_{[\cdot]_i}}+\mu^2\phi_{mnp,\xi\xi}^{[\bullet]_i}\phi_{qrs,\xi}^{\psi_{[\cdot]_i}}\right)\mathrm{d}\xi\mathrm{d}\eta\mathrm{d}\gamma, \tag{E.8}$$

$$\left[\overline{\mathbf{K}}_b^H\right]_{mnpqrs}^{\psi_{[\cdot]_i}\psi_{[\cdot]_i}}=\int_0^1\int_0^1\int_0^1\left(\vartheta_4^{2i-2}\gamma_7^2\phi_{mnp}^{\psi_{[\cdot]_i}}\phi_{qrs}^{\psi_{[\cdot]_i}}+\vartheta_8^{2i-2}\gamma_8^2\phi_{mnp,\xi}^{\psi_{[\cdot]_i}}\phi_{qrs,\xi}^{\psi_{[\cdot]_i}}\right)\mathrm{d}\xi\mathrm{d}\eta\mathrm{d}\gamma, \tag{E.9}$$

$$\left[\overline{\mathbf{K}}_b^H\right]_{mnpqrs}^{\psi_{[\cdot]_i}[\bullet]_i}=\int_0^1\int_0^1\int_0^1\left(\vartheta_4^{2i-2}\gamma_7^2\phi_{mnp,\xi}^{\psi_{[\cdot]_i}}\phi_{qrs}^{[\bullet]_i}+\vartheta_5^{2i-2}\gamma_9^2\phi_{mnp,\xi\xi\xi}^{\psi_{[\cdot]_i}}\phi_{qrs}^{[\bullet]_i}\right)\mathrm{d}\xi\mathrm{d}\eta\mathrm{d}\gamma, \tag{E.10}$$

$$\left[\overline{\mathbf{K}}_b^H\right]_{mnpqrs}^{[\bullet]_i\psi_{[\cdot]_i}}=\int_0^1\int_0^1\int_0^1\left(-\vartheta_4^{2i-2}\gamma_3^2\phi_{mnp,\xi}^{[\bullet]_i}\phi_{qrs}^{\psi_{[\cdot]_i}}-\vartheta_5^{2i-2}\gamma_4^2\phi_{mnp,\xi\xi\xi}^{[\bullet]_i}\phi_{qrs}^{\psi_{[\cdot]_i}}\right)\mathrm{d}\xi\mathrm{d}\eta\mathrm{d}\gamma, \tag{E.11}$$

$$\begin{aligned}&\left[\overline{\mathbf{K}}_b^H\right]_{mnpqrs}^{[\bullet]_i[\bullet]_i}=\int_0^1\int_0^1\int_0^1\Big\{\vartheta_4^{2i-2}\gamma_3^2\phi_{mnp,\xi}^{[\bullet]_i}\phi_{qrs,\xi}^{[\bullet]_i}+\vartheta_6^{2i-2}\phi_{mnp,\xi\xi}^{[\bullet]}\phi_{qrs,\xi\xi}^{[\bullet]}+\overline{C}_{v\|_{(i+2,i)}}^H\left(\kappa\overline{d}\right)^2\\
&\Bigg[\phi_{mnp,\eta}^{[\bullet]_i}\phi_{qrs,\eta}^{[\bullet]_i}+\mu^2\phi_{mnp,\xi\eta}^{[\bullet]_i}\phi_{qrs,\xi\eta}^{[\bullet]_i}-\frac{\left(\kappa\overline{d}\right)^2}{12}\left(\phi_{mnp,\eta\eta}^{[\bullet]_i}\phi_{qrs,\eta\eta}^{[\bullet]_i}+\mu^2\phi_{mnp,\xi\eta\eta}^{[\bullet]_i}\phi_{qrs,\xi\eta\eta}^{[\bullet]_i}\right)\\
&+\frac{\left(\kappa\overline{d}\right)^4}{360}\left(\phi_{mnp,\eta\eta\eta}^{[\bullet]_i}\phi_{qrs,\eta\eta\eta}^{[\bullet]_i}+\mu^2\phi_{mnp,\xi\eta\eta\eta}^{[\bullet]_i}\phi_{qrs,\xi\eta\eta\eta}^{[\bullet]_i}\right)-\frac{\left(\kappa\overline{d}\right)^6}{20160}\left(\phi_{mnp,\eta\eta\eta\eta}^{[\bullet]_i}\phi_{qrs,\eta\eta\eta\eta}^{[\bullet]_i}+\mu^2\phi_{mnp,\xi\eta\eta\eta\eta}^{[\bullet]_i}\phi_{qrs,\xi\eta\eta\eta\eta}^{[\bullet]_i}\right)\Bigg]\\
&+\overline{C}_{v\|_{(i,3-i)}}^H\left(\phi_{mnp}^{[\bullet]_i}\phi_{qrs}^{[\bullet]_i}\right)+2\overline{C}_{v\|_{(i+1,4-i)}}^H\left(\phi_{mnp}^{[\bullet]_i}\phi_{qrs}^{[\bullet]_i}\right)+\overline{C}_{v\perp_{(i+2,i)}}^H\overline{d}^2\Bigg[\phi_{mnp,\gamma}^{[\bullet]_i}\phi_{qrs,\gamma}^{[\bullet]_i}+\mu^2\phi_{mnp,\xi\gamma}^{[\bullet]_i}\phi_{qrs,\xi\gamma}^{[\bullet]_i}\\
&-\frac{\overline{d}^2}{12}\left(\phi_{mnp,\gamma\gamma}^{[\bullet]_i}\phi_{qrs,\gamma\gamma}^{[\bullet]_i}+\mu^2\phi_{mnp,\xi\gamma\gamma}^{[\bullet]_i}\phi_{qrs,\xi\gamma\gamma}^{[\bullet]_i}\right)+\frac{\overline{d}^4}{360}\left(\phi_{mnp,\gamma\gamma\gamma}^{[\bullet]_i}\phi_{qrs,\gamma\gamma\gamma}^{[\bullet]_i}+\mu^2\phi_{mnp,\xi\gamma\gamma\gamma}^{[\bullet]_i}\phi_{qrs,\xi\gamma\gamma\gamma}^{[\bullet]_i}\right)\\
&-\frac{\overline{d}^6}{20160}\left(\phi_{mnp,\gamma\gamma\gamma\gamma}^{[\bullet]_i}\phi_{qrs,\gamma\gamma\gamma\gamma}^{[\bullet]_i}+\mu^2\phi_{mnp,\xi\gamma\gamma\gamma\gamma}^{[\bullet]_i}\phi_{qrs,\xi\gamma\gamma\gamma\gamma}^{[\bullet]_i}\right)\Bigg]+\overline{C}_{v\|_{(i,3-i)}}^H\left(\phi_{mnp}^{[\bullet]_i}\phi_{qrs}^{[\bullet]_i}\right)+2\overline{C}_{v\|_{(i+1,4-i)}}^H\left(\phi_{mnp}^{[\bullet]_i}\phi_{qrs}^{[\bullet]_i}\right)\\
&+\left(\overline{C}_{d\|_{(i+2,i)}}^H+\overline{C}_{d\perp_{(i+2,i)}}^H\right)\overline{d}^2\Bigg[\phi_{mnp,\gamma}^{[\bullet]_i}\phi_{qrs,\gamma}^{[\bullet]_i}+\mu^2\phi_{mnp,\xi\gamma}^{[\bullet]_i}\phi_{qrs,\xi\gamma}^{[\bullet]_i}+\kappa^2\left(\phi_{mnp,\eta}^{[\bullet]_i}\phi_{qrs,\eta}^{[\bullet]_i}+\mu^2\phi_{mnp,\xi\eta}^{[\bullet]_i}\phi_{qrs,\xi\eta}^{[\bullet]_i}\right)\\
&-\frac{\overline{d}^2}{12}\Bigg(\phi_{mnp,\gamma\gamma}^{[\bullet]_i}\phi_{qrs,\gamma\gamma}^{[\bullet]_i}+\mu^2\phi_{mnp,\xi\gamma\gamma}^{[\bullet]_i}\phi_{qrs,\xi\gamma\gamma}^{[\bullet]_i}+6\kappa^2\left(\phi_{mnp,\eta\gamma}^{[\bullet]_i}\phi_{qrs,\eta\gamma}^{[\bullet]_i}+\mu^2\phi_{mnp,\xi\eta\gamma}^{[\bullet]_i}\phi_{qrs,\xi\eta\gamma}^{[\bullet]_i}\right)\\
&+\kappa^4\left(\phi_{mnp,\eta\eta}^{[\bullet]_i}\phi_{qrs,\eta\eta}^{[\bullet]_i}+\mu^2\phi_{mnp,\xi\eta\eta}^{[\bullet]_i}\phi_{qrs,\xi\eta\eta}^{[\bullet]_i}\right)\Bigg)+\frac{\overline{d}^4}{360}\Bigg(\phi_{mnp,\gamma\gamma\gamma}^{[\bullet]_i}\phi_{qrs,\gamma\gamma\gamma}^{[\bullet]_i}+\mu^2\phi_{mnp,\xi\gamma\gamma\gamma}^{[\bullet]_i}\phi_{qrs,\xi\gamma\gamma\gamma}^{[\bullet]_i}\\
&+15\kappa^2\left(\phi_{mnp,\eta\gamma\gamma}^{[\bullet]_i}\phi_{qrs,\eta\gamma\gamma}^{[\bullet]_i}+\mu^2\phi_{mnp,\xi\eta\gamma\gamma}^{[\bullet]_i}\phi_{qrs,\xi\eta\gamma\gamma}^{[\bullet]_i}\right)+15\kappa^4\left(\phi_{mnp,\eta\eta\gamma}^{[\bullet]_i}\phi_{qrs,\eta\eta\gamma}^{[\bullet]_i}+\mu^2\phi_{mnp,\xi\eta\eta\gamma}^{[\bullet]_i}\phi_{qrs,\xi\eta\eta\gamma}^{[\bullet]_i}\right)\\
&+\kappa^6\left(\phi_{mnp,\eta\eta\eta}^{[\bullet]_i}\phi_{qrs,\eta\eta\eta}^{[\bullet]_i}+\mu^2\phi_{mnp,\xi\eta\eta\eta}^{[\bullet]_i}\phi_{qrs,\xi\eta\eta\eta}^{[\bullet]_i}\right)\Bigg)\Bigg]+\left(\overline{C}_{d\|_{(i,3-i)}}^H+\overline{C}_{d\perp_{(i,3-i)}}^H\right)\left(\phi_{mnp}^{[\bullet]_i}\phi_{qrs}^{[\bullet]_i}\right)\\
&+2\left(\overline{C}_{d\|_{(i+1,4-i)}}^H+\overline{C}_{d\perp_{(i+1,4-i)}}^H\right)\left(\phi_{mnp}^{[\bullet]_i}\phi_{qrs}^{[\bullet]_i}\right)\Big\}\mathrm{d}\xi\mathrm{d}\eta\mathrm{d}\gamma,\end{aligned} \tag{E.12}$$

$$
\begin{aligned}
&\left[\overline{\mathbf{K}}_b^H\right]^{[\bullet]_i[\bullet]_{3-i}}_{mnpqrs} = \int_0^1\int_0^1\int_0^1 \Big\{ -\overline{C}^H_{v\|_{(i,3-i)}} \left(\phi^{[\bullet]_i}_{mnp}\phi^{[\bullet]_{3-i}}_{qrs}\right) - 2\overline{C}^H_{v\|_{(i+1,4-i)}} \left(\phi^{[\bullet]_i}_{mnp}\phi^{[\bullet]_{3-i}}_{qrs}\right) + \overline{C}^H_{v\|_{(i+1,4-i)}} \left(\kappa\overline{d}\right)^2 \\
&\Bigg[\phi^{[\bullet]_i}_{mnp,\eta}\phi^{[\bullet]_{3-i}}_{qrs,\eta} + \mu^2\phi^{[\bullet]_i}_{mnp,\xi\eta}\phi^{[\bullet]_{3-i}}_{qrs,\xi\eta} - \frac{\left(\kappa\overline{d}\right)^2}{12}\left(\phi^{[\bullet]_i}_{mnp,\eta\eta}\phi^{[\bullet]_{3-i}}_{qrs,\eta\eta} + \mu^2\phi^{[\bullet]_i}_{mnp,\xi\eta\eta}\phi^{[\bullet]_{3-i}}_{qrs,\xi\eta\eta}\right) \\
&+\frac{\left(\kappa\overline{d}\right)^4}{360}\left(\phi^{[\bullet]_i}_{mnp,\eta\eta\eta}\phi^{[\bullet]_{3-i}}_{qrs,\eta\eta\eta} + \mu^2\phi^{[\bullet]_i}_{mnp,\xi\eta\eta\eta}\phi^{[\bullet]_{3-i}}_{qrs,\xi\eta\eta\eta}\right) - \frac{\left(\kappa\overline{d}\right)^6}{20160}\left(\phi^{[\bullet]_i}_{mnp,\eta\eta\eta\eta}\phi^{[\bullet]_{3-i}}_{qrs,\eta\eta\eta\eta} + \mu^2\phi^{[\bullet]_i}_{mnp,\xi\eta\eta\eta\eta}\phi^{[\bullet]_{3-i}}_{qrs,\xi\eta\eta\eta\eta}\right)\Bigg] \\
&-\overline{C}^H_{v\perp_{(i,3-i)}}\left(\phi^{[\bullet]_i}_{mnp}\phi^{[\bullet]_{3-i}}_{qrs}\right) - 2\overline{C}^H_{v\perp_{(i+1,4-i)}}\left(\phi^{[\bullet]_i}_{mnp}\phi^{[\bullet]_{3-i}}_{qrs}\right) + \overline{C}^H_{v\perp_{(i+1,4-i)}}\overline{d}^2\Bigg[\phi^{[\bullet]_i}_{mnp,\gamma}\phi^{[\bullet]_{3-i}}_{qrs,\gamma} + \mu^2\phi^{[\bullet]_i}_{mnp,\xi\gamma}\phi^{[\bullet]_{3-i}}_{qrs,\xi\gamma} \\
&-\frac{\overline{d}^2}{12}\left(\phi^{[\bullet]_i}_{mnp,\gamma\gamma}\phi^{[\bullet]_{3-i}}_{qrs,\gamma\gamma} + \mu^2\phi^{[\bullet]_i}_{mnp,\xi\gamma\gamma}\phi^{[\bullet]_{3-i}}_{qrs,\xi\gamma\gamma}\right) + \frac{\overline{d}^4}{360}\left(\phi^{[\bullet]_i}_{mnp,\gamma\gamma\gamma}\phi^{[\bullet]_{3-i}}_{qrs,\gamma\gamma\gamma} + \mu^2\phi^{[\bullet]_i}_{mnp,\xi\gamma\gamma\gamma}\phi^{[\bullet]_{3-i}}_{qrs,\xi\gamma\gamma\gamma}\right) \\
&-\frac{\overline{d}^6}{20160}\left(\phi^{[\bullet]_i}_{mnp,\gamma\gamma\gamma\gamma}\phi^{[\bullet]_{3-i}}_{qrs,\gamma\gamma\gamma\gamma} + \mu^2\phi^{[\bullet]_i}_{mnp,\xi\gamma\gamma\gamma\gamma}\phi^{[\bullet]_{3-i}}_{qrs,\xi\gamma\gamma\gamma\gamma}\right)\Bigg] - \left(\overline{C}^H_{d\|_{(i,3-i)}} + \overline{C}^H_{d\perp_{(i,3-i)}}\right)\left(\phi^{[\bullet]_i}_{mnp}\phi^{[\bullet]_{3-i}}_{qrs}\right) \\
&-2\left(\overline{C}^H_{d\|_{(i+1,4-i)}} + \overline{C}^H_{d\perp_{(i+1,4-i)}}\right)\left(\phi^{[\bullet]_i}_{mnp}\phi^{[\bullet]_{3-i}}_{qrs}\right) + \left(\overline{C}^H_{d\|_{(i+1,4-i)}} + \overline{C}^H_{d\perp_{(i+1,4-i)}}\right)\overline{d}^2\Bigg[\phi^{[\bullet]_i}_{mnp,\gamma}\phi^{[\bullet]_{3-i}}_{qrs,\gamma} + \mu^2\phi^{[\bullet]_i}_{mnp,\xi\gamma}\phi^{[\bullet]_{3-i}}_{qrs,\xi\gamma} \\
&+\kappa^2\left(\phi^{[\bullet]_i}_{mnp,\eta}\phi^{[\bullet]_{3-i}}_{qrs,\eta} + \mu^2\phi^{[\bullet]_i}_{mnp,\xi\eta}\phi^{[\bullet]_{3-i}}_{qrs,\xi\eta}\right) - \frac{\overline{d}^2}{12}\Bigg(\phi^{[\bullet]_i}_{mnp,\gamma\gamma}\phi^{[\bullet]_{3-i}}_{qrs,\gamma\gamma} + \mu^2\phi^{[\bullet]_i}_{mnp,\xi\gamma\gamma}\phi^{[\bullet]_{3-i}}_{qrs,\xi\gamma\gamma} + 6\kappa^2\Big(\phi^{[\bullet]_i}_{mnp,\eta\gamma}\phi^{[\bullet]_{3-i}}_{qrs,\eta\gamma} \\
&+\mu^2\phi^{[\bullet]_i}_{mnp,\xi\eta\gamma}\phi^{[\bullet]_{3-i}}_{qrs,\xi\eta\gamma}\Big) + \kappa^4\left(\phi^{[\bullet]_i}_{mnp,\eta\eta}\phi^{[\bullet]_{3-i}}_{qrs,\eta\eta} + \mu^2\phi^{[\bullet]_i}_{mnp,\xi\eta\eta}\phi^{[\bullet]_{3-i}}_{qrs,\xi\eta\eta}\right)\Bigg) + \frac{\overline{d}^4}{360}\Bigg(\phi^{[\bullet]_i}_{mnp,\gamma\gamma\gamma}\phi^{[\bullet]_{3-i}}_{qrs,\gamma\gamma\gamma} + \mu^2\phi^{[\bullet]_i}_{mnp,\xi\gamma\gamma\gamma}\phi^{[\bullet]_{3-i}}_{qrs,\xi\gamma\gamma\gamma} \\
&+15\kappa^2\left(\phi^{[\bullet]_i}_{mnp,\eta\gamma\gamma}\phi^{[\bullet]_{3-i}}_{qrs,\eta\gamma\gamma} + \mu^2\phi^{[\bullet]_i}_{mnp,\xi\eta\gamma\gamma}\phi^{[\bullet]_{3-i}}_{qrs,\xi\eta\gamma\gamma}\right) + 15\kappa^4\left(\phi^{[\bullet]_i}_{mnp,\eta\eta\gamma}\phi^{[\bullet]_{3-i}}_{qrs,\eta\eta\gamma} + \mu^2\phi^{[\bullet]_i}_{mnp,\xi\eta\eta\gamma}\phi^{[\bullet]_{3-i}}_{qrs,\xi\eta\eta\gamma}\right) \\
&+\kappa^6\left(\phi^{[\bullet]_i}_{mnp,\eta\eta\eta}\phi^{[\bullet]_{3-i}}_{qrs,\eta\eta\eta} + \mu^2\phi^{[\bullet]_i}_{mnp,\xi\eta\eta\eta}\phi^{[\bullet]_{3-i}}_{qrs,\xi\eta\eta\eta}\right)\Bigg)\Bigg]\Big\}\,\mathrm{d}\xi\mathrm{d}\eta\mathrm{d}\gamma,
\end{aligned}
\tag{E.13}
$$

$$
\begin{aligned}
&\left[\overline{\mathbf{K}}_b^H\right]^{[\bullet]_i[\circ]_1}_{mnpqrs} = \left(\overline{C}^H_{d\|_{(i+2,i)}} - \overline{C}^H_{d\perp_{(i+2,i)}}\right)\kappa\overline{d}^2\int_0^1\int_0^1\int_0^1\Big\{\phi^{[\bullet]_i}_{mnp,\eta}\phi^{[\circ]_1}_{qrs,\gamma} + \phi^{[\bullet]_i}_{mnp,\gamma}\phi^{[\circ]_1}_{qrs,\eta} + \mu^2\Big(\phi^{[\bullet]_i}_{mnp,\xi\eta}\phi^{[\circ]_1}_{qrs,\xi\gamma} \\
&+\phi^{[\bullet]_i}_{mnp,\xi\gamma}\phi^{[\circ]_1}_{qrs,\xi\eta}\Big) - \frac{\overline{d}^2}{6}\Big[\overline{\nabla}_{\eta\gamma}\left\{\phi^{[\bullet]_i}_{mnp,\eta}\right\}\cdot\overline{\nabla}_{\eta\gamma}\left\{\phi^{[\circ]_1}_{qrs,\gamma}\right\} + \overline{\nabla}_{\eta\gamma}\left\{\phi^{[\bullet]_i}_{mnp,\gamma}\right\}\cdot\overline{\nabla}_{\eta\gamma}\left\{\phi^{[\circ]_1}_{qrs,\eta}\right\} + \mu^2\Big(\overline{\nabla}_{\eta\gamma}\left\{\phi^{[\bullet]_i}_{mnp,\xi\eta}\right\}\cdot \\
&\overline{\nabla}_{\eta\gamma}\left\{\phi^{[\circ]_1}_{qrs,\xi\gamma}\right\} + \overline{\nabla}_{\eta\gamma}\left\{\phi^{[\bullet]_i}_{mnp,\xi\gamma}\right\}\cdot\overline{\nabla}_{\eta\gamma}\left\{\phi^{[\circ]_1}_{qrs,\xi\eta}\right\}\Big)\Big] + \frac{\overline{d}^4}{360}\Big[3\kappa^4\Big(\phi^{[\bullet]_i}_{mnp,\gamma\eta\eta}\phi^{[\circ]_1}_{qrs,\eta\eta\eta} + \phi^{[\bullet]_i}_{mnp,\eta\eta\eta}\phi^{[\circ]_1}_{qrs,\gamma\eta\eta} \\
&+\mu^2\left(\phi^{[\bullet]_i}_{mnp,\xi\eta\eta\gamma}\phi^{[\circ]_1}_{qrs,\xi\eta\eta\eta} + \phi^{[\bullet]_i}_{mnp,\xi\eta\eta\eta}\phi^{[\circ]_1}_{qrs,\xi\eta\eta\gamma}\right)\Big) + 10\kappa^2\Big(\phi^{[\bullet]_i}_{mnp,\eta\eta\eta}\phi^{[\circ]_1}_{qrs,\gamma\gamma\gamma} + \phi^{[\bullet]_i}_{mnp,\gamma\gamma\gamma}\phi^{[\circ]_1}_{qrs,\eta\eta\eta} \\
&+\mu^2\left(\phi^{[\bullet]_i}_{mnp,\xi\eta\eta\eta}\phi^{[\circ]_1}_{qrs,\xi\gamma\gamma\gamma} + \phi^{[\bullet]_i}_{mnp,\xi\gamma\gamma\gamma}\phi^{[\circ]_1}_{qrs,\xi\eta\eta\eta}\right)\Big) + 3\Big(\phi^{[\bullet]_i}_{mnp,\eta\gamma\gamma}\phi^{[\circ]_1}_{qrs,\gamma\gamma\gamma} + \phi^{[\bullet]_i}_{mnp,\gamma\gamma\gamma}\phi^{[\circ]_1}_{qrs,\eta\gamma\gamma} \\
&+\mu^2\left(\phi^{[\bullet]_i}_{mnp,\xi\eta\gamma\gamma}\phi^{[\circ]_1}_{qrs,\xi\gamma\gamma\gamma} + \phi^{[\bullet]_i}_{mnp,\xi\gamma\gamma\gamma}\phi^{[\circ]_1}_{qrs,\xi\eta\gamma\gamma}\right)\Big)\Big]\Big\}\,\mathrm{d}\xi\mathrm{d}\eta\mathrm{d}\gamma,
\end{aligned}
\tag{E.14}
$$

$$\left[\overline{\mathbf{K}}_b^H\right]_{mnpqrs}^{[\bullet]_i[\circ]_2}=\left(\overline{C}_{d\|_{(i+1,4-i)}}^H-\overline{C}_{d\perp_{(i+1,4-i)}}^R\right)\kappa\overline{d}^2\int_0^1\int_0^1\int_0^1\left\{\phi_{mnp,\eta}^{[\bullet]_i}\phi_{qrs,\gamma}^{[\circ]_2}+\phi_{mnp,\gamma}^{[\bullet]_i}\phi_{qrs,\eta}^{[\circ]_2}+\mu^2\left(\phi_{mnp,\xi\eta}^{[\bullet]_i}\phi_{qrs,\xi\gamma}^{[\circ]_2}+\right.\right.$$
$$\left.\phi_{mnp,\xi\gamma}^{[\bullet]_i}\phi_{qrs,\xi\eta}^{[\circ]_2}\right)-\frac{\overline{d}^2}{6}\left[\overline{\nabla}_{\eta\gamma}\left\{\phi_{mnp,\eta}^{[\bullet]_i}\right\}\cdot\overline{\nabla}_{\eta\gamma}\left\{\phi_{qrs,\gamma}^{[\circ]_2}\right\}+\overline{\nabla}_{\eta\gamma}\left\{\phi_{mnp,\gamma}^{[\bullet]_i}\right\}\cdot\overline{\nabla}_{\eta\gamma}\left\{\phi_{qrs,\eta}^{[\circ]_2}\right\}+\mu^2\left(\overline{\nabla}_{\eta\gamma}\left\{\phi_{mnp,\xi\eta}^{[\bullet]_i}\right\}\cdot\right.\right.$$
$$\left.\left.\overline{\nabla}_{\eta\gamma}\left\{\phi_{qrs,\xi\gamma}^{[\circ]_2}\right\}+\overline{\nabla}_{\eta\gamma}\left\{\phi_{mnp,\xi\gamma}^{[\bullet]_i}\right\}\cdot\overline{\nabla}_{\eta\gamma}\left\{\phi_{qrs,\xi\eta}^{[\circ]_2}\right\}\right)\right]+\frac{\overline{d}^4}{360}\left[3\kappa^4\left(\phi_{mnp,\gamma\eta\eta}^{[\bullet]_i}\phi_{qrs,\eta\eta\eta}^{[\circ]_2}+\phi_{mnp,\eta\eta\eta}^{[\bullet]_i}\phi_{qrs,\gamma\eta\eta}^{[\circ]_2}\right.\right.$$
$$\left.+\mu^2\left(\phi_{mnp,\xi\eta\eta\gamma}^{[\bullet]_i}\phi_{qrs,\xi\eta\eta\eta}^{[\circ]_2}+\phi_{mnp,\xi\eta\eta\eta}^{[\bullet]_i}\phi_{qrs,\xi\eta\eta\gamma}^{[\circ]_2}\right)\right)+10\kappa^2\left(\phi_{mnp,\eta\eta\eta}^{[\bullet]_i}\phi_{qrs,\gamma\gamma\gamma}^{[\circ]_2}+\phi_{mnp,\gamma\gamma\gamma}^{[\bullet]_i}\phi_{qrs,\eta\eta\eta}^{[\circ]_2}\right.$$
$$\left.+\mu^2\left(\phi_{mnp,\xi\eta\eta\eta}^{[\bullet]_i}\phi_{qrs,\xi\gamma\gamma\gamma}^{[\circ]_2}+\phi_{mnp,\xi\gamma\gamma\gamma}^{[\bullet]_i}\phi_{qrs,\xi\eta\eta\eta}^{[\circ]_2}\right)\right)+3\left(\phi_{mnp,\eta\gamma\gamma}^{[\bullet]_i}\phi_{qrs,\gamma\gamma\gamma}^{[\circ]_2}+\phi_{mnp,\gamma\gamma\gamma}^{[\bullet]_i}\phi_{qrs,\eta\gamma\gamma}^{[\circ]_2}\right.$$
$$\left.\left.\left.+\mu^2\left(\phi_{mnp,\xi\eta\gamma\gamma}^{[\bullet]_i}\phi_{qrs,\xi\gamma\gamma\gamma}^{[\circ]_2}+\phi_{mnp,\xi\gamma\gamma\gamma}^{[\bullet]_i}\phi_{qrs,\xi\eta\gamma\gamma}^{[\circ]_2}\right)\right)\right]\right\}\mathrm{d}\xi\mathrm{d}\eta\mathrm{d}\gamma, \tag{E.15}$$

where $[.]$=y or z, and $([\bullet],[\circ])$=(v,w) or (w,v).

References

Akgoz, B., Civalek, O., 2017. Effects of thermal and shear deformation on vibration response of functionally graded thick composite microbeams, Compos. Part B-Eng. 129, 77–87. https://doi.org/10.1016/j.compositesb.2017.07.024.

Barretta, R., Canadija, M., de Sciarra, F.M., 2016. A higher-order Eringen model for BernoulliEuler nanobeams, Arch. Appl. Mech. 86, 483–495. https://doi.org/10.1007/s00419-015-1037-0.

Batra, R.C., Sears, A., 2007. Continuum models of multi-walled carbon nanotubes. Int. J. Solids Struct. 44, 7577–7596. https://doi.org/10.1016/j.ijsolstr.2007.04.029.

Besseghier, A., Tounsi, A., Houari, M.S.A., Benzair, A., Boumia, L., Heireche, H., 2011. Thermal effect on wave propagation in double-walled carbon nanotubes embedded in a polymer matrix using nonlocal elasticity. Physica E 43, 1379–1386. https://doi.org/10.1016/j.physe.2011.03.008.

Cebeci, H., de Villoria, R.G., Hart, A.J., Wardle, B.L., 2009. Multifunctional properties of high volume fraction aligned carbon nanotube polymer composites with controlled morphology. Compos. Sci. Technol. 69(15–16), 2649–2656. https://doi.org/10.1016/j.compscitech.2009.08.006.

Chang, T.P., 2013. Stochastic FEM on nonlinear vibration of fluid-loaded double-walled carbon nanotubes subjected to a moving load based on nonlocal elasticity theory. Compos. Part B-Eng 54, 391–399. https://doi.org/10.1016/j.compositesb.2013.06.012.

Chen, G., Davis, R.C., Futaba, D.N., Sakurai, S., Kobashi, K., Yumura, M., Hata, K., 2016. A sweet spot for highly efficient growth of vertically aligned single-walled carbon nanotube forests enabling their unique structures and properties. Nanoscale 8, 162–171. https://doi.org/10.1039/C5NR05537G.

Chen, G., Shin, D.H., Iwasaki, T., Kawarada, H., Lee, C.J., 2008. Enhanced field emission properties of vertically aligned double-walled carbon nanotube arrays. Nanotechnology 19, 415703. https://doi.org/10.1088/0957-4484/19/41/415703.

Choi, W.B., Bae, E., Kang, D., Chae, S., Cheong, B.H., Ko, J.H., Lee, E., Park, W., 2004. Aligned carbon nanotubes for nanoelectronics. Nanotechnology 15, S512. https://doi.org/10.1088/0957-4484/15/10/003.

Choi, W.B., Chu, J.U., Jeong, K.S., Bae, E.J., Lee, J.W., Kim, J.J., Lee, J.O., 2001. Ultrahigh-density nanotransistors by using selectively grown vertical carbon nanotubes. Appl. Phys. Lett. 79, 3696–3698. https://doi.org/10.1063/1.1419236.

Civalek, O., Demir, C., Akgöz, B., 2010. Free vibration and bending analyses of cantilever microtubules based on nonlocal continuum model, Math. Comput. Appl. 15, 289–298. https://doi.org/10.3390/mca15020289.

Demir, C., Civalek, O., 2017. A new nonlocal FEM via Hermitian cubic shape functions for thermal vibration of nano beams surrounded by an elastic matrix. Compos. Struct. 168, 872–884. https://doi.org/10.1016/j.compstruct.2017.02.091.

Demir, ., Civalek, Ö., 2017. On the analysis of microbeams. Int. J. Eng. Sci. 121, 14–33. https://doi.org/10.1016/j.ijengsci.2017.08.016.

Dragoman, M., Grenier, K., Dubuc, D., Bary, L., Plana, R., Fourn, E., Flahaut, E., 2007. Millimeter wave carbon nanotube gas sensor. J. Appl. Phys. 101, 106103. https://doi.org/10.1063/1.2734873.

Eringen, A.C., 1966. Linear theory of micropolar elasticity. J. Math. Mech. 15, 909–923.

Eringen, A.C., 1972. Nonlocal polar elastic continua. Int. J. Eng. Sci. 10, 1–16. https://doi.org/10.1016/0020-7225(72)90070-5.

Eringen, A.C., 2002. *Nonlocal continuum field theories.* Springer-Verlag, NY. https://doi.org/10.1007/b97697

Fang, B., Zhen, Y.X., Zhang, C.P., Tang, Y., 2013. Nonlinear vibration analysis of double-walled carbon nanotubes based on nonlocal elasticity theory. Appl. Math. Model. 37, 1096–1107. https://doi.org/10.1016/j.apm.2012.03.032.

Ghavanloo, E., Fazelzadeh, A.A., 2013. Nonlocal elasticity theory for radial vibration of nanoscale spherical shells. Euro. J. Mech. A/Solids 41, 37–42. https://doi.org/10.1016/j.euromechsol.2013.02.003.

Gupta, S.S., Batra, R.C., 2008. Continuum structures equivalent in normal mode vibrations to single-walled carbon nanotubes. Comp. Mater. Sci. 43, 715–723. https://doi.org/10.1016/j.commatsci.2008.01.032.

Gupta, S.S., Bosco, F.G., Batra, R.C., 2010. Wall thickness and elastic moduli of single-walled carbon nanotubes from frequencies of axial, torsional and inextensional modes of vibration. Comp. Mater. Sci. 47, 1049–1059. https://doi.org/10.1016/j.commatsci.2009.12.007.

Heireche, H., Tounsi, A., Benzair, A., 2008. Scale effect on wave propagation of double-walled carbon nanotubes with initial axial loading. Nanotechnology 19, 185703. https://doi.org/10.1088/0957-4484/19/18/185703.

Hoseinzadeh, M.S., Khadem, S.E., 2014. A nonlocal shell theory model for evaluation of thermoelastic damping in the vibration of a double-walled carbon nanotube. Physica E 57, 6–11. https://doi.org/10.1016/j.physe.2013.10.009.

Hosseini-Hashemi, S., Nazemnezhad, R., Rokni, H., 2015. Nonlocal nonlinear free vibration of nanobeams with surface effects. Euro. J. Mech. A/Solids. 52, 44–53. https://doi.org/10.1016/j.euromechsol.2014.12.012.

Hu, L., Hecht, D.S., Gruner, G., 2004. Percolation in transparent and conducting carbon nanotube networks. Nano Lett. 4, 2513–2517. https://doi.org/10.1021/nl048435y

Hu, Y.G., Liew, K.M., Wang, Q., He, X.Q., Yakobson, B.I., 2008. Nonlocal shell model for elastic wave propagation in single- and double-walled carbon nanotubes. J. Mech. Phys. Solids 56, 3475–3485. https://doi.org/10.1016/j.jmps.2008.08.010.

Jiang, K., Li, Q., Fan, S., 2002. Nanotechnology: Spinning continuous carbon nanotube yarns. Nature 419, 801. https://doi.org/10.1038/419801a.

Jiang, K., Wang, J., Li, Q., Liu, L., Liu, C., Fan, S., 2011. Superaligned carbon nanotube arrays, films, and yarns: a road to applications. Adv. Mater. 23, 1154–1161. https://doi.org/10.1002/adma.201003989.

Ke, L.L., Xiang, Y., Yang, J., Kitipornchai, S., 2009. Nonlinear free vibration of embedded double-walled carbon nanotubes based on nonlocal Timoshenko beam theory. Comp. Mater. Sci. 47, 409–417. https://doi.org/10.1016/j.commatsci.2009.09.002.

Kiani, K., 2014(a). In- and out-of- plane dynamic flexural behaviors of two-dimensional ensembles of vertically aligned single-walled carbon nanotubes. Physica B 449, 164–180. https://doi.org/10.1016/j.physb.2014.04.044.

Kiani, K., 2014(b). Nonlocal discrete and continuous modeling of free vibration of stocky ensembles of single-walled carbon nanotubes. Curr. Appl. Phys. 14, 1116–1139. https://doi.org/10.1016/j.cap.2014.05.018.

Kiani, K., 2015. Wave characteristics in aligned forests of single-walled carbon nanotubes using nonlocal discrete and continuous theories. Int. J. Mech. Sci. 90, 278–309. https://doi.org/10.1016/j.ijmecsci.2014.11.011.

Kiani, K., 2016. Free vibration of in-plane-aligned membranes of single-walled carbon nanotubes in the presence of in-plane-unidirectional magnetic fields. J. Vib. Control 22, 3736–3766. https://doi.org/10.1177/1077546314565684.

Kiani, K., 2018(a). Application of nonlocal higher-order beam theory to transverse wave analysis of magnetically affected forests of single-walled carbon nanotubes. Int. J. Mech. Sci. 138–139, 1–16. https://doi.org/10.1016/j.ijmecsci.2018.01.033.

Kiani, K., 2018(b). Nonlocal dynamic response of periodic arrays of single-walled carbon nanotubes in the presence of longitudinal thermal and magnetic fields. Comp. Math. Appl. 75, 3849–3872. https://doi.org/10.1016/j.camwa.2018.02.033.

Kiani, K., Pakdaman, H., 2018. Nonlocal vibrations and potential instability of monolayers from double-walled carbon nanotubes subjected to temperature gradients. Int. J. Mech. Sci. 144, 576–599. https://doi.org/10.1016/j.ijmecsci.2018.06.018.

Kiani, K., Wang, Q., 2018. Nonlocal magneto-thermo-vibro-elastic analysis of vertically aligned arrays of single-walled carbon nanotubes. Euro. J. Mech. A-Solids 72, 497–515. https://doi.org/10.1016/j.euromechsol.2018.05.017.

Koratkar, N., Wei, B., Ajayan, P.M., 2002. Carbon nanotube films for damping applications. Adv. Mater. 14, 997–1000. https://doi.org/10.1002/1521-4095(20020705)14:13/14%3C997::AID-ADMA997%3E3.0.CO;2-Y.

Koratkar, N.A., Wei, B., Ajayan, P.M., 2003. Multifunctional structural reinforcement featuring carbon nanotube films. Compos. Sci. Technol. 63(11), 1525–1531. https://doi.org/10.1016/S0266-3538(03)00065-4.

Lan, Y., Wang, Y., Ren, Z.F., 2011. Physics and applications of aligned carbon nanotubes. Adv. Phys. 60, 553–678. https://doi.org/10.1080/00018732.2011.599963.

Lin, W., Moon, K.S., Wong, C.P., 2009. A combined process of in situ functionalization and microwave treatment to achieve ultrasmall thermal expansion of aligned carbon nanotube polymer nanocomposites: toward applications as thermal interface materials. Adv. Mater. 21, 2421–2424. https://doi.org/10.1002/adma.200803548.

Liu, C., Kim, K.S., Baek, J., Cho, Y., Han, S., Kim, S.W., Min, N.K., Choi, Y., Kim, J.U., Lee, C.J., 2009(a). Improved field emission properties of double-walled carbon nanotubes decorated with Ru nanoparticles. Carbon 47, 1158–1164. https://doi.org/10.1016/j.carbon.2008.12.054.

Liu, K., Sun, Y., Zhou, R., Zhu, H., Wang, J., Liu, L., Fan, S., Jiang, K., 2009(b). Carbon nanotube yarns with high tensile strength made by a twisting and shrinking method. Nanotechnology 21, 045708. https://doi.org/10.1088/0957-4484/21/4/045708.

Meng, L., Zou, D., Lai, H., Guo, Z., He, X., Xie, Z., Gao, C., 2018. Semi-analytic solution of Eringens two-phase local/nonlocal model for Euler-Bernoulli beam with axial force. Appl. Math. Mech. 39, 1805–1824. https://doi.org/10.1007/s10483-018-2395-9.

Mercan, K., Civalek, Ö., 2017. Buckling analysis of Silicon carbide nanotubes (SiCNTs) with surface effect and nonlocal elasticity using the method of HDQ. Compos. Part B-Eng. 114, 34–45. https://doi.org/10.1016/j.compositesb.2017.01.067.

Murmu, T., Adhikari, S., 2012. Nonlocal elasticity based vibration of initially pre-stressed coupled nanobeam systems. Euro. J. Mech A/Solids, 34, 52–62. https://doi.org/10.1016/j.euromechsol.2011.11.010.

Murmu, T., McCarthy, M.A., Adhikari, S., 2012. Vibration response of double-walled carbon nanotubes subjected to an externally applied longitudinal magnetic field: a nonlocal elasticity approach. J. Sound Vib. 331, 5069–5086. https://doi.org/10.1016/j.jsv.2012.06.005.

Ngo, Q., Cruden, B.A., Cassell, A.M., Sims, G., Meyyappan, M., Li, J., Yang, C.Y., 2004. Thermal interface properties of Cu-filled vertically aligned carbon nanofiber arrays. Nano Lett. 4, 2403–2407. https://doi.org/10.1021/nl048506t.

Numanoglu, H.M., Akgöz, B., Civalek, Ö., 2018. On dynamic analysis of nanorods. Int. J. Eng. Sci. 130, 33–50. https://doi.org/10.1016/j.ijengsci.2018.05.001.

Ogasawara, T., Moon, S.Y., Inoue, Y., Shimamura, Y., 2011. Mechanical properties of aligned multi-walled carbon nanotube/epoxy composites processed using a hot-melt prepreg method. Compos. Sci. Technol. 71(16), 1826–1833. https://doi.org/10.1016/j.compscitech.2011.08.009.

Patel, A.M., Joshi, A.Y., 2014. Investigation of double walled carbon nanotubes for mass sensing. Proc. Tech. 14, 290–294. https://doi.org/10.1016/j.protcy.2014.08.038.

Qu, L., Dai, L., 2007. Gecko-foot-mimetic aligned single-walled carbon nanotube dry adhesives with unique electrical and thermal properties. Adv. Mater. 19, 3844–3849. https://doi.org/10.1002/adma.200700023.

Qu, L., Dai, L., Stone, M., Xia, Z., Wang, Z.L., 2008. Carbon nanotube arrays with strong shear binding-on and easy normal lifting-off. Science 322, 238–242. https://doi.org/10.1126/science.1159503

Rahmani, O., Refaeinejad, V., Hosseini, S.A.H., 2017. Assessment of various nonlocal higher order theories for the bending and buckling behavior of functionally graded nanobeams. Steel Compos. Struct. 23, 339–350. http://dx.doi.org/10.12989/scs.2017.23.3.339.

Shen, H.S., Zhang, C.L., 2010. Torsional buckling and postbuckling of double-walled carbon nanotubes by nonlocal shear deformable shell model. Compos. Struct. 92, 1073–1084. https://doi.org/10.1016/j.compstruct.2009.10.002.

Sohn, J.I., Lee, S., Song, Y.H., Choi, S.Y., Cho, K.I., Nam, K.S., 2011. Patterned selective growth of carbon nanotubes and large field emission from vertically well-aligned carbon nanotube field emitter arrays. Appl. Phys. Lett. 78, 901–903. https://doi.org/10.1063/1.1335846.

Sudak, L.J., 2003. Column buckling of multiwalled carbon nanotubes using nonlocal continuum mechanics. J. Appl. Phys. 94, 7281–7287. https://doi.org/10.1063/1.1625437.

Suhr, J., Koratkar, N., Keblinski, P., Ajayan, P., 2005. Viscoelasticity in carbon nanotube composites. Nat. Mater. 4(2), 134. https://doi.org/10.1038/nmat1293.

Tong, T., Zhao, Y., Delzeit, L., Kashani, L., Meyyappan, M., Majumdar, A. 2007. Dense vertically aligned multiwalled carbon nanotube arrays as thermal interface materials. IEEE T. Compon. Pack. T. 30, 92–100. https://doi.org/10.1109/TCAPT.2007.892079.

Tounsi, A., Benguedia, S., Adda, B., Semmah, A., Zidour, M., 2013. Nonlocal effects on thermal buckling properties of double-walled carbon nanotubes. Adv. Nano Res. 1, 1–11. http://dx.doi.org/10.12989/anr.2013.1.1.001.

Tounsi, A., Heireche, H., Berrabah, H.M., Benzair, A., Boumia, L., 2008. Effect of small size on wave propagation in double-walled carbon nanotubes under temperature field. J. Appl. Phys. 104, 104301. https://doi.org/10.1063/1.3018330.

Wang, Q., Varadan, V.K., 2006. Vibration of carbon nanotubes studied using nonlocal continuum mechanics. Smart Mater. Struct 15, 659. https://doi.org/10.1088/0964-1726/15/2/050.

Wei, C., Dai, L., Roy, A., Tolle, T.B., 2006. Multifunctional chemical vapor sensors of aligned carbon nanotube and polymer composites. J. Am. Chem. Soc. 128, 1412–1413. https://doi.org/10.1021/ja0570335.

Yamamoto, N., Hart, A.J., Garcia, E.J., Wicks, S.S., Duong, H.M., Slocum, A.H., Wardle, B.L., 2009. High-yield growth and morphology control of aligned carbon nanotubes on ceramic fibers for multifunctional enhancement of structural composites. Carbon 47(3), 551–560. https://doi.org/10.1016/j.carbon.2008.10.030.

Yang, Z.P., Ci, L., Bur, J.A., Lin, S.Y., Ajayan, P.M., 2008. Experimental observation of an extremely dark material made by a low-density nanotube array. Nano Lett. 8, 446–451. https://doi.org/10.1021/nl072369t

Zeighampour, H., Tadi Beni, Y., Dehkordi, M.B., 2018. Wave propagation in viscoelastic thin cylindrical nanoshell resting on a visco-Pasternak foundation based on nonlocal strain gradient theory, Thin. Wall. Struct. 122, 378–386. https://doi.org/10.1016/j.tws.2017.10.037.

Acknowledgement

The financial supports of the Iran National Science Foundation (INSF) as well as K.N. Toosi University of Technology from the undertaken work are highly appreciated.

Captions of the Tables:

Table 1. The predicted fundamental frequencies (THz) of the nanosystem with BC1 and BC2 for different slenderness ratios as well as small-scale parameters (N_y=N_z=20).

Table 2. The predicted fundamental frequencies (THz) of the nanosystem by both discrete models and continuous models for different numbers of DWCNTs and slenderness ratios.

Captions of the figures:

Fig. 1. A layer-by-layer assembly of vertically aligned DWCNTs.

Fig. 2. An illustration of the continuum-based jungle of vertically aligned DWCNTs embedded in an elastic matrix.

Fig. 3. Influence of the elastic properties of the matrix on the fundamental frequency for different numbers of DWCNTs: ((...) NRBT, (—) NHOBT; (○) N_y=N_z=5, (□) N_y=N_z=8, (△) N_y=N_z=15, λ_1=17).

Fig. 4. Influence of the number of DWCNTs on the fundamental frequency for various slenderness ratios for two cases: (a) all exterior DWCNTs are fixed, (b) all cornered DWCNTs are fixed; ((...) NRBT, (—) NHOBT; (○) λ_1=12, (□) λ_1=22, (△) λ_1=32).

Fig. 5. Influence of the slenderness ratio on the fundamental frequency for different numbers of DWCNTs: ((...) NRBT, (—) NHOBT; (○) N_y=N_z=5, (□) N_y=N_z=15, (△) N_y=N_z=500).

Fig. 6. Influence of the intertube distance on the fundamental frequency for different numbers of DWCNTs: ((...) NRBT, (—) NHOBT; (○) N_y=N_z=5, (□) N_y=N_z=8, (△) N_y=N_z=28, λ_1=22, $d_N = \dfrac{d - 2r_{m_1}}{t_b}$).

Fig. A1. Schematic representation of a doubly adjacent DWCNTs accounting for linear modeling of the variation of vdW forces due to their lateral vibrations.

Table 1.

		λ_1					
	e_0a (nm)	10	15	20	100	250	500
BC1							
NRBT	0	3.227616	1.497925	0.869338	0.319643	0.517675	0.733319
	1	2.957756	1.438934	0.850265	0.319643	0.517675	0.733319
	2	2.431720	1.297280	0.800243	0.319643	0.517675	0.733319
NHOBT	0	2.767708	1.379718	0.828275	0.319636	0.517675	0.733319
	1	2.536513	1.325567	0.810211	0.319636	0.517675	0.733319
	2	2.086087	1.195575	0.762849	0.319636	0.517675	0.733319
BC2							
NRBT	0	3.226638	1.495641	0.865285	0.289690	0.468558	0.663737
	1	2.956687	1.436555	0.846119	0.289690	0.468558	0.663737
	2	2.430416	1.294640	0.795837	0.289690	0.468558	0.663737
NHOBT	0	2.766487	1.377191	0.823990	0.289683	0.468558	0.663737
	1	2.535179	1.322936	0.805830	0.289683	0.468558	0.663737
	2	2.084462	1.192657	0.758194	0.289683	0.468558	0.663737

Table 2.

	λ_1	$N_y = N_z$				
		4	8	12	16	20
DMs†						
NRBT	14	1.856185	1.530893	1.477310	1.459810	1.452037
	24	1.322751	0.770947	0.652175	0.609453	0.589659
	34	1.243575	0.610682	0.448592	0.382733	0.349820
NHOBT	14	1.767080	1.412661	1.353022	1.333443	1.324729
	24	1.316200	0.757205	0.635421	0.591335	0.570842
	34	1.242809	0.608348	0.445237	0.378729	0.345404
CMs‡						
NRBT	14	1.854956	1.530588	1.477135	1.459677	1.451922
	24	1.321878	0.770652	0.652031	0.609369	0.589604
	34	1.242765	0.610321	0.448388	0.3826035	0.349731
NHOBT	14	1.765888	1.412392	1.352884	1.3333467	1.324651
	24	1.315323	0.756905	0.635274	0.5912495	0.570786
	34	1.241997	0.607985	0.445032	0.3785986	0.345314

† and ‡: DMs and CMs in order stand for discrete models and continuous models.

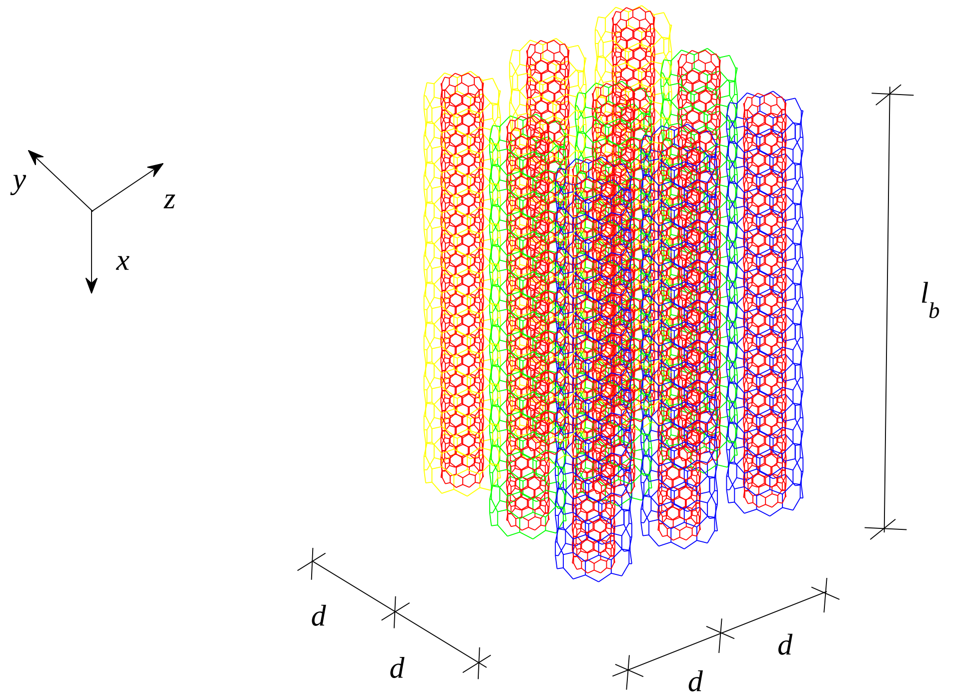

Fig. 1.

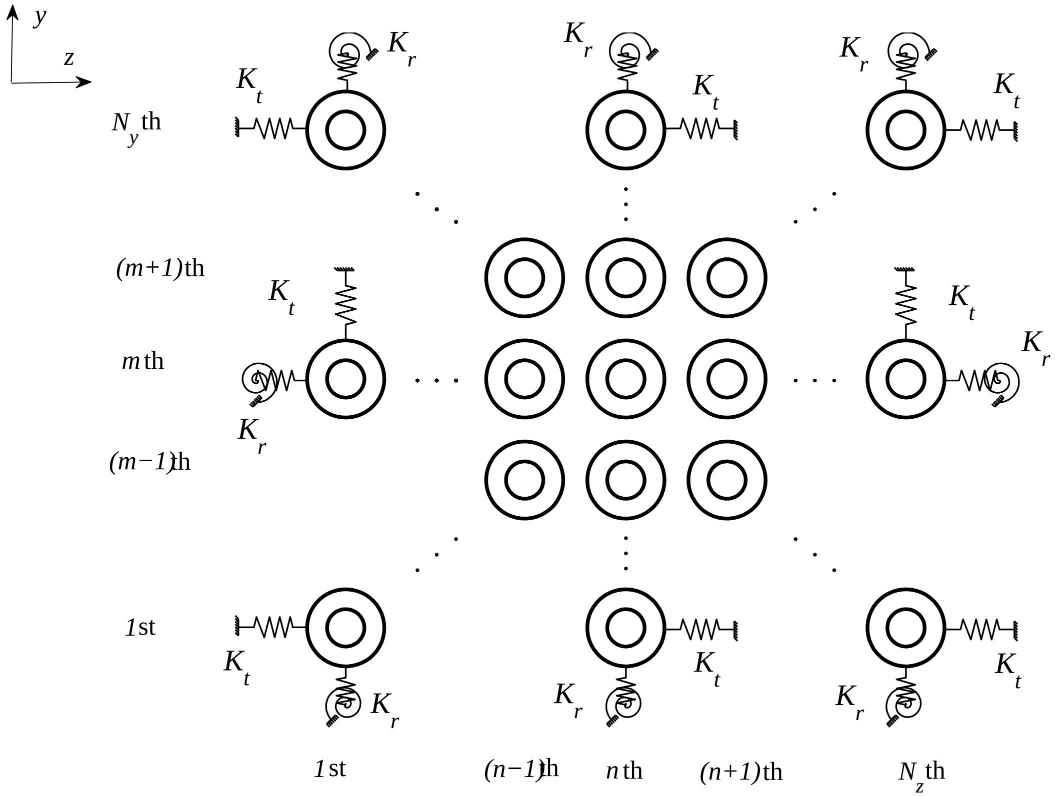

Fig. 2.

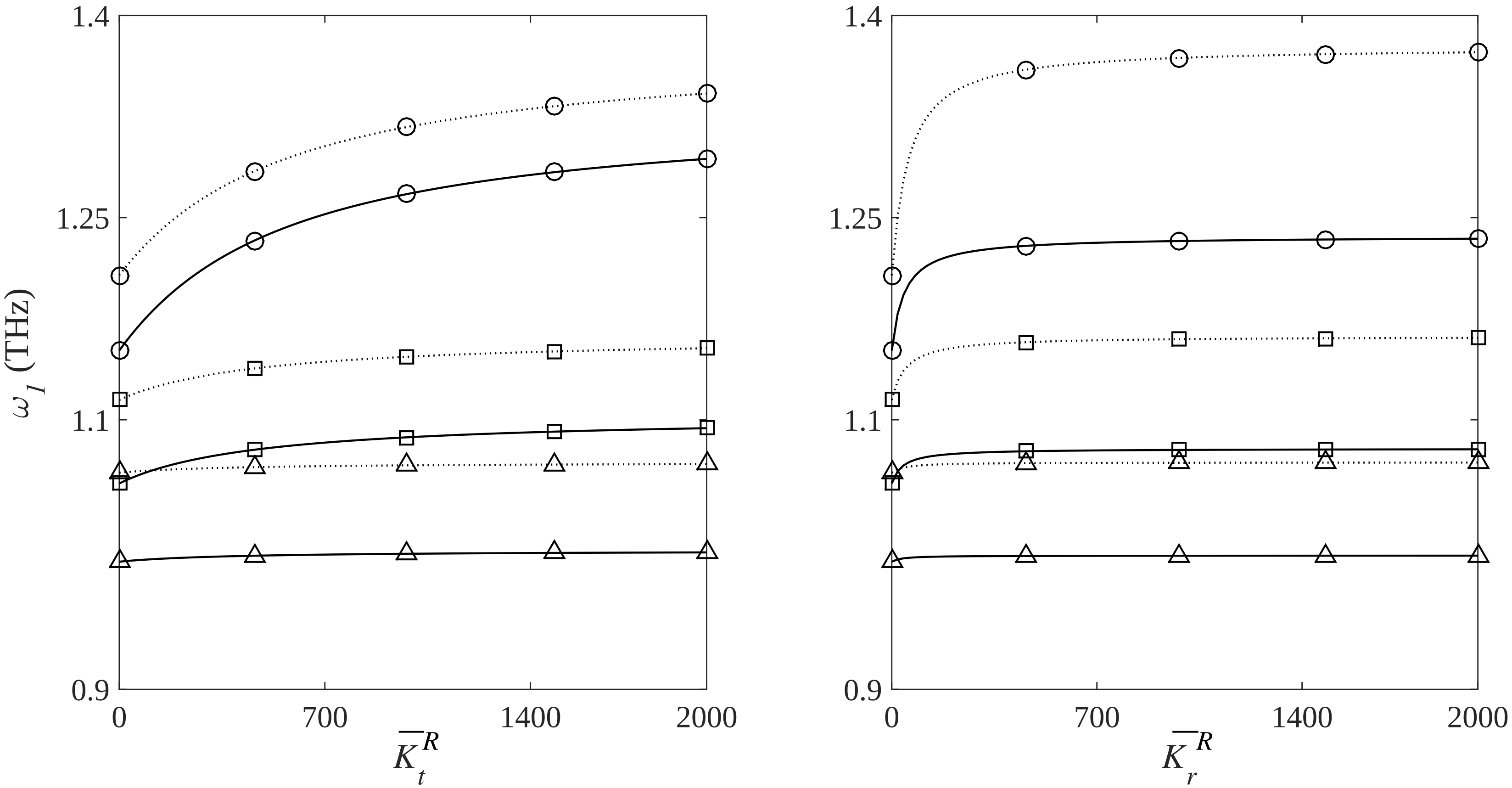

1.4
1.25
1.1
0.9
ω1 (THz)
0
700
1400
2000
K̄tR
1.4
1.25
1.1
0.9
0
700
1400
2000
K̄rR

Fig. 3.

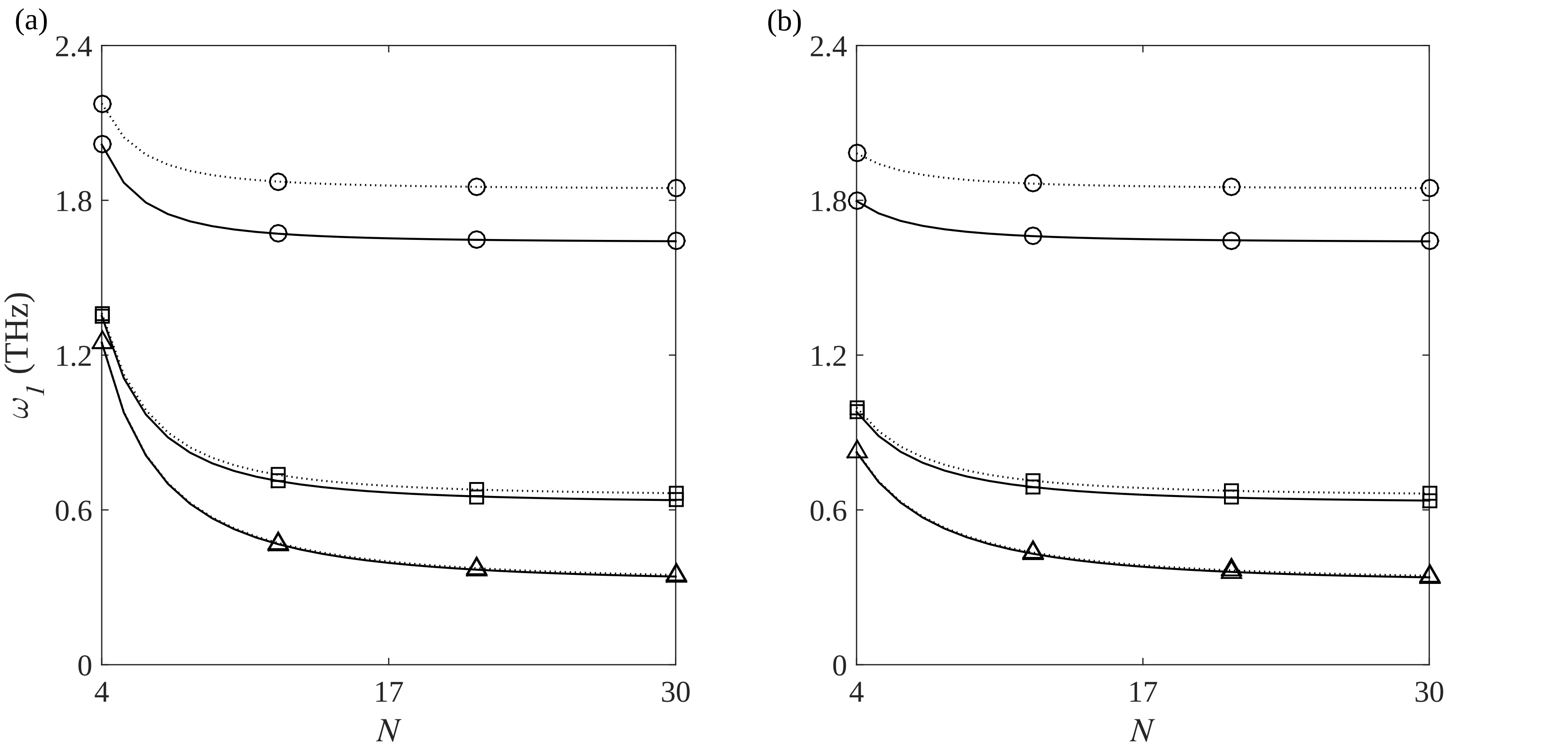

Fig. 4.

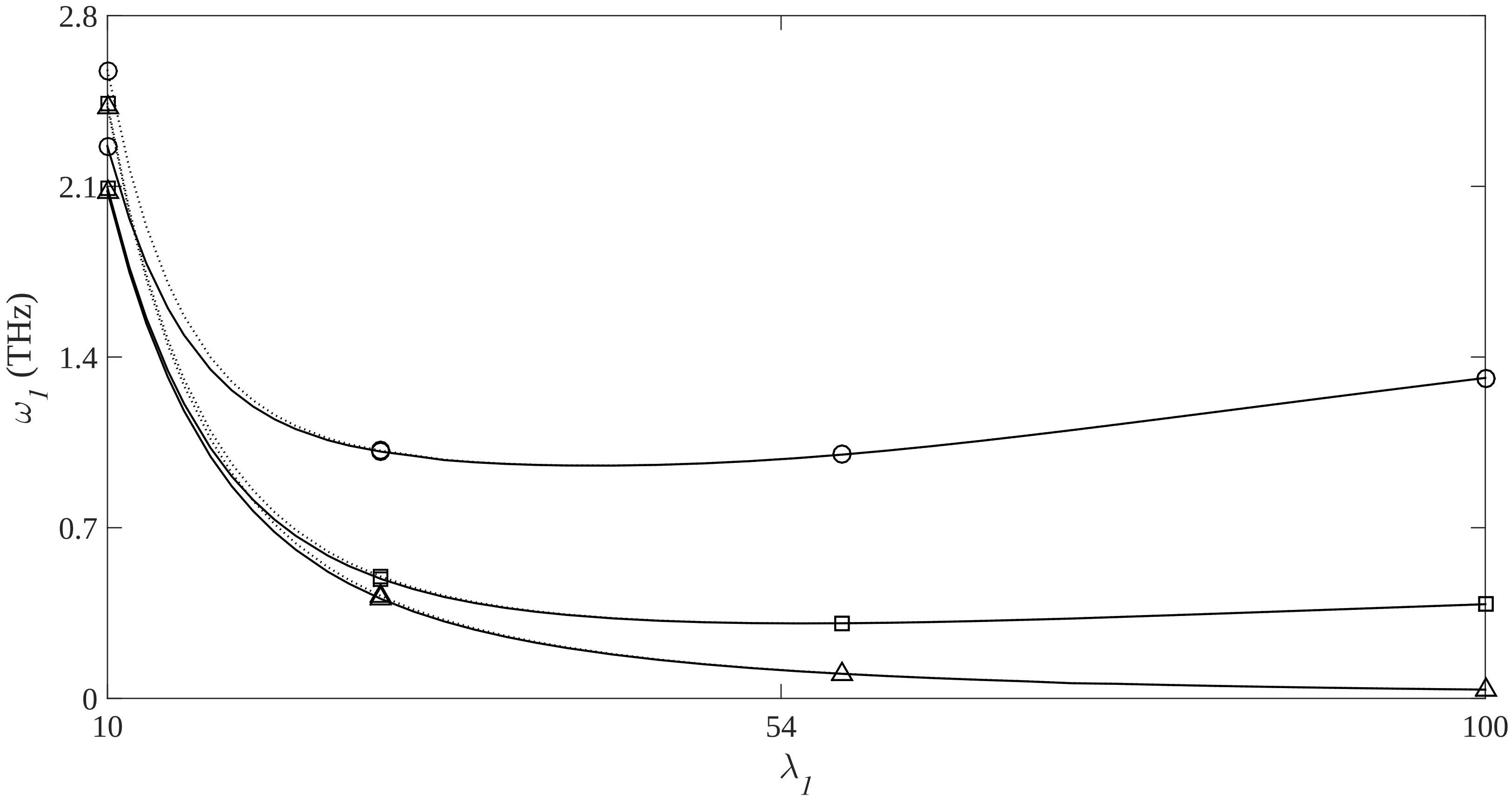

Fig. 5.

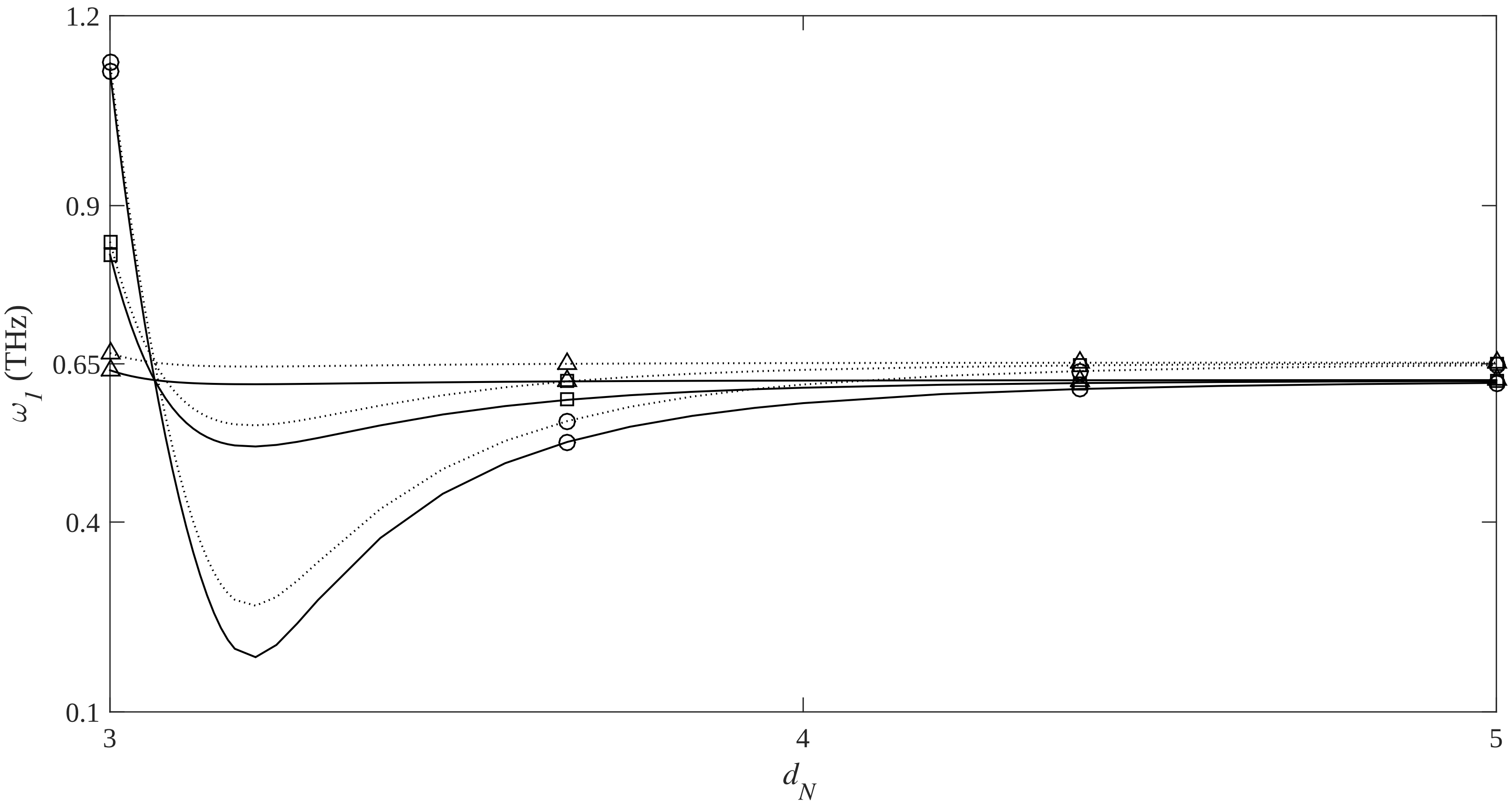

Fig. 6.

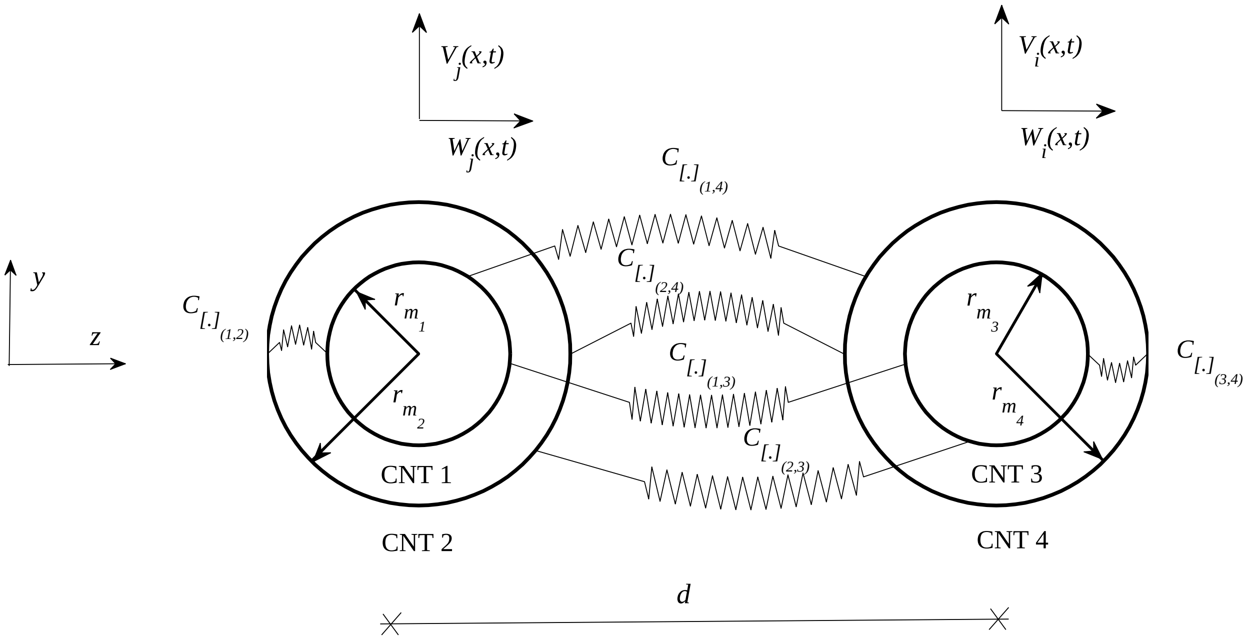

$V_j(x,t)$
$W_j(x,t)$
$V_i(x,t)$
$W_i(x,t)$
$C_{[.]_{(1,4)}}$
$C_{[.]_{(2,4)}}$
$C_{[.]_{(1,3)}}$
$C_{[.]_{(2,3)}}$
$C_{[.]_{(1,2)}}$
$C_{[.]_{(3,4)}}$
y
z
r_{m_1}
r_{m_2}
r_{m_3}
r_{m_4}
CNT 1
CNT 2
CNT 3
CNT 4
d

Fig. A1.

Highlights of the present research:

- Nonlocal-bilateral dynamics of layer-by-layer assembly of DWCNTs are studied.
- The Rayleigh and higher-order beams are adopted for modeling of constitutive tubes.
- The complex rigorous-intertube vdW forces are taken into account for the models.
- Roles of intertube distance, shear, and population on vibrations are displayed.
- Novel-nonlocal-continuous-based models are also established and verified.

Dear Prof. Tvergaard,

The authors of the paper do not feel any conflict of interest for the carried out theoretical study in the present work.

Best regards,

Keivan Kiani, PhD

Associate Professor,
Department of Civil Engineering,
K.N. Toosi University of Technology,
Tehran, Iran
Email(s): k_kiani@kntu.ac.ir , keivankiani@yahoo.com
Homepage: http://wp.kntu.ac.ir/k_kiani/
Tel: +98 21 88779473
Fax: +98 21 88779476
P.O. Box: 15875-4416